





29192038



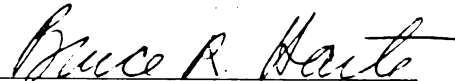
This is to certify that the

dissertation entitled  
FINITE ELEMENT MODELING OF OXYGEN  
DIFFUSION AND DEGRADATION OF VITAMIN C  
IN PACKAGED LIQUID FOODS

presented by  
FELIX H. BARRON

has been accepted towards fulfillment  
of the requirements for

Ph. D. Food Science  
degree in

  
Major professor

Date July 1990

PLACE IN RETURN BOX to remove this checkout from your record.  
TO AVOID FINES return on or before date due.

DATE DUE	DATE DUE	DATE DUE
JUN 13 1994 28	_____	_____
SEP 06 1995 012	_____	_____
JUN 11 1996 103	_____	_____
SEP 10 1997	_____	_____
_____	_____	_____
DEC 13 2001 11	_____	_____
MAY 01 2002 091602	_____	_____
_____	_____	_____

MSU Is An Affirmative Action/Equal Opportunity Institution

c:\circ\data\due.pm3-p.1

**FINITE ELEMENT MODELING OF OXYGEN DIFFUSION  
AND DEGRADATION OF VITAMIN C IN PACKAGED  
LIQUID FOODS**

**By**

**FELIX HECTOR BARRON**

**AN ABSTRACT OF A DISSERTATION**

**Submitted to  
Michigan State University  
in partial fulfillment of the requirements  
for the degree of**

**DOCTOR OF PHILOSOPHY**

**Department of Food Science and Human Nutrition**

**1990**



6760-11-11

**ABSTRACT**  
**FINITE ELEMENT MODELING OF OXYGEN DIFFUSION AND**  
**DEGRADATION OF VITAMIN C IN PACKAGED LIQUID FOODS**

By

**Felix Hector Barron**

The simultaneous diffusion of oxygen and its reaction with vitamin C was studied using water and apple juice. The liquids, supplemented with vitamin C (range 0.113 mM to 11.35 mM) were packaged in a cylindrical container, permeable to oxygen. The container was made of High Density Polyethylene (HDPE). The liquids, contained in a graduated glass cylinder were also studied when exposed to air in the absence of the HDPE membrane.

The diffusion-reaction process was simulated using the Finite Element Method (FEM) through the implementation of three main computer programs applicable to finite, semi-infinite and cylindrical liquid systems with no convective movements. The FEM was selected due to its potential application in many different situations, including irregular container shapes and boundary conditions.

Three main parameters, necessary for the computer simulation were determined: Oxygen diffusion coefficient in the liquids, kinetic rate constants for oxygen and vitamin C rate expressions, and the permeability constant for HDPE.

The permeability constant value of 10,593.1cc-mil/m<sup>2</sup>.atm.day was determined using the Isostatic Method. Oxygen diffusion coefficients in water and apple juice at 25°C were 1.2x10<sup>-3</sup>cm<sup>2</sup>/min and 8.5x10<sup>-4</sup>cm<sup>2</sup>/min respectively. The values were determined by applying the diffusion equation to the semi-infinite water and apple juice systems.

Kinetic rate constants for rate equations (oxygen) were determined in the liquids supplemented with vitamin C, at 25°C. The closed systems, with initial oxygen levels of 0.21 atm, and low vitamin contents yielded first order rate constants of 0.0049 min<sup>-1</sup> for water, and 0.0073 min<sup>-1</sup> for apple juice. A zero order rate constant (1.567 x 10<sup>-4</sup> atm/min) was obtained for water with a high vitamin content of 11.35 mM.

The kinetic rate constants for rate equations (vitamin C) were not as simple as for the constants determined for oxygen. Empirical power model rate equations were obtained for water with 0.341 mM vitamin C, and for apple juice with 3.157 mM Vit. C. The model parameters were different for each liquid.

An apparent zero order rate constant (2.7x10<sup>-7</sup> M/min) was observed for apple juice containing 0.272 mM vitamin C. No significant changes in vitamin C content (11.35 mM) in water were observed in a closed system with initial oxygen levels ranging from 0.08 to 0.21 atm.

Non-consistent kinetic models suggested a more complex reaction mechanism for the oxidation of vitamin C under the experimental conditions used in this work. The kinetic models, however, were appropriate for the computer simulation used in this study.

The three main parameters were used to validate the Finite Element computer models, by coupling oxygen diffusion with and without a chemical reaction. Acceptable predictions were obtained reflecting the flexible applicability of the FEM and the corresponding models.

**To my wife Florencia, for her love,  
enduring patience, support and her  
precious years sacrificed**

**To my children: Piero and Guendalina,  
for their faith, love and patience.**

## ACKNOWLEDGMENTS

The author is sincerely indebted to Dr. Bruce Harte, Associate Professor, School of Packaging and Department of Food Science and Nutrition for his interest and advise in this work. This study could not have been undertaken without his encouragement and arrangements for financial support.

The author acknowledges and thanks Dr. J. Giacin and Dr. R. Hernandez (School of Packaging) for their assistance in this study.

Appreciation is also extended to Dr. J. Lee, Dr. Heidi Hoojjat (School of Packaging), Dr. L. Segerlind (Agricultural Engineering), Dr. J. Cash and Dr. M. Uebersax (Food Science and Human Nutrition) for their valuable advise during the period of this work.

The author thanks Mr. Ron Norris (Biochemistry workshop) for his help in the building of the plexiglass diffusion cells.

## TABLE OF CONTENTS

	Page
ACKNOWLEDGEMENTS. . . . .	iii
TABLE OF CONTENTS. . . . .	iv
LIST OF TABLES. . . . .	viii
LIST OF FIGURES. . . . .	x
 I. INTRODUCTION. . . . .	 1
II. LITERATURE REVIEW. . . . .	4
2.1 Computer simulation of food quality. . . . .	4
2.1.1 The Finite Element and other computer models. . . . .	4
2.2 Oxidation of vitamin C. . . . .	10
2.3 Oxygen permeability of polymeric plastic materials. . . . .	17
2.4 Oxygen diffusivity in aqueous solutions. . . . .	18
2.5 Oxygen absorption and chemical reaction in aqueous solutions and liquid foods. . . . .	20
 III. MATERIALS AND METHODS. . . . .	 24
3.1 The Finite Element Method. . . . .	24
3.1.1 Description of the Finite Element Method: One Dimension. . . . .	24
3.1.2 Description of the Finite Element Method in two and three dimensions, with derivative boundary conditions. . . . .	28
3.1.3 The Finite Element Method: Simultaneous oxygen absorption and chemical reaction . . . . .	41
3.2 Micro-Oxygen Electrodes. . . . .	42
3.2.1 Oxygen partial pressure measurements. . . . .	42
3.2.2 Calibration of micro-oxygen electrodes. . . . .	43
3.2.3 Oxygen solubility in water. . . . .	45

3.3	Oxygen Diffusion Cells. . . . .	47
3.3.1	Cell for one dimensional oxygen diffusion. . . . .	47
3.3.2	Determination of the oxygen diffusion coefficient in liquids. . . . .	49
3.3.3	Oxygen permeable cylindrical cells. . . . .	52
3.3.4	Mathematical model for the radial diffusion of oxygen in non moving water and apple juice. . . . .	54
3.4	Oxygen permeability tester: OX-TRAN 100. . . . .	57
3.4.1	Measurement of the permeability constant in Alethan and HDPE. . . . .	57
3.5	Permeability testing cell in the gas phase. . . . .	59
3.5.1	Verification of the HDPE permeability constant. . . . .	59
3.6	Cell systems for the diffusion of oxygen and autooxidation of ascorbic acid. . . . .	64
3.6.1	Optimum conditions for kinetic experiments. . . . .	64
3.6.1.1	Open system exposed to surface air. . . . .	65
3.6.2	Open system with continuous bubbling air. . . . .	66
3.6.3	Closed system . . . . .	67
3.6.3.1	Closed system and changes in dissolved oxygen. . . . .	67
3.6.3.1.1	Closed system and water added with vitamin C. . . . .	68
3.6.3.1.2	Closed system and apple juice added with vitamin C. . . . .	69
3.6.3.2	Closed system and changes in vitamin C content. . . . .	69
3.6.3.2.1	Closed system and water added with vitamin C. . . . .	70
3.6.3.2.2	Closed system and apple juice added with vitamin C. . . . .	71

3.7	Kinetic models. . . . .	71
IV	RESULTS AND DISCUSSION. . . . .	73
4.1	Calibration of oxygen sensors in liquid and gas phases. . .	73
4.1.1	Gas phase. . . . .	73
4.1.2	Liquid phase. . . . .	73
4.2	Oxygen diffusivity in liquids. . . . .	76
4.2.1	Oxygen diffusivity in water. . . . .	76
4.2.2	Oxygen diffusivity in apple juice. . . . .	82
4.3	Oxygen permeability constants. . . . .	85
4.4	Lumped gas model for testing cylindrical permeable cells. . .	88
4.5	Experimental determination of kinetic rate constants. . . .	92
4.5.1	Optimum experimental conditions. . . . .	92
4.6	Experimental kinetic models. . . . .	97
4.6.1	Kinetic rate equations expressed in terms of oxygen partial pressure. . . . .	97
4.6.1.1	Water with added vitamin C (25 <sup>0</sup> C). . . .	97
4.6.1.2	Apple juice with added vitamin C (25 <sup>0</sup> C). . .	102
4.6.2	Kinetic rate equations expressed in terms of vitamin C. . . . .	102
4.6.2.1	Water added with vitamin C. . . . .	104
4.6.2.2	Apple juice added with vitamin C. . . .	105
4.7	Liquid resistance to oxygen absorption. . . . .	109
4.8	Experimental retention of vitamin C. . . . .	111

4.9	Finite Element computer models. . . . .	113
4.9.1.	Rectangular coordinates (one dimension). . . . .	113
4.9.1.1	Oxygen diffusion. . . . .	113
4.9.1.2	Oxygen diffusion and chemical reaction . . . . .	116
4.9.2	Cylindrical coordinates (two dimensions). . . . .	119
4.9.2.1	Oxygen diffusion. . . . .	119
4.9.2.2	Oxygen diffusion and chemical reaction. . . . .	119
4.10	Validation of the Finite Element computer models. . . . .	122
4.10.1	Model verification for oxygen diffusion. . . . .	126
4.10.2	Model verification for simultaneous oxygen diffusion and chemical reaction with vitamin C. . . . .	131
4.11	Effects of packaging variables on oxygen diffusion. . . . .	136
V	CONCLUSIONS. . . . .	148
	APPENDIX A. . . . .	153
	APPENDIX B. . . . .	154
	APPENDIX C. . . . .	155
	APPENDIX D. . . . .	156
	REFERENCES. . . . .	157



## LIST OF TABLES

Table	Page
3.1      Summary of computer programming parameters for the three dimensional isoparametric thermal solid representing the finite element: STIF 70 (ANSYS,1987). . . . .	34
3.2      Summary of element printout explanations generated from the finite element program involving the three dimensional thermal solid (ANSYS, 1987). . . . .	35
3.3      Summary of computer parameters for the lumped thermal mass finite element (ANSYS, 1987). . . . .	40
3.4      Summary of element printout explanations generated from the finite element program involving the lumped thermal mass finite element: STIF: 71 (ANSYS, 1987). . . . .	40
3.5.     Sets of kinetic experiments to determine rate constants in terms of oxygen levels (atm) in water added with vitamin C. . . . .	68
3.6      Sets of kinetic experiments to determine rate constants in terms of vitamin C in water added with vitamin C. . . . .	70
4.1      Kinetic data for water containing 0.341 mM vitamin C in a closed system (25°C). The first order rate constant was $0.0049 \text{ min}^{-1}$ . . . . .	98
4.2      Kinetic data for water containing 11.35 mM vitamin C in a closed system (25°C). The zero order rate constant was $1.567 \times 10^{-4} \text{ atm/min}$ . . . . .	98
4.3      Kinetic data for apple juice (0.272 mM vitamin C) at 25°C in a closed system. The first order reaction rate constant was $0.0073 \text{ min}^{-1}$ . . . . .	103
4.4      Kinetic data for vitamin C degradation in water at 25°C, with constant supply of oxygen and initial vitamin C content of 0.341 mM. . . . .	106
4.5      Kinetic data for vitamin C degradation in apple juice at 25°C with constant supply of oxygen and initial vitamin C content of 0.272 mM. . . . .	106
4.6      Kinetic data for vitamin C degradation in apple juice at 25°C with constant supply of oxygen and initial vitamin content of 3.157 mM. . . . .	108

4.7	Experimental retention values of vitamin C in water and apple juice at 25°C. Semi-infinite and cylindrical cell systems. . . . .	108
4.8	Description of input parameters to the ANSYS computer program. Oxygen diffusion in a semi-infinite liquid system. . . . .	114
4.9	Description of input parameters to the ANSYS computer program . Oxygen diffusion in a semi-infinite liquid system with simultaneous chemical reaction. . . . .	117
4.10	Description of input parameters to the ANSYS computer program. Oxygen diffusion in a cylindrical permeable cell. . . . .	121
4.11	Description of input parameters to the ANSYS computer program. Simultaneous oxygen diffusion and chemical reaction in food liquids packaged in a permeable cylindrical cell. . . . .	123

## LIST OF FIGURES

Figure	Page
3.1	Summary of ANSYS analysis types (ANSYS, 1983). . . . . 30
3.2	Three dimensional thermal solid representing the geometry, nodal locations, and faces of the finite element STIF 70. . . . . 33
3.3	Lumped thermal mass (STIF 71) representing a point finite element used in conjunction with the three dimensional thermal solid. . . . . 37
3.4A	One-dimensional oxygen diffusion cell. . . . . 48
3.4B	Symmetrical diffusion system for the one-dimensional oxygen diffusion cell. . . . . 48
3.5	Semi-infinite oxygen diffusion system. . . . . 51
3.6	Oxygen permeable cylindrical cell. . . . . 53
4.1	Calibration of oxygen sensors in gas mixtures. . . . . 74
4.2	Calibration of oxygen sensors in water at 25°C. . . . . 75
4.3	Calibration of oxygen sensors in water and in air at 25°C. . . . . 77
4.4	Linear plot for determination of the oxygen diffusion coefficient in water at 25°C (Equation 3.1). . . . . 78
4.5	Determination of the oxygen diffusion coefficient in water at 25°C. Semi-infinite system. . . . . 79
4.6	Experimental determination of the oxygen diffusion coefficient in apple juice (25°C) using absorption data from a semi-infinite system. . . 84
4.7	Determination of oxygen permeability constant in High Density Poly Ethylene (Isostatic Method: OX-TRAN 100). . . . . 86
4.8	Unsteady state diffusion from air into a cylindrical permeable (HDPE) container. Experimental values and lumped model predictions. . . . . 89

4.9	Lumped model predictions of accumulating oxygen in a cylindrical, permeable (HDPE) container. . . . .	90
4.10	Preliminary kinetic experiments to test oxygen sensor response to effects of a chemical reaction in water. . . . .	93
4.11	Preliminary kinetic experiments in water to visualize the effects of vitamin contents on oxygen changes (semi-infinite system, no HDPE). . .	94
4.12	Preliminary zero order chemical reaction for degradation of vitamin C in apple juice. Shaker water bath system at 25°C. . . . .	96
4.13	Linear plot representing a first order rate equation for degradation of vitamin C (0.341 mM) in water. . . . .	100
4.14	Linear plot representing a zero order rate equation for degradation of vitamin C (11.35 mM) in water. . . . .	101
4.15	Effect of vitamin C content on the resistance to oxygen absorption in apple juice (Cylindrical permeable (HDPE) package). . . . .	110
4.16	Effect of vitamin C content on the resistance to oxygen absorption in water packaged in a cylindrical permeable (HDPE) container. . . .	112
4.17	Semi-infinite liquid system: (A) Physical representation (B) Finite Element model. . . . .	115
4.18	Finite Element model for a cylindrical permeable cell. Representation of a cylindrical (slice) section. . . . .	120
4.19	Predicted dissolved oxygen in water packaged in a cylindrical permeable (Alethan) container. Analytical and Finite Element estimates. . . . .	125
4.20	Predicted (FE) and experimental oxygen levels in a semi-infinite water system. One dimensional diffusion. . . . .	127
4.21	Predicted (FE, Segerlind, 1984) and experimental dissolved oxygen in a 0.5 cm layer of water at 25°C. One dimensional diffusion. . . .	128
4.22	Predicted (FE) and experimental oxygen levels in a semi-infinite apple juice system. One dimensional diffusion. . . . .	129
4.23	Predicted (FE) and experimental oxygen levels in water packaged in a cylindrical permeable (Alethan) container. . . . .	130

4.24	Predicted (FE) and experimental oxygen levels in a semi-infinite water system reacting with vitamin C (0.341 mM). . . . .	133
4.25	Predicted (FE) and experimental oxygen levels in water (HDPE) with simultaneous diffusion and reaction (0.341 mM vitamin C). . . .	134
4.26	Predicted (FE) and experimental oxygen levels in apple juice (HDPE) with simultaneous diffusion and reaction (1.303 mM vitamin C). . . .	135
4.27	Oxygen profile in a semi-infinite water system with simultaneous diffusion and reaction with vitamin C (0.341 mM). . . . .	137
4.28	Unsteady state oxygen diffusion and reaction in a semi-infinite water system (0.341 mM vitamin C). . . . .	138
4.29	Oxygen levels as a function of time and location in a cylindrical HDPE water system reacting with vitamin C (0.341 mM). . . . .	140
4.30	Unsteady state oxygen diffusion and reaction in a cylindrical HDPE water system (0.341 mM vitamin C). . . . .	142
4.31	Oxygen as a function of time and location in a cylindrical HDPE apple juice system reacting with vitamin C (1.303 mM). . . . .	143
4.32	Unsteady state oxygen diffusion and reaction in a cylindrical HDPE apple juice system (1.303 mM vitamin C). . . . .	144
4.33	Predicted (FE) oxygen levels in a liquid food, with and without a zero order reaction (HDPE cylindrical container). . . . .	146
4.34	Unsteady state oxygen diffusion with and without reaction in a liquid food system (HDPE cylindrical container). . . . .	147

## I. INTRODUCTION

The presence of dissolved oxygen in food products has a deteriorative effect on the quality of foods. This may be reflected in color changes in beer and wine, nutritional changes in fruit juices and drinks due to loss of vitamin C, and many other comparable changes.

The oxygen necessary for changes in color, nutritional value or flavor may be found in the head space of a container and dissolved in the liquid food. Oxygen may be also permeating through the package. In order to minimize these negative effects, the food industry is using packaging materials with low permeability to oxygen, deaeration operations, or inert gas packaging among others (Quast and Karel, 1971).

It has been shown that deaeration of apple juice provides only slight improvements in taste and appearance, as compared to non deaerated juice. However, disagreement exists in the food industry regarding the use of deaeration operations in the manufacture of apple juice.

Recent advances in packaging technology has created not only numerous ways to design polymer food packages, but also new problems such as punctured film, loss of seal integrity, thermal instability, lack of film uniformity, migration of toxic substances, and permeating oxygen through the package (Saddler, 1984). Such problems must be taken into consideration in package design, processing and shelf life determinations.

Quality prediction models are desirable due to time and cost savings; however, if many parameters are involved, and the physical system is complex, these models are difficult to develop. Complicated simulation models generally use computers and numerical techniques such as finite differences and finite element methods in order to obtain good approximation values of a desired quality related parameter.

Fruit juices and drinks, contained in permeable packages, represent a complex system due to the simultaneous oxygen diffusion and degradation of vitamin C. Oxygen uptake is affected by the degradation reaction and the permeable membrane of a package.

The goal of this study is to implement a finite element computer model capable of simulating the simultaneous oxygen diffusion and reaction of vitamin C in water and apple juice packaged in a cylindrical permeable cell.

..

The specific objectives were:

1. To develop appropriate physical systems and methods to determine necessary input model parameters.
2. To determine the oxygen diffusion coefficient in apple juice and water.
3. To determine the oxygen permeability constant in high and low density polyethylene packaging materials.
4. To determine the kinetic rate constants for degradation of vitamin C in apple juice and water added with vitamin C.
5. To implement finite element computer models to simulate the simultaneous oxygen diffusion and reaction in apple juice and water packaged in a cylindrical permeable cell.

..



## II. LITERATURE REVIEW

### 2.1. Computer simulation of food quality

#### 2.1.1. The Finite Element and other computer models

Quality in foods may be defined in different terms, including: texture, color flavor, aroma, and nutritional content; each of these terms has a certain degree of importance depending on the main use of that particular food.

The complexity of defining food quality may be demonstrated by reviewing the different descriptions which may be used to represent a single quality characteristic. As an example, texture which may be defined in terms of brittleness, hardness, and adhesiveness (Barron, 1981).

Nutritional value may be expressed in terms of vitamin content, essential amino acids, fatty acids, and minerals. Other quality factors such as color, flavor and aroma have their own terminology (Fennema, 1976).

This complexity of terminology is further influenced by the physical state of the food (liquid or solid), and is what makes food quality very difficult to predict or simulate. In order to make more accurate predictions, the quality parameter of interest must be singled out.

All of the methods used for prediction or simulation of food quality can be included in three categories: numerical, analytical and empirical. The analytical and numerical methods are preferred due to the more fundamental (scientific) concepts involved and their wider applications (Heldman, 1978).

Numerical procedures such as the finite element and finite differences methods, represent excellent alternatives to predict quality changes in foods, whenever the analytical approach can not be applied to a particular problem regarding the simulation of food quality.

The finite element is of particular importance, due to its wider applicability as compared to finite differences (Chapra and Canale, 1988).

The finite element method has been applied to heat conduction and mass transfer problems since it was first proposed in 1965 (Zienckiewicz and Cheng, 1965).

However, little work has been done regarding its application to mass transfer problems in food liquids undergoing a chemical degradative reaction, with surface situations (boundary conditions) involving oxygen permeable barriers.

De Baerdemaeker et al. (1977) illustrated the application of the finite element method to heat transfer in foods. Several hypothetical cases were modeled, including cooked foods packaged in cylindrical cans, the cooling of a pear, cooking of a chicken leg, and pan frying of a steak.

A single computer program was developed which was applicable to a wide variety of food shapes, thermal properties, and surface conditions. No experimental work was performed to verify the computer model.

Purwadaria (1980) developed a finite element computer program to predict food freezing rates of anomalous food shapes.

Variable surface heat transfer resistance (heat transfer coefficient) situations were incorporated into the computer model. Experimental tests were conducted to verify the model. Good predictions were obtained for ground beef molded into elliptical and trapezoidal shapes.

Hayakawa et al. (1983) reported an application of a finite element computer program to predict temperature histories during a freezing process in cylindrically shaped cellulose and rectangularly trimmed lean beef meat. Heat loss was assumed to occur by convection and radiation at the surface of the cellulose and beef.

Other finite element computer programs have been developed to predicting moisture transfer in different solid products:

Zhang et al. (1984) simulated moisture diffusion in rice during a soaking process. His two dimensional finite element included a concentration dependent moisture diffusivity, and change of size of the rice kernel.

Lomauro and Bakshi (1985) obtained acceptable predictions of moisture for selected foods including raisins. It was observed that the actual elliptical shape of raisins, as compared to the cylindrical model, was in part responsible for significant prediction deviations. In two other foods, predictions were improved by using a variable diffusion coefficient as compared to its constant value.

Hongh et al. (1986) also obtained good predictions of moisture histories in raisins and peanuts (finite cylinders), banana chips (semi infinite slab), and slivered almonds (infinite slab). None of the above cited works include in the finite element model, the use of a heat generation rate factor, nor a permeable surface.

Probably, the most unified approach is represented by the work of Comini et al. (1974). Their computer model was directed to solve, at least in theory, heat conduction problems in one, two and three dimensions. The model accounted also for the simultaneous temperature dependence of thermal conductivity, heat capacity, rate of internal heat generation, and surface heat transfer coefficients.

No experimental work was carried out; only illustrative examples were demonstrated. Good agreement was shown between finite element predictions and the analytical solution for the following cases:

Freezing of an infinite slab of liquid

Freezing of a corner region in a liquid with  
radiation surfaces, and

Ground freezing.

Successful simulation of food quality, using procedures other than the finite element method are reported in the literature.

Singh (1974) developed a finite differences computer program to predict degradation of vitamin C in an infant liquid formula packaged in glass bottles.

Lee and Heldman (1977) developed a computer model based on empirical equations experimentally obtained regarding the destruction of vitamin C in tomato juice as a function of temperature, pH and copper concentration.

Sadler (1984) utilized the analytical solution to the diffusion equation for a semi infinite medium with constant surface concentration to predict vitamin C degradation in orange juice and lycopene changes in tomato juice.

A weighted oxygen diffusion coefficient for the liquid food had to be determined in order to take into account the oxygen diffusion resistance at the polymer membrane.

Sadler was able to use the analytical solution without actually employing the variable permeable surface information in direct form. The solution included the simultaneous oxygen diffusion and a first order chemical reaction.

**A**t this point, it can be concluded that much work remains to **b**e done in the area of computer simulation of oxygen diffusion in foods in conjunction with chemical reactions during storage.

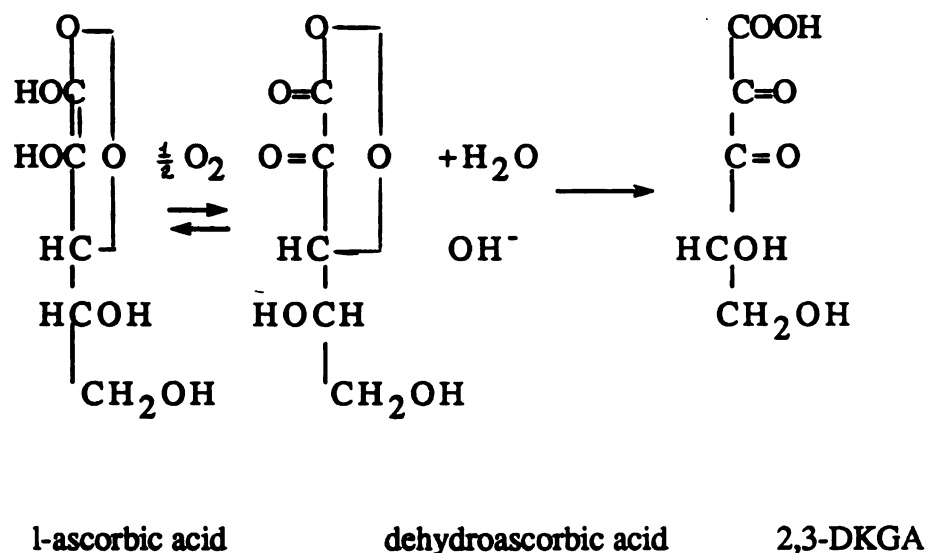
## **2.2. Oxidation of vitamin C**

Vitamin C (Ascorbic Acid) is a highly water soluble hexose derivative (1 gram in approximately 3 ml) (Hay et al., 1967), which has strong reducing properties, due to its enediol structure (conjugated with the carbonyl group in a lactone ring).

Many factors are important in the degradation of vitamin C, including temperature, salt and sugar concentrations, pH, oxygen, enzyme, metal catalysts, amino acids, etc. (Fennema, 1976).

The most important component of the ascorbic acid degradative reaction is the reversible formation of dehydroascorbic acid which is further oxidized to 2,3-diketogulonic acid (DKGA). This causes its loss of the vitamin activity, therefore, its nutritional value.

The oxidation steps can be summarized as follows:



Subsequent oxidation of DKGA produces brown pigments, typically associated with vitamin C loss in fruit products.

The degradation of vitamin C has been studied by many researchers, who have subjected the vitamin C to several different reacting conditions, including aerobic and anaerobic media.

Singh (1974) reported a second order rate constant for the oxidation of vitamin C in a liquid infant formula. Three main factors were taken into consideration:

- low and high concentrations of initial dissolved oxygen
- low and high concentrations of vitamin C and
- light intensity



A first order reaction was observed when dissolved oxygen was abundant.

Eison-Perchonok (1982) reported a second order reaction, first order with respect to vitamin C and oxygen respectively. In her experiment, oxygen was replenished continuously through an increased gas flow to the vitamin C solution in order to maintain constant dissolved oxygen.

Robertson and Samaniego (1986) studied the effect of initial dissolved oxygen levels on the degradation of vitamin C, and browning of lemon juice at 36°C under dark conditions.

They observed a rapid disappearance of oxygen in the juice samples, reaching a low constant level after three days (0.12 - 0.15 mg/L).

Degradation of vitamin C reached a relatively low constant value of 50% after 28 days. The reported first order rate constants were: 1.67, 1.65, and  $1.8 \times 10^{-6} \text{ day}^{-1}$  for juice samples with initial dissolved oxygen levels of 0.41, 1.44, and 3.74 mg/L respectively.

They also reported a second order rate constant of

$2.58 \times 10^{-4} / \%$ -day for the same experiments. The second order rate constant was proportional to the square of the vitamin C concentration, and it had a better fit than the first order values.

They concluded that anaerobic degradation was the major mode of vitamin C destruction, since after seven days, all three juice samples showed relatively low levels of dissolved oxygen.

Evidences of the anaerobic degradation was the unaffected (by oxygen levels) presence of furfural in the reacted lemon juice. In the presence of oxygen, vitamin C degrades aerobically to furfural as well as hydroxyfurfural.

Huelin (1953) reported a first order reaction for the anaerobic decomposition of vitamin C in solutions of citrate-phosphate buffer with a vitamin C concentration of 0.01M, at different pH levels and temperatures (30<sup>0</sup>, 40<sup>0</sup>, and 100<sup>0</sup>C).

The rate constant values under optimum conditions of 30<sup>0</sup>C, pH 3 and 4 were 0.8 and  $8.97 \times 10^{-7} \text{ min}^{-1}$  respectively. Huelin also studied the effect of added fructose and sucrose, and demonstrated that a 0.5M addition of each sugar, in separate experiments, accelerated the reaction, as indicated by the decrease in time necessary for half of the vitamin C to be destroyed from 70 weeks (no sugar added) to 57 and 58 weeks for solutions containing fructose and sucrose respectively.

**D**egradation of vitamin C at 90°C and 100°C canned orange juice, tomato juice, apricots, and spinach, followed a first order reaction (Branner et al. 1948).

A summary review of studies reporting on the oxidation of vitamin C, from 1939 to 1977 was presented by Davidson and Grieger-Block (1977). They mentioned that previous studies of copper-ion catalyzed ascorbic acid autoxidation have indicated zero order, first order, or Michaelis-Menten dependence of rate on ascorbic acid or copper concentrations, and first or half order dependence on oxygen concentration.

In their experimental work, the dissolved oxygen was monitored in a system with no gas-liquid interface, thus eliminating the coupling of oxygen transfer and reaction.

The experiment consisted of a closed vessel completely filled with ascorbic acid solution. A biological oxygen demand probe and oxygen meter were used to monitor the reaction.

Catalyst was injected into the system containing high concentrations of ascorbic acid used to keep the amount of these species approximately constant during a run.

Measurements of oxygen concentration as a function of time provided estimates of initial reaction rates and forms of rate expressions. Plots of  $[O_2]^{1/2}$  vs time were linear, implying a half order dependence (of the rate) on oxygen, which indicates that the reaction occurs by a chain mechanism (Jameson and Blackburn, 1976).

Russel et al. (1943) performed experiments which showed that the autoxidation of vitamin C occurs very slowly in solutions at pH below 8.0 in the absence of copper; however, the rate of the reaction increased as the pH increased above pH 8.0 until reaching a maxima in highly alkaline solutions.

When copper was present, the reaction took place readily in both acid and alkaline solutions; minimum rates occurred between pH 8.0 and 10.0; maximum rates between pH 6.0 and 8.0. Russel also observed that the volume of oxygen absorbed in the presence of one part of copper per ten million parts of solution, varied from 0.5 moles in highly acid solutions, to approximately one mole in highly alkaline solutions.

Increasing the concentration of copper decreased the volume of oxygen absorbed. They demonstrated that the extent of vitamin C oxidation, at various times, has been determined by following the change in the concentrations of vitamin C in a specific solution.

Most of the studies cited utilize a batch reactor, which is simply a container which holds the reacting species in order to determine the characteristic rate equation.

The oxidation of vitamin C is not yet totally understood, being highly variable due to the many parameters influencing the reaction.

**R**ate equations may be obtained through theoretical considerations, or simply by empirical curve fitting procedures. There are two methods used to analyze the kinetic data: the integral and the differential methods.

In the integral method of analysis, a rate equation is estimated, and after appropriate integrations and mathematical manipulations, a plot of certain concentration function versus time should yield a straight line. The rate equation is then said to satisfactorily fit the data.

In the differential method, the rate expression is tested to fit the data directly, without integration.

The integral method can only test a particular mechanism or rate form, while the differential method can be used to develop or build a rate equation to fit the data (Levenspiel, 1976).

## **2.3. Oxygen permeability of polymeric plastic materials**

Permeation of gases and vapor in polymeric food packaging materials is of great importance due to its direct effect on the preservation of foods, especially when the permeating gas is oxygen.

Brown (1981) described several methods used to determine permeability coefficients of polymers. In the manometric method, the quantity of gas which permeates through a test piece at a given time, or a change in volume and pressure is measured.

A transmission cell is used, with the test piece forming a dividing barrier between two chambers in the cell. A constant high pressure (one atm) is maintained in one chamber, and a low pressure (vacuum) is initially established in the other chamber.

In the constant pressure method, the pressure is kept constant in the low pressure chamber, and the volumetric change in permeating gas is measured.

**In** the quasi isostatic method (carrier gas technique), a gas **is** allowed to flow across each side of the test piece at equal pressure. Basically, the test gas flows at a constant rate through one chamber, and a second gas, the carrier, flows through the other chamber at a constant rate. The test gas permeating the polymer is swept away to a detector. A strip chart records the changes of oxygen in terms of millivolts, to be used to calculate properties such as permeability constant.

#### **2.4. Oxygen diffusivity in aqueous solutions**

Oxygen diffusion coefficients are key parameters necessary to determine oxygen absorption by liquid foods, and are essential whenever mathematical modeling is desired. Their magnitude is important since it may significantly differ from one food to another, and it may be quite different in value when compared to non-gaseous components participating in an oxidation reaction, such as the destruction of vitamin C.

There are two basic procedures to measure gaseous diffusion coefficients in liquids (Goldstick and Fatt, 1970):

The steady state (liquid jet and diaphragm cell), and

The unsteady state (diffusion into non-moving liquid).

A major disadvantage of steady state methods is that they yield only the product of the diffusion coefficient and the solubility of the gas, not the coefficient alone. Additional uncertainty to the method is that often, the utilized devices need to be calibrated with a material of known coefficient.

A great advantage of unsteady state methods is that the rate of absorption (of oxygen) by a still layer of liquid yields an absolute value of the diffusion coefficient (Crank, 1956). Gas solubility data is not required to analyze gas concentrations as a function of time.

Several types of oxygen electrodes (Fatt, 1976) can be utilized to record the oxygen partial pressure in the liquid. The authors used a polarographic oxygen sensor to determine oxygen diffusivities at 25°C in pure water, saline solutions, serum albumen, and hemoglobin.

The respective values were: 2.13, 2.07, 1.8, and  $0.76 \times 10^{-5}$  cm<sup>2</sup>/sec. The experimental data suggested that the coefficients decrease slowly with increasing solute concentrations.

Sadler (1984) used the same general method, slightly modified as Goldstick and Fatt (1970), obtaining an oxygen diffusivity of  $1.65 \times 10^{-5}$  cm<sup>2</sup>/sec for orange juice, and  $1.71 \times 10^{-5}$  cm<sup>2</sup>/sec for tomato juice.



Hayduk and Laudie (1974) demonstrated that diffusivity coefficients of liquids, gases, and solids, dissolved in water, can be predicted by any of three mathematical correlations, with an average error of 9.5%. The Wilkes and Chang correlation is the most widely used, due to its smallest prediction error.

## 2.5. Oxygen absorption and chemical reaction in aqueous solutions and liquid foods

Literature citations of oxygen absorption and diffusion, coupled with a chemical reaction is very limited in liquid foods. The most recent work found is the study reported by Sadler (1984). He treated the coupled phenomena as a semi infinite medium in which simultaneous oxygen absorption, diffusion and a first order chemical reaction between dissolved oxygen and vitamin C took place.

Oxygen diffusion in the packaging plastic membrane and in the liquid foods were compacted in a single weighted diffusion coefficient. He used this approximated coefficient to predict oxygen concentrations in the foods.

Luh and Sharpe (1982) investigated the degradation of vitamin C and color changes in tomato pastes, packaged in plastic pouches in laminate form. In their study, they did not feel that the laminates (polyethylene-mylar and polyethylene-saran-mylar) were good oxygen barriers, since significant loss of vitamin C was observed during the storage temperature experiments. Their analysis did not include the coupled diffusion-reaction problem.

Singh (1974) developed a computer model, based on finite differences, to simulate successfully the oxygen and vitamin C diffusion in an infant liquid formula packaged in glass bottles. Earlier studies in the chemical engineering area present a more detailed mathematical analysis of simultaneous diffusion and reaction in simple solution. Most of the work has been done on a theoretical basis, and much research is needed on the application of the developed theory to the food engineering problem.

Standard diffusion equations (Crank, 1956) without chemical reaction for spheres, cylinders, parallelepipeds, and semi infinite geometries were the basis to develop corresponding equations including a first order chemical reaction rate (Danckwerts, 1951).

These latter, developed equations were mathematically solved to predict concentrations and absorption (oxygen) rates for each geometrical reacting system.

Van de Vusse (1961) dealt with the mathematical analysis of zero order reactions coupled with gas transfer. His theoretical work was due to the fact that most oxidation reactions of liquid hydrocarbons by oxygen belong to the zero order type. The resulting mathematical solution to the diffusion equation expresses the concentration of the gas (oxygen) and the non-gaseous reacting component as a function of time and location.

The diffusion and reaction equations were also solved for a semi infinite system by Brian (1964). His proposed general kinetic order "n" was assigned to the gas (oxygen) and order "m" was assigned to the non-gaseous component. Orders "n" and "m" include zero and first order chemical reactions.

His mathematical treatment of the diffusion equations illustrates the effect of the form of the chemical reaction kinetic equation upon the gas absorption rate. It also demonstrates its usefulness for determining reaction kinetics from absorption rate measurements (Gilliland, 1958).

He concluded that any chemical reaction which appears to have a reaction order less than unity must undoubtedly change over at a very low concentrations to a reaction order greater than or equal to unity.

Hikita and Asai (1964) derived approximate solution equations (semi infinite system) for gas absorption, coupled with an irreversible reaction of order  $m$  with respect to the dissolving gas, and by an irreversible reaction of order  $n$  with respect to a reactant solute. The proposed equations were applicable to a reaction of any order, integer or fraction, and to any system whose reaction velocity is a power function of the concentrations of the reactants.

It is evident that the computer modeling of liquid food system where oxygen diffusion and chemical reaction are coupled remains practically unexplored, at least in the food science and food engineering areas.

### III. MATERIALS AND METHODS

#### 3.1. The Finite Element Method

##### 3.1.1. Description of the Finite Element Method: One dimension

The following description of the Finite Element (FE) Method (FEM) was derived from the work of Segerlind (1984). The solution to the partial differential equation (DE) in one dimension, was obtained from one of his computer programs, slightly modified to better suit the physical problem in this study. Another FE computer program was used to solve the partial DE's in two dimensions (cylindrical coordinates); its description will be presented later in this chapter.

The method has two main characteristics, different from any other numerical method:

1. The FE method utilizes an integral formulation to generate a system of algebraic equations.
2. The solution is found by approximating the unknown quantities through the use of continuous piecewise smooth equations described in detail in the method (Segerlind, 1984).

The general procedure to determine the FE solution of the time-dependent one dimensional equation (3.1) is to evaluate the Galerkin residual integral with respect to the space coordinates for a fixed instant of time. This yields a system of DE's that can be solved to obtain the variation of the quantity  $p$  with time  $t$ .

$$D\partial^2 p/\partial x^2 + k_{v,0} = \lambda \partial p/\partial t \quad (3.1)$$

Where:

$D$  = Oxygen diffusion coefficient in the system (liquid)

$p$  = Oxygen partial pressure in the system

$x$  = Space coordinate

$t$  = Time

$k_{v,0}$  = Constant

$\lambda$  = Constant

Rearranging Equation (3.1) into

$$D\partial^2 p/\partial x^2 + k_{v,0} - \lambda \partial p/\partial t = 0 \quad (3.2)$$

The residual integral is:

$$\{R^{(e)}\} = \int_{-X_i}^{X_j} [W]^T D\partial^2 p/\partial x^2 + k_{v,0} - \lambda \partial p/\partial t dx \quad (3.3)$$

Where:

$[W]^T$  contains the Galerkin weighing functions.

Equation (3.3) can be expressed as

$$\{R^{(e)}\} = \{R_D^{(e)}\} + \{R_\lambda^{(e)}\} \quad (3.4)$$

Segerlind (1984) describes in detail the evaluation of the residuals  $\{R^{(e)}\}$ 's.

Numerical oscillations consist of the deviated predictions below or above the correct solution value at every time step during the solution process of the FE method.

The best way to avoid numerical oscillations when using the FE method, is the lumped formulation, satisfying the time step requirement

$$\Delta t < \lambda L^2 / 4D(1 - \theta) \quad (3.5)$$

Where:

$\theta$  = Ratio of time step . (= 2/3 for the Galerkin method)

$L$  = Element length

The derivative boundary conditions for the one dimensional problem in this study were of the following types:

I. The oxygen partial pressure  $p$  is known over the top surface of the liquid, corresponding to the equilibrium saturation condition of the dissolved oxygen concentration (0.21 atm).

II. The other boundary condition involving permeability (or convective) constants is of the type

$$D\partial p/\partial x = -Mp_b + S \quad (3.6)$$

Where:

$p_b$  = Unknown value of  $p$  at the boundary.

$M$  = Constant

$S$  = Constant.

$M$  and  $S$  are related to the geometry of the system, and to the permeating or convecting properties of the boundary.

When  $M = S = 0$ ; Equation 3.6 reduces to:

$$D\partial p/\partial x = 0 \quad (3.7)$$

and

$$\partial p/\partial x = 0 \quad (3.8)$$

This situation occurs on an insulated or impermeable boundary or on axes of symmetry.



The derivative boundary conditions (3.6), different than zero, are included in the FE analysis through the use of an interelement vector  $\{I^{(e)}\}$  described by Segerlind (1984).

### 3.1.2. Description of the Finite Element Method in two and three dimensions, with derivative boundary conditions.

The diffusion of oxygen through the polyethylene (PE) membranes in a cylindrical container occurs in the radial direction, and requires the use of cylindrical coordinates. This system can be numerically analyzed as an isoparametric solid, with three dimensional capabilities, as long as the liquid inside is not moving.

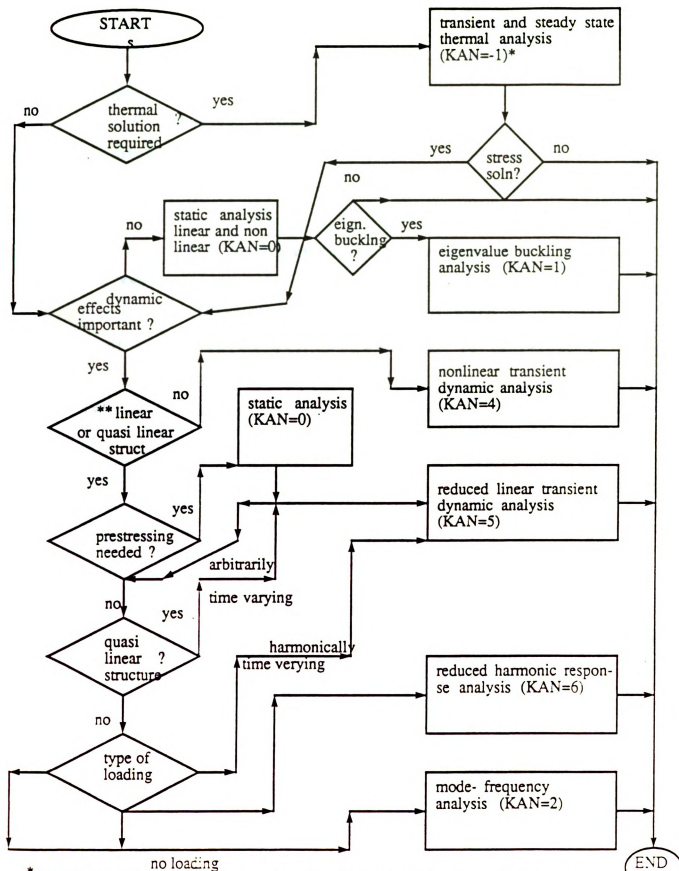
Simulation of oxygen diffusion in water and apple juice, and its absorption through the PE membranes of a cylindrical container was accomplished by the FE computer program developed by Swanson Analysis Systems Inc. (SASI) (ANSYS, 1983) and available at the Case Center, Michigan State University.

The following description of the ANSYS FE computer program was derived from manuals or seminar notes from SASI (ANSYS, 1982, 1983, 1988).

Figure 3.1 presents a summary of all the options available to the user with the ANSYS FE computer program. The total analysis of a particular system may require partial analysis, such as thermal or static. In this study, thermal analysis was the only option being utilized, due to its similarity to mass transfer, to simulate the oxygen diffusion process with or without accompanying chemical reaction.

A description of the fundamental concepts of the ANSYS FE formulation for heat transfer with boundary conditions can be found in the heat transfer notes published by SASI (ANSYS, 1988). The analysis of a physical problem by the ANSYS program depends on many factors, including the composition of the material, its physical properties, its geometrical shape, its physical state: liquid, solid, or gas, its equilibrium conditions, flowing or stagnant conditions etc.

Therefore, in order to accomplish the correct analysis, the program contains a series of commands to guide the user to the proper input sequence of parameters needed for the numerical solution.



\* KAN is the key input on the KAN command to select the analysis type. QUASI LINEAR- the structure is linear except for gaps.

FIGURE 3.1. SUMMARY OF ANSYS ANALYSIS TYPES (ANSYS 1983)

The user must be able to provide the right information such as the analysis desired (thermal), the best element to represent the physical system (linear, triangular, etc.), the proper location of the boundary conditions, a consistent set of units for length, force, time, temperature (or pressure) etc.

In this study, two elements were used to represent the liquid system packaged in a cylindrical permeable cell. The elements were identified as STIF 70 and STIF 71. Another element identified as STIF 33 was used to represent a liquid (semi-infinite system) contained in a long graduated glass cylinder. These systems will be described later in this chapter.

STIF 70 represents an isoparametric thermal solid element that has three dimensional thermal conduction capability, with eight nodal points, and the possibility to apply an average internal heat generation rate to the element.

Due to its similarity to mass transfer, the temperature and the average generation rate are equivalent to partial pressures (or concentrations) and a zero order kinetic rate constant respectively.

This means that proper dimensional units must be provided by the user as input for the computer program in order to perform the correct solution with the FE model.

The element geometry, coordinate system, nodal point locations, and face element numbers for the isoparametric element are shown in Figure 3.2.

The element must have other than a zero volume, and it may be numbered as shown or it may have the planes IJKL and MNOP interchanged. A prism tetrahedron shaped element may be formed by defining duplicate node numbers.

Free surfaces of the element that are not subject to boundary constraints are assumed to be adiabatic. A summary of the parameters for the thermal solid element is shown in Table 3.1.

The temperature (partial pressure) distribution for this element is obtained from the numerical solution to Equation (3.9)

$$\rho C_p \frac{\partial T}{\partial t} = (\frac{\partial}{\partial x})(k_x \frac{\partial T}{\partial x}) + (\frac{\partial}{\partial y})(k_y \frac{\partial T}{\partial y}) + (\frac{\partial}{\partial z})(k_z \frac{\partial T}{\partial z}) + q \quad (3.9)$$

Where:

- $\rho$  = Density
- $C_p$  = Specific heat
- $k$  = Thermal conductivity
- $q$  = Internal heat generation rate

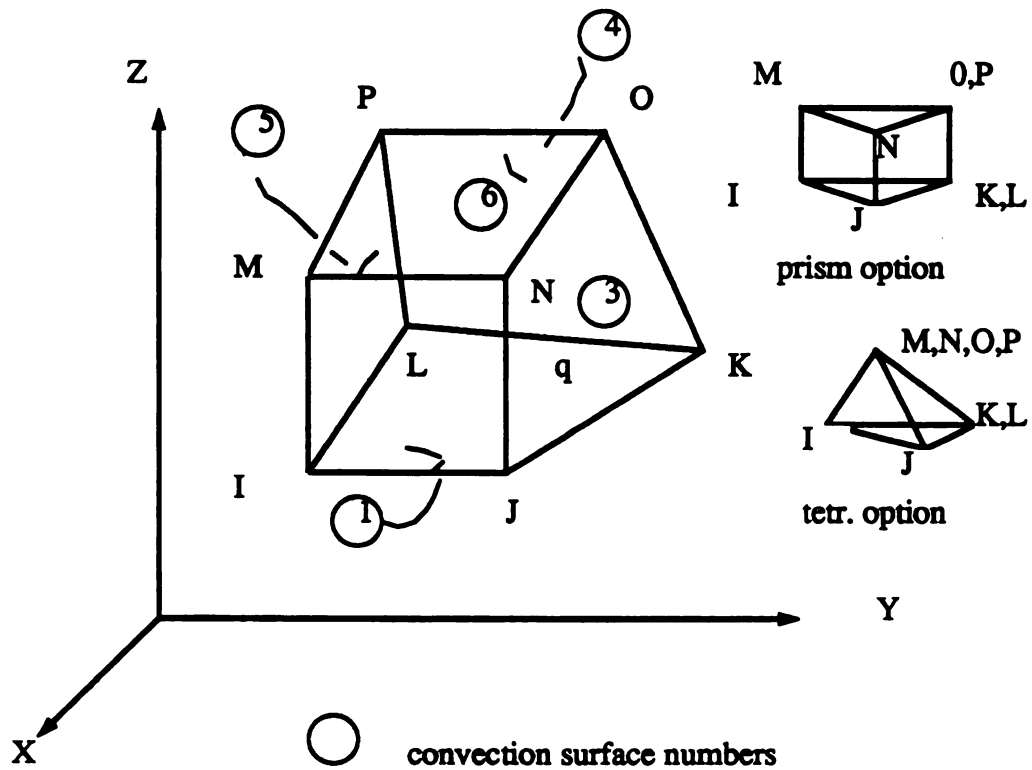


FIGURE 3.2. THREE DIMENSIONAL THERMAL SOLID REPRESENTING THE GEOMETRY, NODAL LOCATIONS, AND FACES OF THE FINITE ELEMENT STIF 70. (ANSYS,1983).

The solution printout is obtained in two forms:

1. The node temperatures are included in the overall nodal temperature solution printout , and
2. The element printout as shown in Table 3.2.

**Table 3.1. Summary of computer programming parameters for the three dimensional isoparametric thermal solid representing the finite element: STIF 70 (ANSYS, 1987).**

ELEMENT NAME	STIF 70
NO. OF NODES	8 I,J,K,L,M,N,O,P .
DEGREES OF FREEDOM PER	
NODE	1 TEMP
MATERIAL PROPERTIES	5 KXX,KYY,KZZ (GLOBAL), DENS, C
CONVECTION FACES	6 IJKL, IJNM, JKON, KLPO, LIMP, MNOP
HEAT GENERATION RATES	1 AVERAGE

**Table 3.2. Summary of element printout explanations generated from the finite element program involving the three dimensional thermal solid (ANSYS, 1987).**

LABEL	NO. OF CONSTS.	EXPLANATION
LINE 1 (PRINTED ONLY IF CONVECTION OR KEYOPT (5) OR (7)=1)		
EL	1	ELEMENT NUMBER
NODES	8	NODES I, J, K, L, M, N, O, P
MAT	1	MATERIAL NUMBER
VOL	1	VOLUME
LINE 2		
TG (X,Y,Z,SUM)	4	THERMAL GRADIENT COMPONENTS AND VECTOR SUM AT CENTROID
TF (X,Y,Z,SUM)	4	THERMAL FLUX (HEAT FLUX RATE/CROSS SEC. AREA) COMPONENTS AND VECTOR SUM AT CENTROID
LINE 3 (PRINTED ONLY IF CONVECTION)		
FACE	1	CONVECTION FACE NUMBER
NODES	4	NODES AT THIS FACE
AREA	1	CONVECTION FACE AREA
HFILM	1	FILM COEFFICIENT
TAVG,TBULK	2	AVG. FACE TEMP, FLUID BULK TEMP.
LINES 4-8 (SAME AS ABOVE FOR OTHER CONVECTION FACES, IF DEFINED)		



STIF 71 is the name given to the lumped thermal mass element, with variable heat generation. This element may be used in an unsteady-state thermal analysis to represent a body having thermal capacitance capability, but negligible internal thermal resistance, that is, no significant temperature gradients within the body.

The element has the capability to process a temperature dependent heat generation rate ( $q(T)$ ), and it may be applied to one, two or three dimensional analysis.

The lumped thermal mass element, shown in Figure 3.3, is defined by one nodal point and a thermal capacitance (heat/degree). For an axisymmetric analysis, the thermal capacitance should be input on a per radian basis.

A temperature dependent heat generation rate in the form of a polynomial may be input as:

$$q(T) = A_1 + A_2T + A_3T^4 + A_5T^6 \quad (3.10)$$

Where T is the temperature of the previous iteration.

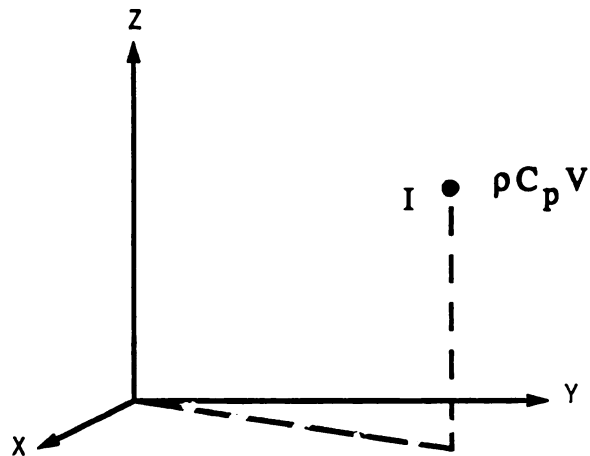


FIGURE 3.3. LUMPED THERMAL MASS (STIF 71) REPRESENTING A POINT FINITE ELEMENT USED IN CONJUNCTION WITH THE THREE DIMENSIONAL THERMAL SOLID (ANSYS, 1983)

A summary of the lumped thermal mass element parameters is given in Table 3.3, and the element printout explanation in Table 3.4. The numerical solution to Equation (3.11) describes the temperature of the element.

$$\rho C_p V \partial T / \partial t = q(T) \quad (3.11)$$

STIF 33 is the name given to a conducting bar element with the ability to conduct heat transfer (or oxygen) between its two nodal points (Figure 4.17). Other parameters defining this element are the cross-sectional area and the material properties: thermal conductivity, density and specific heat. An average heat generation rate may be applied to the element.

The temperature distribution for this element is obtained from the numerical solution of the following equation:

$$\rho C_p \partial T / \partial t = \partial / \partial x (K_x \partial T / \partial x) + q \quad (3.12)$$

All parameters in Equation (3.12) were previously defined.

A non-restrictive data input gives the user more flexibility to inputting data to the ANSYS program than the standard FORTRAN conventions. The ANSYS program also has the capability of creating one, two or three dimensional plots on screen or printout, based on a particular numerical solution, or on a geometrical shape with the desired number of nodes and elements.

**Table 3.3. Summary of computer parameters for the lumped thermal mass finite element (ANSYS, 1987).**

ELEMENT NAME	STIF 71
NO. OF NODES	1 I
DEGREES OF FREEDOM	
PER NODE	1 TEMP
REAL CONSTANTS	7 THERMAL CAPACITANCE ( $\text{RHO} \cdot \text{C} \cdot \text{VOL}$ )
SPECIAL FEATURES	NONLINEAR IF HEAT GEN, IS DEFINED AS A FUNCTION OF TEMPERATURE

**Table 3.4. Summary of element printout explanations generated from the finite element program involving the lumped thermal mass finite element: STIF 71 (ANSYS, 1987).**

LABEL	NO. OF CONSTANTS	EXPLANATION
LINE 1	(PRINTED ONLY IF HEAT RATE IS NONZERO)	
EL	1	ELEMENT NUMBER
NODE	1	NODE I
TEMP	1	ELEMENT (NODE) TEMPERATURE
HEAT RATE	1	HEAT GENERATION RATE INTO NODE

### 3.1.3. The Finite Element Method: Simultaneous oxygen absorption and chemical reaction.

Due to its similarity to heat transfer, the corresponding mass (oxygen) transfer relationships can be developed based on Equations (3.9) through (3.11) by substituting temperature for oxygen partial pressure, thermal conductivity for oxygen diffusivity, and heat generation rate for a reaction rate constant. These substitutions, with proper dimensional units allow the FE model to solve Equations (3.9) through (3.11).

Since the ANSYS FE computer program does not provide with the solution for simultaneous absorption and chemical reaction with a single element type, it was necessary to couple two different elements: STIF 70 and STIF 71 in order to obtain the proper numerical solution, as will be described in the Results and Discussion section.

## 3.2 Micro - Oxygen Electrodes

### 3.2.1. Oxygen partial pressure measurements

The MI-730 oxygen-electrodes (Microelectrodes, Inc.) were used to measure the oxygen partial pressure which would be in equilibrium with the physically dissolved oxygen in water or apple juice. The electrodes have a total length of 6.3 cm with an outer diameter at the tip of 0.3 cm, and a response time of less than 20 seconds. The reference electrode is of the Ag type. The oxygen electrode is contained in an acrylic housing with a teflon membrane incorporated in the housing tip.

The preparation of the electrodes includes the addition of the electrolyte solution (provided by Microelectrodes, Inc.) into the acrylic housing. Caution must be taken to avoid creation of air bubbles that may affect oxygen detection.

The signal output from the oxygen electrode is transmitted to a biological OM-2 oxygen meter (Microelectrodes, Inc.), which has direct read out in atm or percentage of oxygen. The oxygen meter is connected to a data acquisition system (PCLAB, SP0141, V02.00, Data Translation, Inc.), which records the information as volts.

### 3.2.2. Calibration of micro-oxygen electrodes

Calibration of the electrodes is carried out in gas mixtures of oxygen and nitrogen. Calibration was also carried out in water and apple juice in absence of chemical reaction.

The gas phase calibration was obtained, using a gas flow meter to introduce desired gas mixtures of compressed air and nitrogen into a sealed glass bottle (cell) in which the electrode is mounted. Gas Chromatograph (Carle GC Instruments, Inc.) measurements were used to compare with oxygen meter readings.

A stainless steel GC column (80°C) with 60/80 molecular sieve was used for oxygen determinations.

The sensors were calibrated by introducing pure nitrogen and waiting until the meter readings stabilized. At that point the meter was set to read 0 atm (0% oxygen), then maintained at that value for at least 30 minutes.

In the next step air was introduced into the cell, and the oxygen meter was set to read that value constantly for at least 30 minutes. Intermediate points are obtained by introducing desired gas mixtures of air-nitrogen into the cell, and allowing the system to equilibrate. Readings were compared to GC measurements.



The liquid phase calibration was similar, in principle, to the gas phase calibration, since the readings for the sensor in the liquid were set to read the oxygen partial pressure, which would be in equilibrium with the physically dissolved oxygen in the water or apple juice.

The sensor in the liquid phase will read the oxygen partial pressure corresponding to the gas phase. Partial pressures can be converted into dissolved oxygen concentration in the liquid, using Henry's law.

### 3.2.3. Oxygen solubility in water

Since the predicted and experimental values were obtained in terms of oxygen partial pressures, conversion to dissolved oxygen concentrations was necessary.

In this study, Henry's law constant was utilized for the conversion of oxygen partial pressures into dissolved oxygen concentrations in the liquid as follows (Battino and Clever, 1966):

$$p_g = H_1 x_1 \quad (3.13)$$

or

$$p_g = H_2 C_1 \quad (3.14)$$

or

$$C_g = H_c C_1 \quad (3.15)$$

Where:

$p_g$  = Oxygen partial pressure of the gas (mm Hg)

$x_1$  = mol fraction of Oxygen

$C_1$  = Concentration of Oxygen in the liquid phase

$C_g$  = Concentration of Oxygen in the gas phase

$H_1$  = Henry's law constant (mm Hg)

$H_2$  = Henry's law constant

((mmHg)(L of solvent)/mol of gas)

$H_c$  = Henry's law constant (dimensionless)

Determination of Henry's law constants can be obtained through a series of interconversions of the solubility expressions:

$$H_1 = 17.033 \times 10^6 \rho / (\alpha M_s) + 760 \quad (3.16)$$

$$H_2 = 17,033/\alpha = 22,414 \times 760 / (1000\alpha) \quad (3.17)$$

$$H_c = 1/L_c \quad (3.18)$$

Where:

$\alpha$  = Bunsen coefficient (0.02847 at 25 °C, 1 atm)

$\rho$  = Density of the solution

$M_s$  = Molecular weight of the solvent

$L_c$  = Ostwald coefficient (dimensionless)

$T$  = Absolute temperature (°K)

### 3.3. Oxygen Diffusion Cells

#### 3.3.1. Cell for one dimensional Oxygen diffusion.

The one dimensional oxygen diffusion experiments were performed in still water contained in an open glass bottle (Figure 3.4A and 3.4B), 2.3 cm in diameter, with a layer of water of known thickness.

The oxygen partial pressure (p) was monitored using the Oxygen electrode (sensor), with its tip positioned in slight contact with the bottom surface. The placing of the sensor in this position allowed the physical system to be analyzed as a symmetrical mathematical problem.

The sensor was connected to an oxygen meter, and a data acquisition (PCLAB) system was used to store the experimental data as volts. The system was kept at  $25^{\circ}\text{C} \pm 0.2$  in a water bath.

The initial, low levels of dissolved oxygen were achieved by bubbling Nitrogen through the liquid sample, prior to initiation of the experiments. During the diffusion experiments, the top surface of the water remained in direct contact with air (0.21 atm).

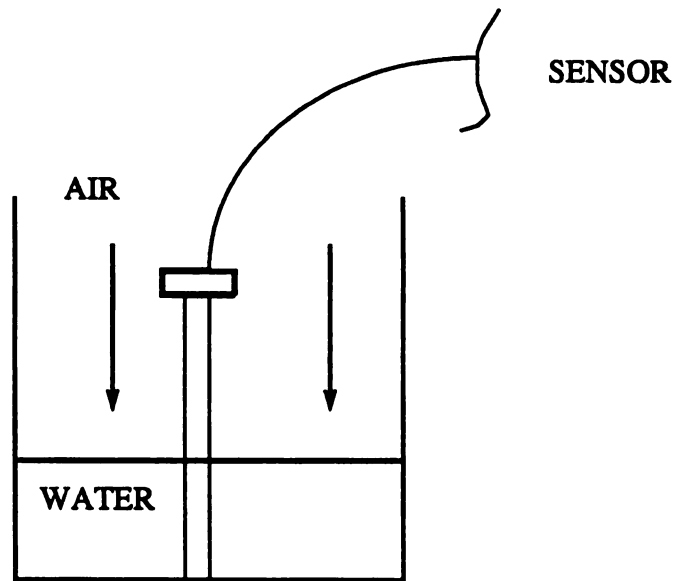


FIGURE 3.4A. ONE-DIMENSIONAL OXYGEN DIFFUSION CELL

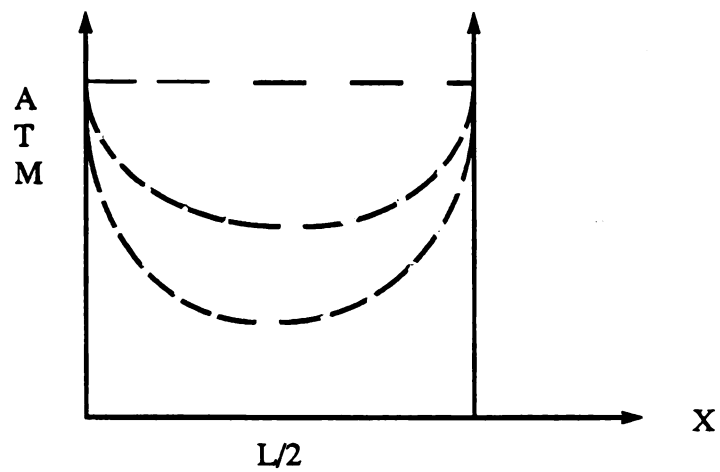


FIGURE 3.4B. SYMMETRICAL DIFFUSION SYSTEM FOR THE ONE DIMENSIONAL OXY-GEN DIFFUSION CELL

The usefulness of this experiment was dual:

1. To determine the Oxygen diffusion coefficient using a mathematical model, and
2. To simulate the one dimensional Oxygen diffusion in non moving water, using the FE computer program (Seegerlind, 1984).

### 3.3.2. Determination of the oxygen diffusion coefficient in liquids.

Two methods were employed to determine the oxygen diffusion coefficient (D) in water :

The first method (two trials) involved the generation of a linear equation derived from the analytical solution to Equation (3.1) (Appendix A).

The diffusion coefficient D was then calculated from the slope of the line as follows:

$$D = (2.303) (\text{slope}) (4)(L^2)/(\pi^2) \quad (3.19)$$

and L is the thickness of the water layer in the glass bottle.

The second method (two trials) uses the analytical solution of the diffusion equation for a semiinfinite system; its development is presented in Appendix B.

The semiinfinite system was created using a long (20 cm) graduated cylinder (100 ml) containing the liquid. The application of the semiinfinite analysis was based on the criterion (Pitts and Sissom,1977):

$$2x\sqrt{4Dt} > 0.5 \quad (3.20)$$

Where  $2x$  is the thickness (or length) of the semiinfinite system (20cm).

The sensor was located 1.5 cm below the top surface of the water or apple juice as shown in Figure 3.5. The experiment was carried out at  $25^{\circ}\text{C} \pm 0.2$  in a controlled atmosphere chamber.

In this case,  $D$  is calculated from the slope of a linear equation, obtained by plotting the absorption rate of oxygen per unit area against the square root of time.

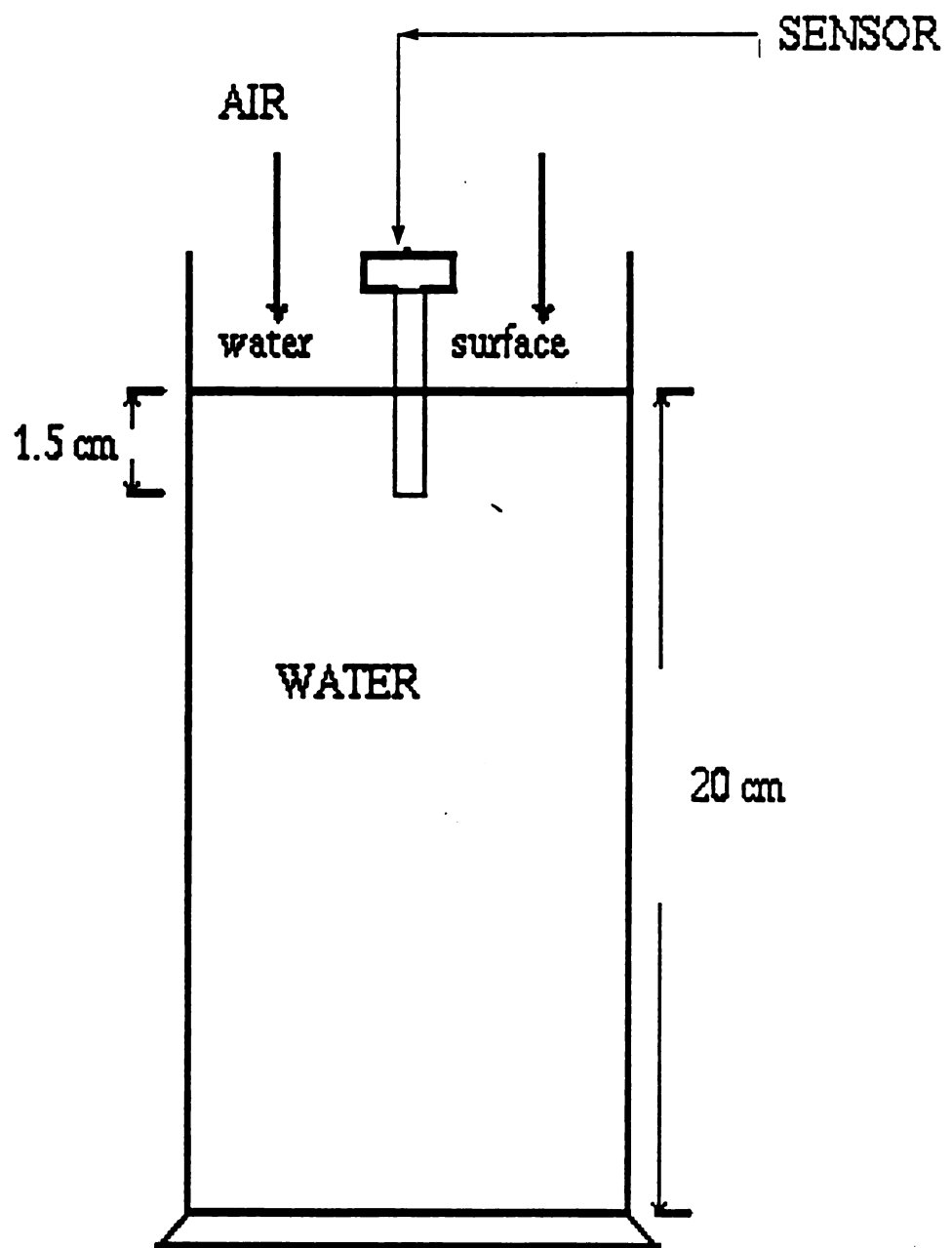


FIGURE 3.5 SEMI-INFINITE OXYGEN DIFFUSION SYSTEM



### 3.3.3. Oxygen permeable cylindrical cells

Two types of oxygen permeable cylindrical cells, using two different PE membranes were made. The top and bottom of the cylinders were made of solid acrylic in order to mount the sensor from the top, and to create the cylindrical shape. The acrylic is impermeable to oxygen (Figure 3.6).

The cylindrical wall of one cell was made of High Density Poly Ethylene (HDPE), the wall of the other cell was made of Alethan (Poly Ethylene). The radius, length, and volume of the cells were determined prior to any experiment. Both PE membranes were provided directly from the manufacturer

PE membrane samples were carefully selected, to avoid imperfections such as holes, cracks etc. The selected portion of the membrane was glued to the edges of the top and bottom surfaces, and allowed to dry before use.

Location of the sensor was 1.37 cm from the radial wall of the Alethan cell (2.425 cm radius), and for the HDPE cell (3.512 cm), the sensor was located at the center.

Water and apple juice were introduced from the top surface through ready to seal valves (feeding and exhausting).

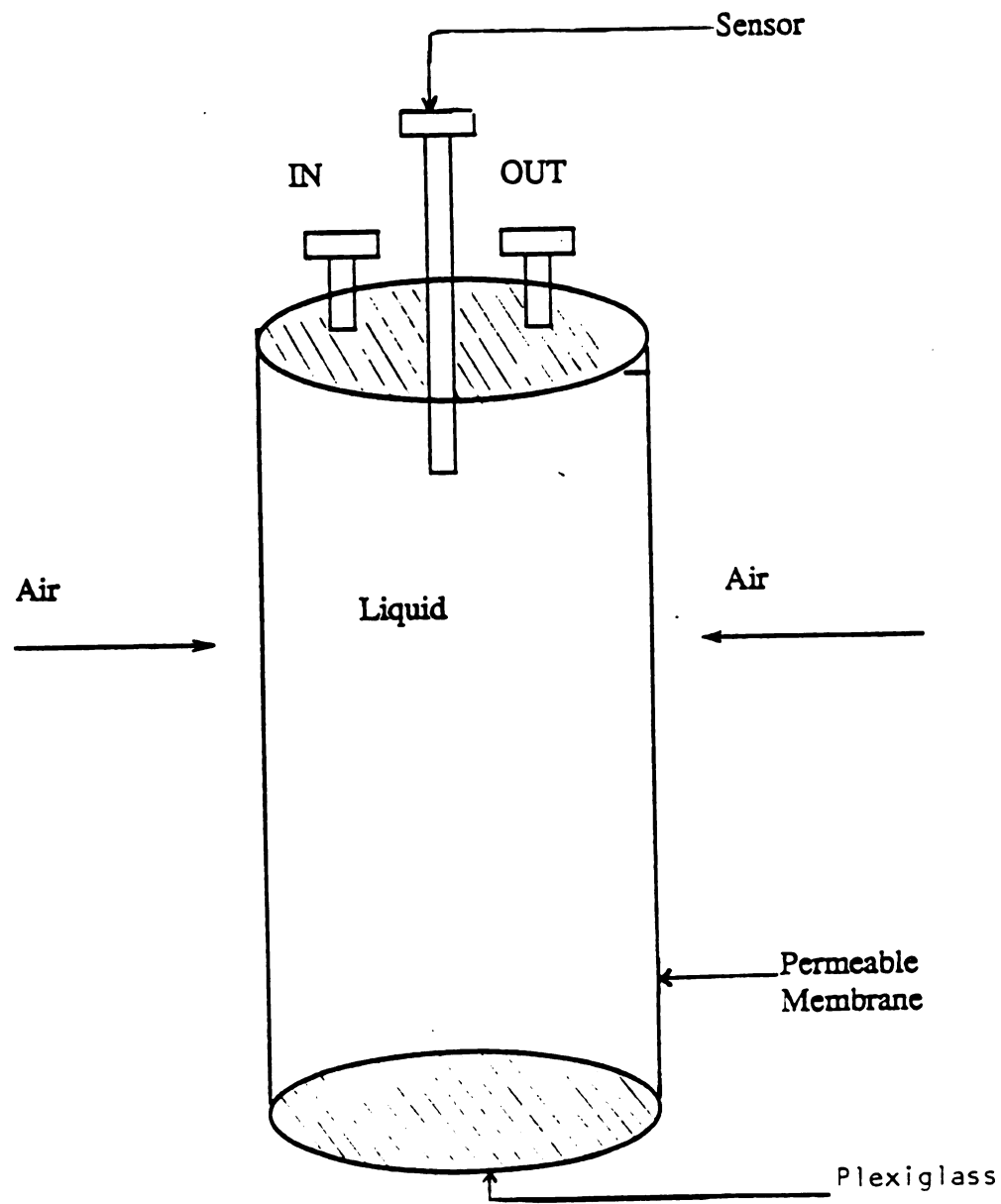


FIGURE 3.6 OXYGEN PERMEABLE CYLINDRICAL CELL

3.3.4. Mathematical model for the radial diffusion of oxygen in non moving water and apple juice.

The following set of equations (Crank, 1975) and the corresponding analytical solution were utilized to develop the analytical model to predict the oxygen partial pressure in the cylindrical cell.

$$\partial C / \partial t = 1/r(\partial / \partial r)(rD\partial C / \partial r) \quad (3.21)$$

$$\text{I.C. } C = C_0, 0 \leq r \leq R, t = 0 \quad (3.22)$$

$$\text{B.C.1 } D\partial C / \partial r = k'(C_b - C^*), r = R, t > 0 \quad (3.23)$$

$$\text{B.C. 2 } D\partial C / \partial r = 0, r = 0, t > 0 \quad (3.24)$$

According to Henry's Law, oxygen concentrations  $C$  in an aqueous solution is proportional to oxygen partial pressures  $p$ , through the oxygen solubility constant  $S$ , such that:

$$C = Sp \quad (3.25)$$

The boundary condition (see also Eq. 3.6) at the liquid surface  $r=R$ , is obtained applying Fick's first law for determination of the net rate of oxygen transfer ( $F$ ) through the packaging film.

$$F = (P_m/\delta)(p_b - p^*) \quad (3.26)$$

This Equation is applied at time intervals during the model simulation.

Substitution of Equation 3.25 into 3.21 through 3.24, and carrying out the necessary operations, one obtains, after cancelling S:

$$\partial p / \partial t = 1/r(\partial / \partial r)(rD\partial p / \partial r) \quad (3.27)$$

$$\text{I.C. } p = p_o, 0 \leq r \leq R, t = 0 \quad (3.28)$$

$$\text{B.C.1 } D\partial p / \partial r = (P_m/\delta)(p_b - p^*), r = R, t > 0 \quad (3.29)$$

$$\text{B.C.2 } D\partial p / \partial r = 0, r = 0, t > 0 \quad (3.30)$$

The corresponding solution is:

$$(p - p_o)/(p^* - p_o) = 1 - \sum_{n=1}^{\infty} \{2LJ_o(r\beta_n/R)\exp(-\beta_n^2 Dt/R^2)\}/(\beta_n^2 + L^2)J_o(\beta_n) \quad (3.31)$$

Where:

$$L = R(P_m/\delta)/D \quad (3.32)$$

S = Oxygen solubility coefficient in liquid

$P_m$  = Oxygen permeability constant

$\delta$  = Film thickness

$k'$  = Mass transfer coefficient

$r$  = Radial distance. 0 at center, R at walls

$p_o$  = Initial oxygen partial pressure

$p^*$  = Equilibrium oxygen partial pressure

$p_b$  = Oxygen partial pressure at surface just within  
cylinder wall

$C_o$  = Initial oxygen concentration

$C^*$  = Equilibrium oxygen concentration

$C_b$  = Oxygen concentration at surface just within  
cylinder wall

$J_0(\beta)$ , and  $J_1(\beta)$  = Bessel functions of the zero and first  
order respectively

$\beta_n$  = Roots of  $J_1(\beta) - LJ_0(\beta) = 0$

### 3.4. Oxygen permeability tester: OX-TRAN 100

#### 3.4.1. Measurement of the permeability constant in Alethan and HDPE.

Measurement (two replicates) of the oxygen permeability constant ( $P_m$ ) of the PE membranes was obtained by the isostatic method (25°C, 85% RH) using the OX-TRAN 100 Oxygen permeability tester, made by modern Controls, Inc. The test procedure, described in Appendix C, was based on the "Standard Methods of Test for Oxygen Gas Transmission Rate Through Plastic Film and Sheet Using a Coulometric Sensor" as proposed by ASTM committee D-20 on plastics (subcommittee D- 20.70 on Analytical Methods).

#### 3.4.2. Measurement of the oxygen diffusion coefficient in HDPE.

The oxygen diffusion coefficient ( $D_m$ ) of permeable membranes is a fundamental physical property, related to  $P_m$  as follows:

$$P_m = S_m \cdot D_m \quad (3.33)$$

Where  $S_m$  is the solubility coefficient of oxygen in the membrane.

The use of  $D_m$  or  $P_m$  should be consistent with the set of units in which other parameters are expressed, such as oxygen partial pressures or dissolved oxygen concentrations.

$D_m$  in HDPE was determined by using the same experimental data as for the  $P_m$  determination (three replicates). The method consists of solving Fick's first and second law of the diffusion equations, with proper boundary conditions, using a Newton-Raphson method (Hernandez, 1984).

For comparative purposes, another recursive method, consisting of an integration procedure of time versus current output was also used (Aiba and Huang, 1969) to determine the diffusion coefficient for HDPE. The value for  $D_m$  is calculated from the following equation:

$$D_m = \delta^2 I_s / (6(I_s t_s - q_s)) \quad (3.34)$$

Where:

$I_s$  = Current output value

$t_s$  = Time to reach the steady state

$q_s$  = Integration value of time vs output  $I_t$

$I_s$  = Current output at time  $t$

### 3.5. Permeability testing cell in the gas phase.

#### 3.5.1. Verification of the HDPE permeability constant.

-

Three are the most important factors to be considered in the design of a permeable cell: the permeability constant, the dimensions, and the integrity of the cell (no leaks).

Therefore a procedure for checking on the accuracy of these factors is necessary. A lumped system analysis is a suitable alternative for this matter.

In this study, the lumped system consisted of the HDPE permeability cell, the sensor located at the center of the top surface, and oxygen passing through the HDPE membrane from the environment.

Oxygen was totally eliminated from the cell before starting the diffusion process, by flushing pure nitrogen into the cell until the sensor reading indicated a zero percentage of oxygen inside the cell. The experiment was performed under controlled conditions of temperature ( $25^{\circ}\text{C}\pm 0.2$ ) and relative humidity (45%) in a controlled atmosphere chamber.



A system is said to be lumped (Meyer, 1974) when the variation, in this case, of the oxygen partial pressure with time is much more important than the variation with position (inside the cell), which may be overlooked; the only mass transfers to be considered are:

1. Convection between the object (cell) and the environment, and
2. Accumulation of oxygen in the cell.

A lumped analysis is acceptable when the parameter  $NB_i$ , called the Biot number is less than 0.1, which indicates that the internal resistance to oxygen transfer is negligible.

Due to its similarity to heat transfer, the Biot number can be defined by Equation (3.35).

$$NB_i = (K_c)x/D_g \quad (3.35)$$

Where:

$x$  = Characteristic dimension ( $r/2$ ).

$D_g$  = Oxygen diffusion coefficient in the air

$K_c$  = Mass transfer coefficient (cm/sec)

$K_c$  can be calculated through several numerical conversions (Geankoplis, 1978) starting from:

$$K_g = P_m/\delta \quad (\text{gmol O}_2/\text{cm}^2.\text{sec.atm}) \quad (3.36)$$

Where  $K_g$  is the "equivalent" mass transfer coefficient in the gas phase.

$K_c$  can be obtained by the relationship

$$(K_c \cdot P)/(R.T.) = K_g \cdot P \quad (3.37)$$

Where  $P$  is the total pressure (atm) of the system. It follows that (description of symbols is shown in page 63).

$$K_c = K_g \cdot R.T. \quad (\text{cm/sec}) \quad (3.38)$$

Following is the development of the mathematical model, used in this study, for a lumped system, which has the capability to predict the oxygen partial pressures inside the cell.

Comparisons between predicted and experimental data are essential to determine the accuracy of the overall system design.

The mathematical model was established using the following oxygen balance in the cylindrical system:

Oxygen IN through HDPE = Change in Amount of O<sub>2</sub> in cell

Expressing the above balance using rate equations it follows that:

$$(P_m/\delta)A(p_a - p) = dp/dt \quad (3.39)$$

However, Equation (3.39) needs to be dimensionally balanced, depending on the units for  $P_m$ . For example, if  $P_m$  is given in cc-mil/cm<sup>2</sup>.atm.min, then the resulting balanced equation is

$$(P_m/\delta)A(p_a - p) dt/22414 = Vdp/RT \quad (3.40)$$

Solution to Equation (3.39) is obtained through integration as follows:

$$[(P_m ART/\delta V)] \int_{t=0}^{t=t} dt = \int_{p=0}^{p=p} dp/(p_a - p) \quad (3.41)$$

and

$$\exp[-(P_m A R T / \delta V) t] = (p - p_a) / (p_o - p_a) \quad (3.42)$$

Where the oxygen partial pressure  $p$  can be determined as follows:

$$\text{Defining } L = P_m A R T / 22414 \delta V \quad (3.43)$$

$$p = p_a + (p_o - p_a) \exp(-L t) \quad (3.44)$$

Where:

$P_a$  = Oxygen partial pressure in ambient (atm)

$p_o$  = Initial oxygen partial pressure (atm)

$V$  = Volume of cylindrical cell (cc)

$A$  = Surface area of cell ( $\text{cm}^2$ )

$T$  = Absolute temperature (K)

$R$  = Gas constant (82.057 cc.atm/gmol K)

### 3.6. Cell Systems for the Diffusion of Oxygen and Autooxidation of Ascorbic Acid.

#### 3.6.1. Optimum conditions for kinetic experiments.

Preliminary experiments were necessary to find proper experimental conditions regarding reaction kinetics in three fruit juices, sources of vitamin C, and water.

Desired experimental conditions were represented by detectable changes in vitamin C (degradation) in the selected fruit juice at 25°C and constant room light intensity; detectable changes in dissolved oxygen in the corresponding liquid, and a zero or first order kinetic rate constant, required by the FE model.

Bottled, pasteurized lemon juice, grapefruit juice, and apple juice were simultaneously purchased in a local grocery store, carefully selecting them according to production date and code number to insure sample homogeneity.

The juices were kept at room temperature (22°C) to approximately maintain the environmental shelf conditions as in the grocery store. After opening for sampling, bottles were stored at 5°C to avoid further degradation of vitamin C

#### 3.6.1.1. Open System Exposed to Surface Air.

The open system for this preliminary experiment was created by placing approximately 50 ml of desired fruit juice (source of vitamin C) in a narrow neck, clear, glass bottle (10.7 cm length, and 5.3 cm diameter).

The glass bottles were then located, directly exposed to air, in a constant temperature ( $25^{\circ}\text{C} \pm 0.3$ ) shaker bath (Dubnoff Metabolic Shaking Incubator). Bottles were removed one at a specific time interval, making sure enough time was allowed for at least 75% completion of the reaction

In this case, it was assumed that the shaking action maintained oxygen saturation conditions within the juice sample.

Withdrawn sampling bottles were immediately frozen to stop the reaction and storage for two or three days, until measurement of vitamin C. Frozen samples, containing the reacted fruit juice, were thawed at  $5^{\circ}\text{C}$ , before determination of vitamin C in triplicate for each withdrawn sample, following a modified indophenol technique (Morell, 1941) described in Appendix D.

### 3.6.2 Open system with continuous bubbling of air.

-

This open system consisted of an Erlenmeyer glass flask (1000 ml), containing approximately 500 ml of apple juice or water with specific percentages of vitamin C. (0.272 mM and 3.157 mM for apple juice, 0.341 mM for water). The outside surface of the container was covered with a layer of HDPE to approximate the same light intensity passing through the membrane in the cylindrical HDPE cell. This covering of the flasks was necessary since the determined kinetic rate constant was also applied to the HDPE cell.

Compressed air was continuously bubbled through the liquid, assuring constant supply of oxygen for the reaction to occur.

The complete system was kept at  $25^{\circ}\text{C} \pm 0.2$  and 45% RH in a controlled atmosphere chamber. Distilled, deionized water, or apple juice, were conditioned to  $25^{\circ}\text{C}$ , whenever was necessary. Temperature conditioning was achieved rapidly (approximately one minute) by microwave heating. Saturation levels of dissolved oxygen in water or apple juice were achieved prior to add vitamin C and starting the experiment.

### 3.6.3. Closed System

The oxidation reaction involving vitamin C and dissolved oxygen in apple juice and water, was followed in two different ways using two samples; one to monitor changes in dissolved oxygen, and the other to monitor changes in vitamin C content.

The former yields a kinetic rate constant in terms of oxygen, the latter in terms of vitamin C. In this study, a rate constant in terms of oxygen is preferred since the FE model simulates oxygen diffusion, not ascorbic acid diffusion. The rate constant in terms of vitamin C is useful in determining the extent of vitamin C degradation.

#### 3.6.3.1. Closed system and changes in dissolved oxygen

This system consists of a cylindrical, plexyglass (acrylic) cell (24.4 cm length, and 7.6 cm diameter), covered with a layer of HDPE, and totally filled with water or apple juice. An oxygen sensor was located on the top surface to monitor dissolved oxygen changes within the corresponding liquid. The system was kept at  $25^{\circ}\text{C} \pm 0.2$  and at 45% RH in a controlled atmosphere chamber.



3.6.3.1.1. Closed system and water added with  
vitamin C

The following kinetic experiments (Table 3.5) were performed using distilled, deionized water added with vitamin C to determine the kinetic rate constant in terms of oxygen levels (atm).

Table 3.5. Sets of kinetic experiments to determine rate constants in terms of oxygen levels (atm) in water added with vitamin C.

Vit. C	Initial O <sub>2</sub>
<u>(mM)</u>	<u>(atm)</u>
0.341	0.21
11.35	0.21
11.35	0.117
11.35	0.10
11.35	0.086

#### 3.6.3.1.2 Closed system and apple juice added with vitamin C.

The kinetic rate constant in terms of oxygen levels (atm) for apple juice, was determined based on three experiments at saturation levels of oxygen (0.21 atm) and 0.272 mM vitamin C.

#### 3.6.3.2. Closed system and changes in vitamin C content

-  
This system was designed using sealed, clear glass bottles (9.6 cm length, and 2.7 cm diameter), covered with a layer of HDPE for reasons already explained, totally filled with apple juice or water.

One bottle at a time (specific time intervals) was withdrawn from the controlled chamber ( $25^{\circ}\text{C} \pm 0.2$ , 45% RH), and rapidly frozen to stop the reaction, and later determination of vitamin C as described earlier.

3.6.3.2.1. Closed system and water added with  
vitamin C.

The following kinetic experiments (Table 3.6) were performed for added water. Vitamin C was measured in three replicates for each withdrawn sample.

Table 3.6 Sets of kinetic experiments to determine rate constants in terms of vitamin C in water added with vitamin C.

Vit.C	Initial O <sub>2</sub>
<u>(mM)</u>	<u>(atm)</u>
11.35	0.08
11.35	0.12
11.35	0.21
0.284	0.21

#### 3.6.3.2.2. Closed system and apple juice added with vitamin C

Two kinetic experiments were performed for apple juice with saturating oxygen levels (0.21 atm). One with 0.227 mM and the other with 2.236 mM vitamin C.

Vitamin C was determined in three replicates for each withdrawn juice sample.

### 3.7. Kinetic models

Due to the capability of the FE model to simulate oxygen diffusion and chemical reaction, the kinetic models, regarding the zero and first order chemical reactions must be expressed as follows:

A zero order chemical reaction of the form:

$$-dp/dt = k_{v,0} \quad (3.45)$$

Where  $p$  is oxygen partial pressure in the corresponding liquid,  $t$  is time and  $k_{v,0}$  is the kinetic rate constant.

In this case,  $k_{v,0}$  is independent of  $p$  or vitamin C. This is the easiest case for modeling purposes. It is equivalent to a constant heat generation rate ( $q$ ) in Equations (3.9) and (3.11).

A first order chemical reaction is represented by

$$-dp/dt = k_{v,1} \cdot (p) \quad ( 3.46 )$$

Here, the first order rate constant  $k_{v,1}$  depends on the oxygen partial pressure  $p$ . The degree of difficulty for modeling purposes is increased by the dependence of  $k_{v,1}$  on  $p$ . In this case, the FE model uses the element STIF 71, Equation (3.10) to simulate Equation (3.46), as described earlier.

Kinetic models regarding vitamin C will be described in the Results and Discussion section.

## IV RESULTS AND DISCUSSION

### 4.1. Calibration of oxygen sensors in liquid and gas phases.

#### 4.1.1. Gas phase.

The oxygen sensor calibration was carried out using several gas mixtures of nitrogen and oxygen covering a range containing zero to 21% oxygen. The amounts were quantified using GC and compared to sensor voltage readings, which were directly proportional to oxygen partial pressure.

The sensor accurately measured (less than 2% error) the oxygen level in the gas mixtures, as confirmed by GC measurements (Figure 4.1).

#### 4.1.2. Liquid phase.

Calibration of sensors in the liquid phase was done by locating the sensor within the water to monitor changes in oxygen levels. Sensor readings corresponded directly to GC measurements with an error of less than 2% (Figure 4.2).

In order to verify that the oxygen levels (pressure) detected within the water were the same as in the gas phase, one sensor was located in the liquid phase and other sensor was located in the gas phase just above the liquid.

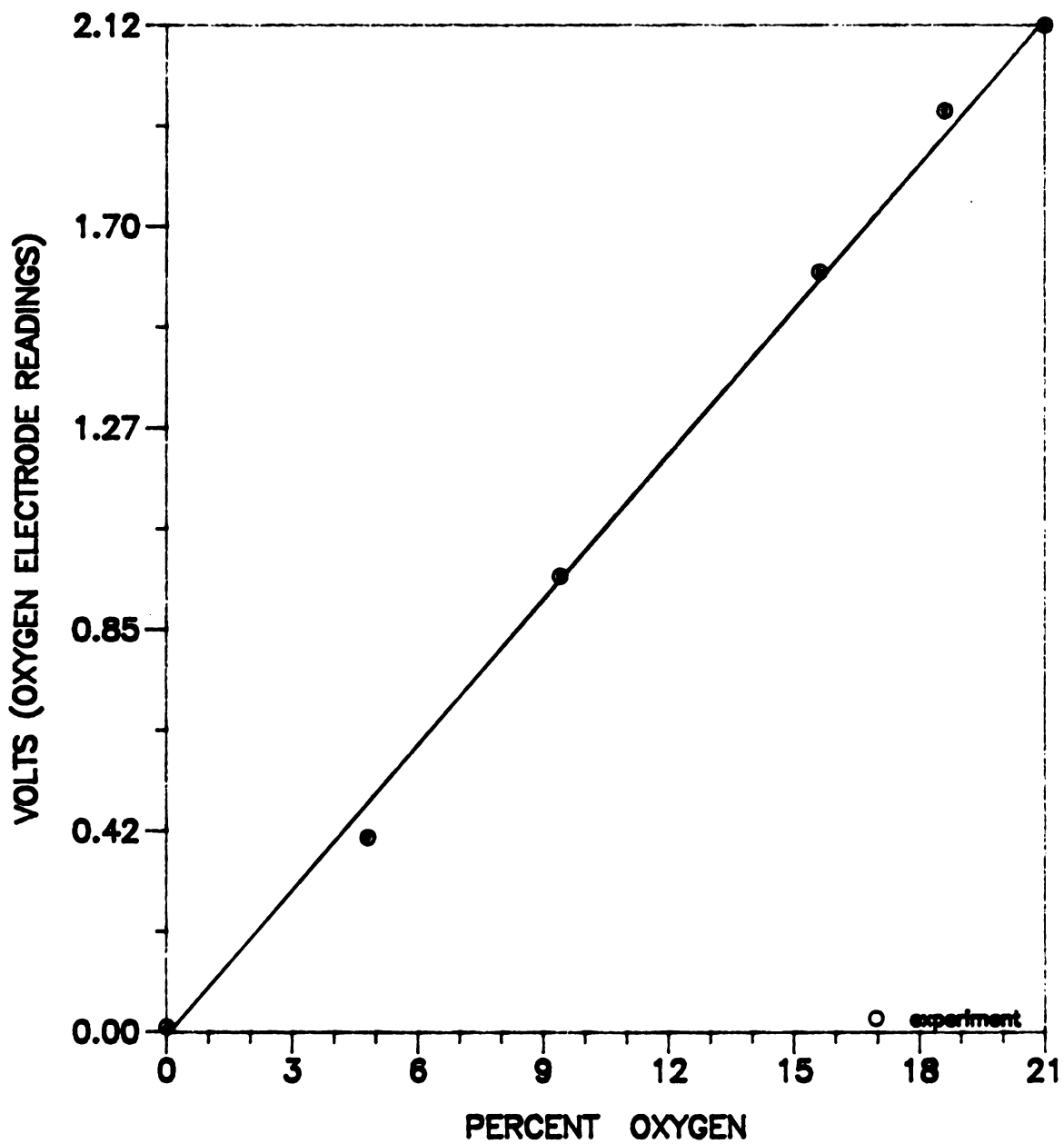


FIGURE 4.1 CALIBRATION OF OXYGEN SENSORS IN GAS MIXTURES

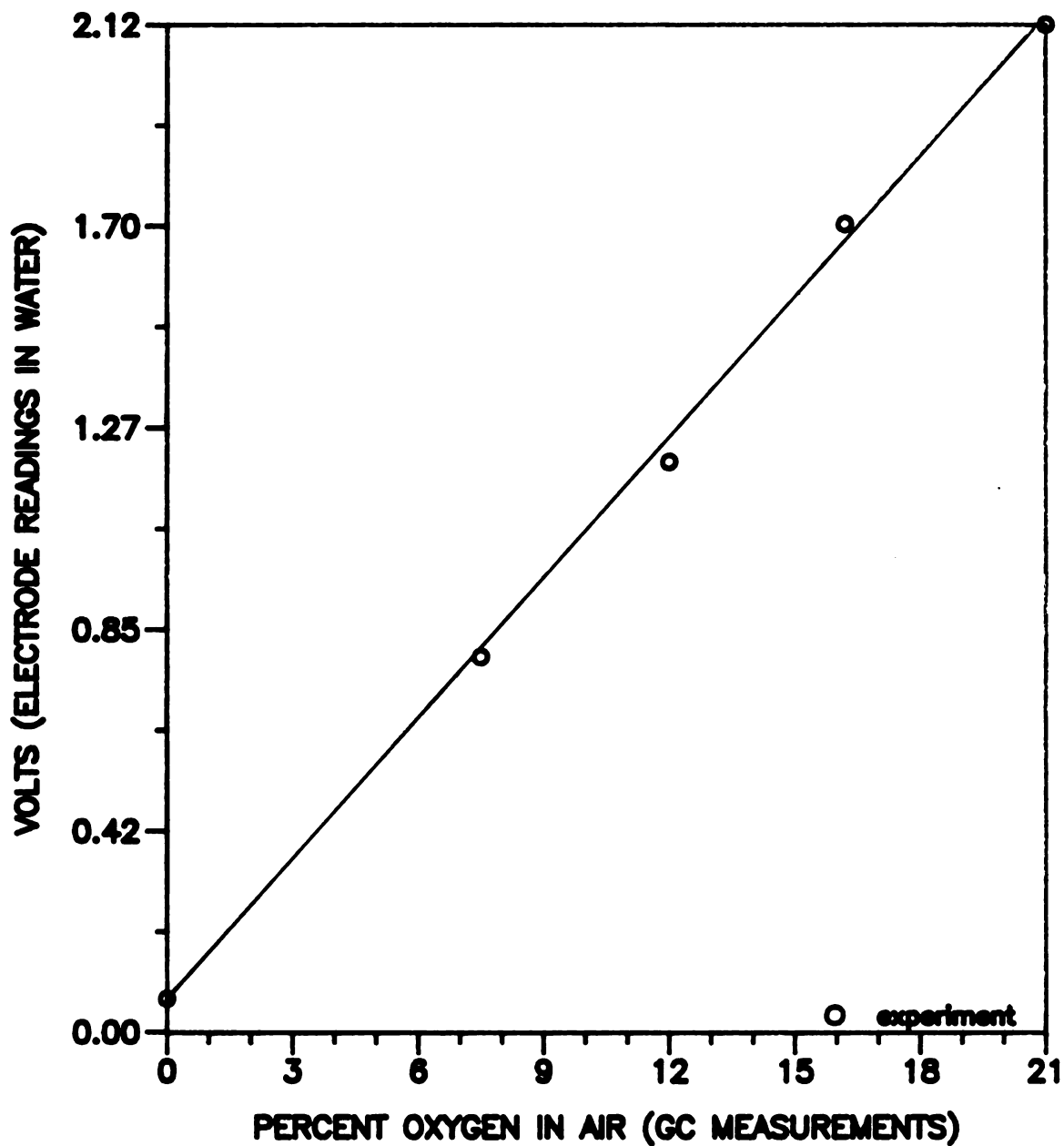


FIGURE 4.2 CALIBRATION OF OXYGEN SENSORS IN WATER



The oxygen voltage readings in the liquid phase were the same as for the gas phase (Figure 4.3); indicating the oxygen partial pressure in the gas is the same as for the liquid. Sensor readings were confirmed with GC measurements. The response was linear indicating with an error of less than 2%.

#### 4.2. Oxygen diffusivity in liquids.

##### 4.2.1. Oxygen diffusivity in water.

The oxygen diffusion coefficient in water at 25°C was determined using two different approaches (described later) yielding similar values of  $1.2 \times 10^{-3} \text{ cm}^2/\text{min}$ . Reported literature values (Saddler, 1984; Perry and Chilton, 1983) range from  $1.13 \times 10^{-3}$  to  $1.37 \times 10^{-3} \text{ cm}^2/\text{min}$  indicating that the methods used in this study are provided reasonable data.

Using the first approach, an example of the linear plot obtained by applying Equation 3.1 (Appendix A) is shown in Figure 4.4. From the slope of the straight line the diffusion coefficient is calculated.

The second approach, using Equation AB.8 (Appendix B) for a semi infinite system is presented in Figure 4.5. The straight line was obtained by plotting the amount of oxygen

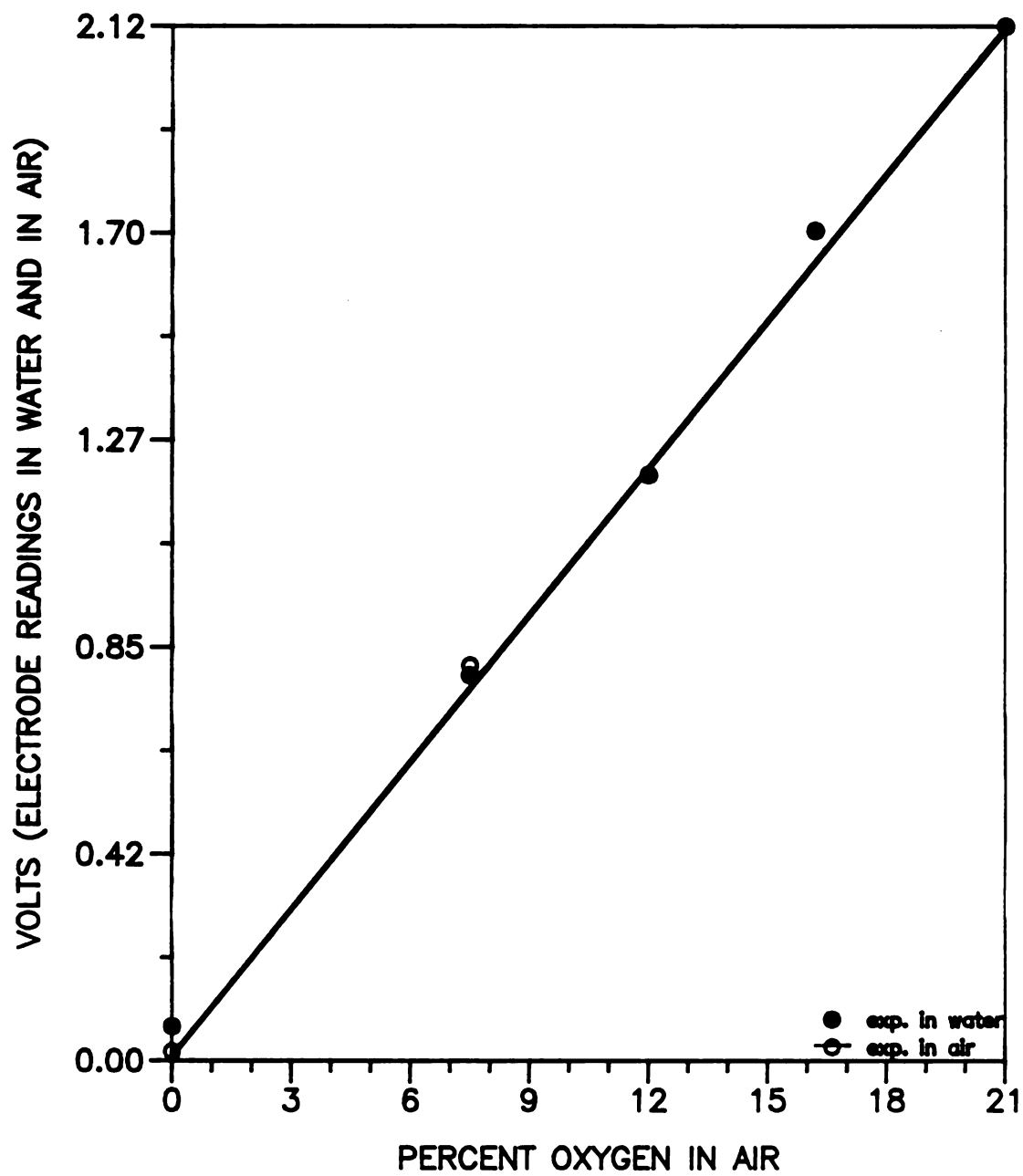


FIGURE 4.3 CALIBRATION OF OXYGEN SENSORS IN WATER AND IN AIR AT 25°C

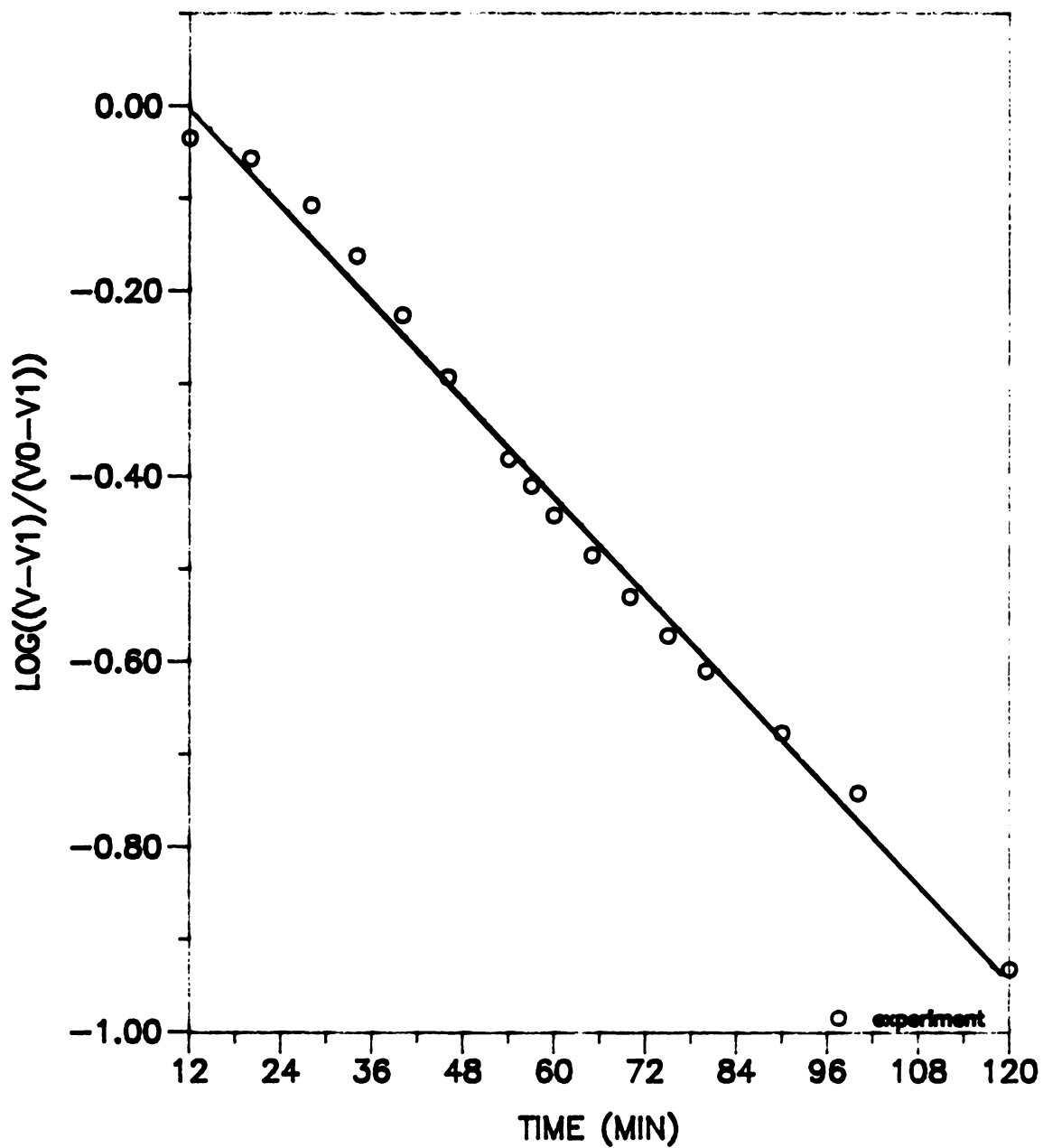


FIGURE 4.4 LINEAR PLOT FOR DETERMINATION OF THE  
OXYGEN DIFFUSION COEFFICIENT IN WATER AT 25°C  
(EQUATION 3.1)

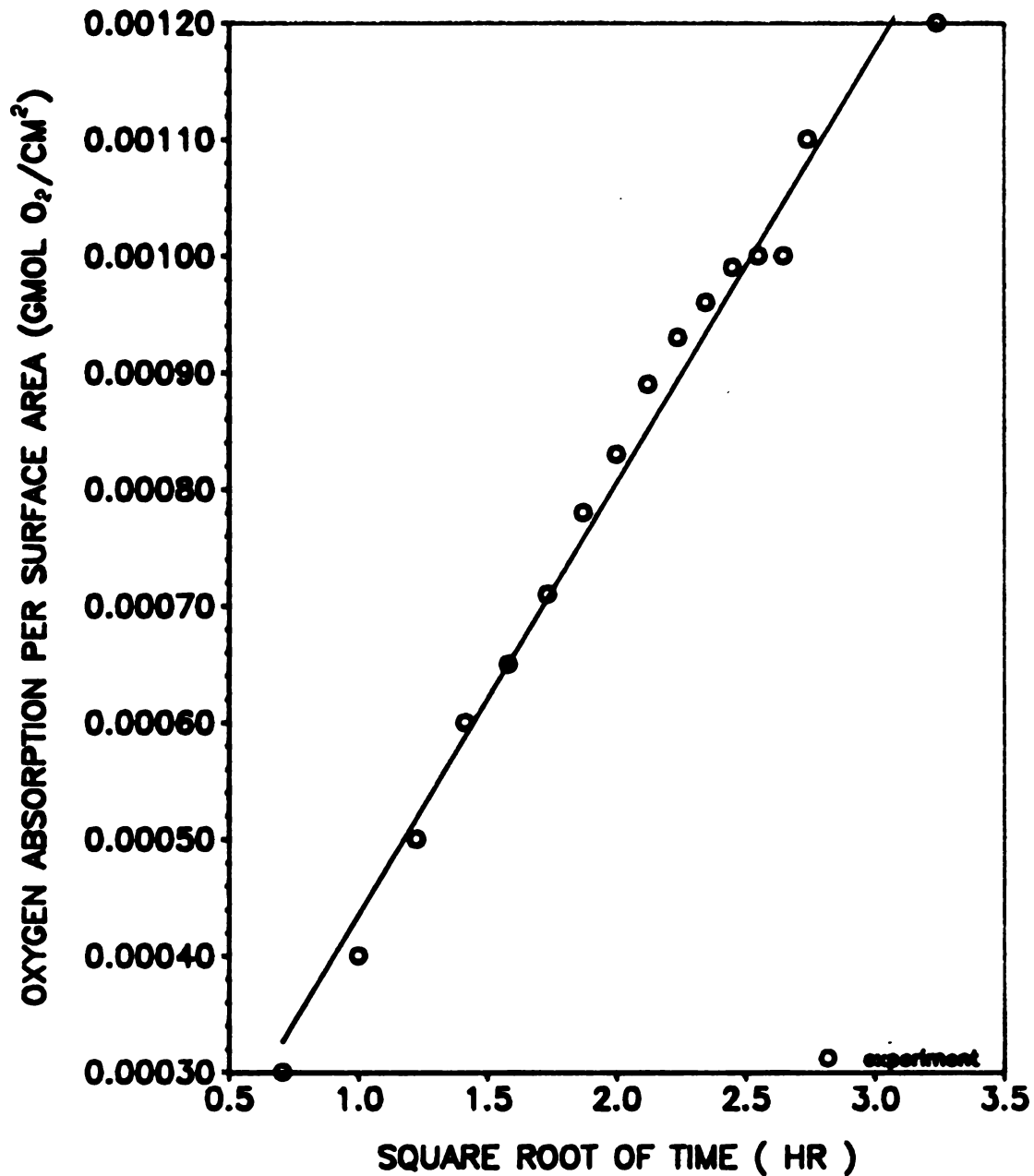


FIGURE 4.5 DETERMINATION OF THE OXYGEN DIFFUSION COEFFICIENT IN WATER AT 25C. SEMI-INFINITE SYSTEM

absorbed (at specific time intervals) per unit surface area ( $Q/A : \text{gmol O}_2/\text{cm}^2$ ) against the square root of time ( $\sqrt{t}$ ).

$Q/A$  was determined as indicated by Equation 4.1:

$$Q/A = LpS \quad (4.1)$$

Where:

$L$  = Distance (1.5 cm; sensor location below water surface)

$p$  = oxygen partial pressure (atm; in water at particular times)

$S$  = Oxygen solubility in water ( $1.27 \times 10^{-6} \text{ gmol O}_2/\text{cc.atm}$ )

$Q$  = Amount of oxygen absorbed (gmol )

$A$  = Surface area ( $\text{cm}^2$ )

The oxygen diffusivity was calculated from Equation (AB.8):

$$\text{slope} = 2 (C^* - C_o) \sqrt{(D/\pi)} \quad (\text{AB.8})$$

Where  $C^*$  and  $C_o$  are dissolved oxygen concentrations at equilibrium, and initially, respectively.

Verification of the oxygen diffusion coefficient is shown in Figure 4.20. This was achieved by using its value to predict oxygen partial pressures in the semi infinite system (Equation AB.8, Appendix B).

The average absolute error (Equation 4.2) was 8%.

$$E_{abs} = (1/n) \sum_{i=1}^{i=n} (|Y_i - Y_{i,e}| / Y_{i,e}) \times 100 \quad (4.2)$$

Where:

$E_{abs}$  = Average absolute error (%)

$n$  = Number of data points

$Y_i$  = Predicted value

$Y_{i,e}$  = Experimental value

The semi infinite approach is preferred due to its simplicity, and because the sensor tip is free within the liquid therefore being subject to less experimental error. In the first approach, the sensor's membrane tip must slightly touch the bottom surface of the glass diffusion cell, thus reducing the diffusing area.

#### 4.2.2. Oxygen diffusivity in apple juice.

The oxygen diffusion coefficient in apple juice at 25°C was similarly obtained applying Equation 4.3 to the semi-infinite system.

$$\text{slope}_a = 2 (p^* - p_O) \sqrt{D/\pi} \quad (4.3)$$

Where:

$p^*$  = Oxygen partial pressure equilibrium (atm)

$p_O$  = Oxygen partial pressure in the juice (atm)

$\text{slope}_a$  = Slope resulting from plotting  $Lp$  (cm-atm) vs  $\sqrt{t}$

Notice that as a result of dimensional analysis of the above Equation, the use of oxygen solubility in the juice was not necessary. This analysis was convenient since oxygen solubility data in apple juice was not available.

The diffusivity  $D$  was calculated from Equation (4.3).

Before setting up the diffusion experiments, apple juice was treated with 0.2% sodium azide as a preservative to avoid fermentation reactions requiring oxygen. The juice was also treated with about 5 units of ascorbate oxidase for at least 6 hours prior to the experiment in order to destroy any vitamin C present in the bottled juice purchased.

In all bottled juice samples, zero percent oxygen was found in the liquid phase as measured immediately after opening the bottles. Vitamin C concentration varied from sample to sample, ranging from about 0.113 to 1.249 mM.

In Figure 4.6 an example is shown of the resulting straight line derived from Equation AB.8. The average diffusion coefficient ( 2 replicates) is  $8.5 \times 10^{-4} \text{ cm}^2/\text{min}$ . Based on theoretical information about increasing molecular interaction (friction) by the soluble solids in the apple juice; this lower value, as compared to water, was expected. (Fatt, 1976).

A soluble solids contents of 11.2mg in apple juice was determined using a refractometer (Abbe - 3L; Busch and Lomb, Inc.)

Estimates of diffusion coefficients in liquids, in absence of data can be made using the Wilke and Chang correlation (Hayduk and Laudie, 1974): Equation (4.3). A diffusion coefficient value of  $7.7 \times 10^{-4} \text{ cm}^2/\text{min}$  was obtained using Equation (4.4).

This estimated value was very similar to the experimental value found in this work. The agreement between these two values confirms that the experimental approach provides reasonable data for diffusion coefficient in liquids.



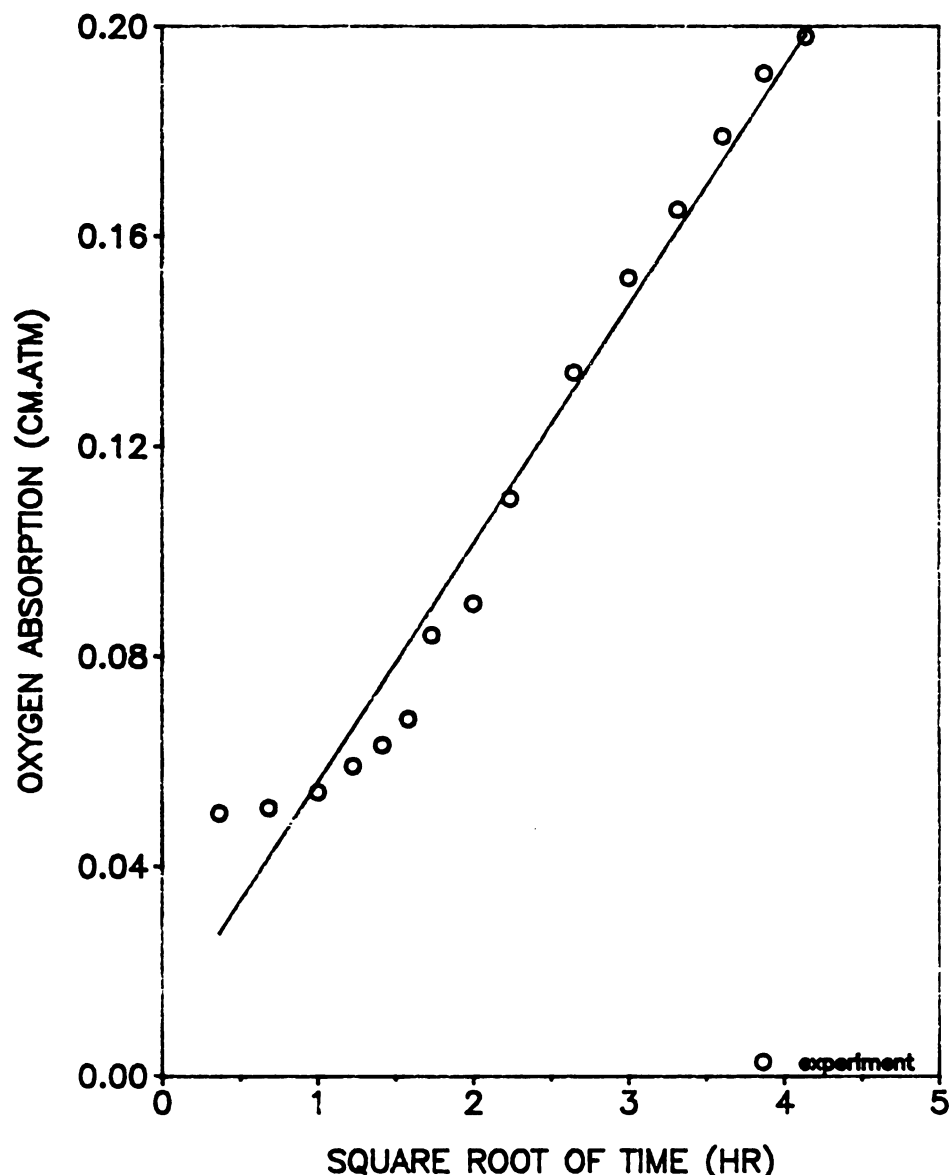


FIGURE 4.6 EXPERIMENTAL DETERMINATION OF THE  
OXYGEN DIFFUSION COEFFICIENT IN APPLE JUICE (25°C)  
USING ABSORPTION DATA FROM A SEMI INFINITE SYSTEM

$$D = 7.4 \times 10^{-8} T (\phi M)^{1/2} / (\mu V)^{0.6} \quad (4.4)$$

Where:

$T = 298.15\text{K}$  ( $25^{\circ}\text{C}$ )

$\phi = 2.26$ : Association factor

$M = 18 \text{ g/gmole}$ : Molecular weight of solvent (water)

$\mu = 5.575 \text{ cp}$ : viscosity of apple juice

$V = 25.6 \text{ cc/gmole}$ : molecular volume of oxygen

The viscosity ( $\mu$ ) ( $5.575 + 0.0959 \text{ cp}$ ) of apple juice was determined using the Wells-Brookfield microviscometer (Brookfield Engineering Laboratories, Inc., Stoughton, MA).

#### 4.3. Oxygen permeability constants.

The permeability constant  $P_m$  for HDPE was determined using the isostatic method as described in Appendix C. In Figure 4.7 an example is shown of the experimental data. The average for 3 replicates was  $10593.1 \text{ cc-mil/m}^2\text{-atm-day}$ . The average thickness of the film was  $0.85 \text{ mil}$ .

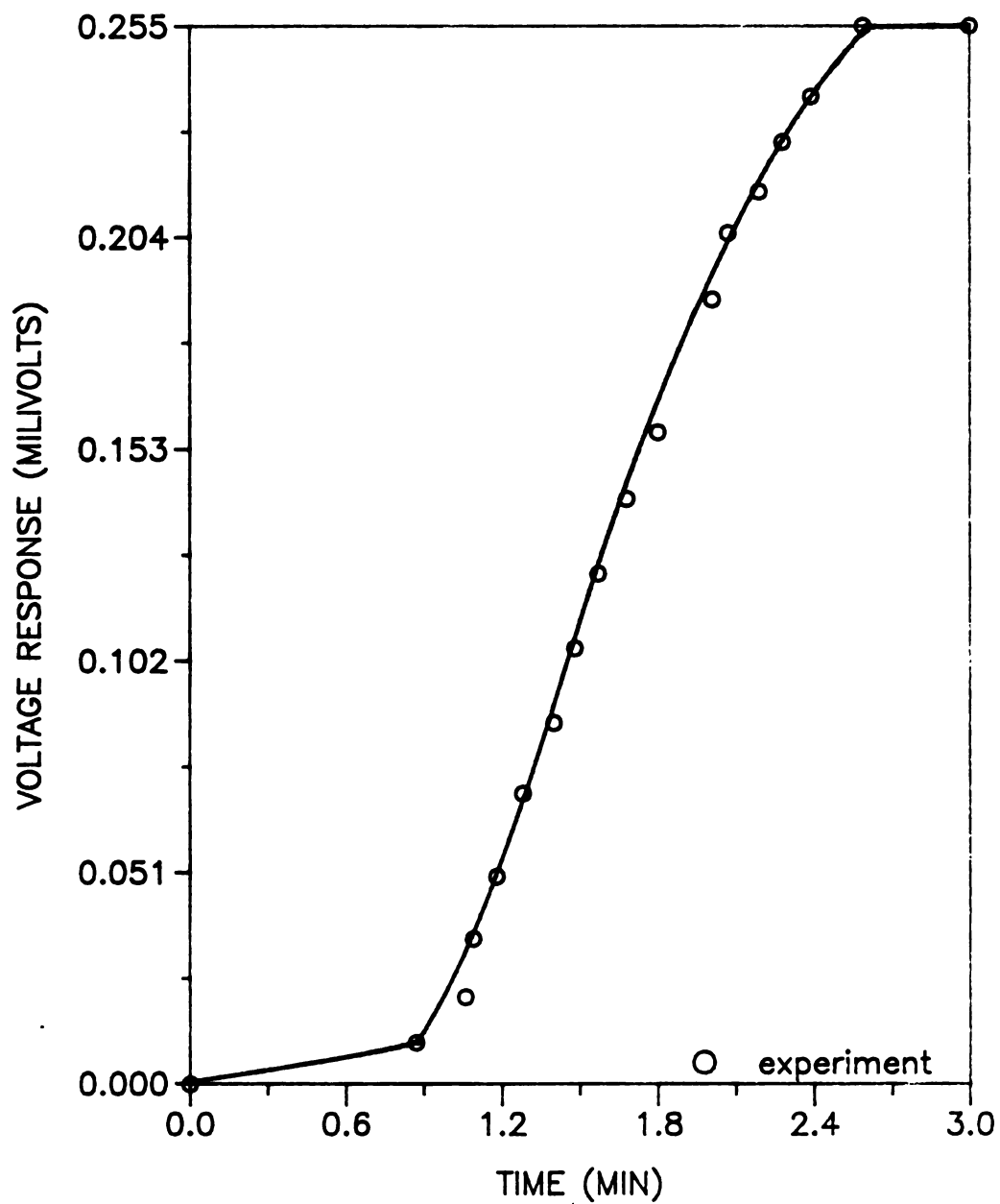


FIGURE 4.7 DETERMINATION OF OXYGEN PERMEABILITY  
CONSTANT IN HIGH DENSITY POLYETHYLENE  
(ISOSTATIC METHOD; OX-TRAN 100)

The permeability constant for Alethan was determined using the isostatic and the quasi-isostatic methods. Both methods yielded very similar permeability values (8450 and 8636) with a Pm average of 8543 cc-mil/m<sup>2</sup>-atm-day. The average thickness of the film was 2 mil. Due to limited supply and restricted use in this study, only one determination per method was performed.

#### 4.4. Lumped gas model for testing cylindrical permeable cells

This procedure was designed to evaluate the integrity of the cylindrical permeable cells, its cell dimensions, leaking areas, and the film permeability to oxygen.

In order to apply the lumped model as explained in section 3.5; a Biot number less than 0.1 must be first demonstrated; oxygen partial pressures and accumulated oxygen volume can then be predicted to quantify the experimental error in these conditions (no liquid inside the cell).

Results show that for a cylindrical cell with the following characteristics:

Height = 4.80 cm

Radius = 3.83 cm

Surface area = 115.51 cm<sup>2</sup>

Volume = 221.2 cm<sup>3</sup>

HDPE thickness = 0.85 mil

$P_m = 6.8 \times 10^{-4}$  cc-mil/cm<sup>2</sup>-atm-min

The Biot number is  $1.777 \times 10^{-4}$ , which is much less than 0.1, indicating the applicability of the lumped analysis.

Comparison of the predicted (Equation 3.44) oxygen partial pressures and experimental results are shown in Figure 4.8 with an average absolute error of 7.4%.

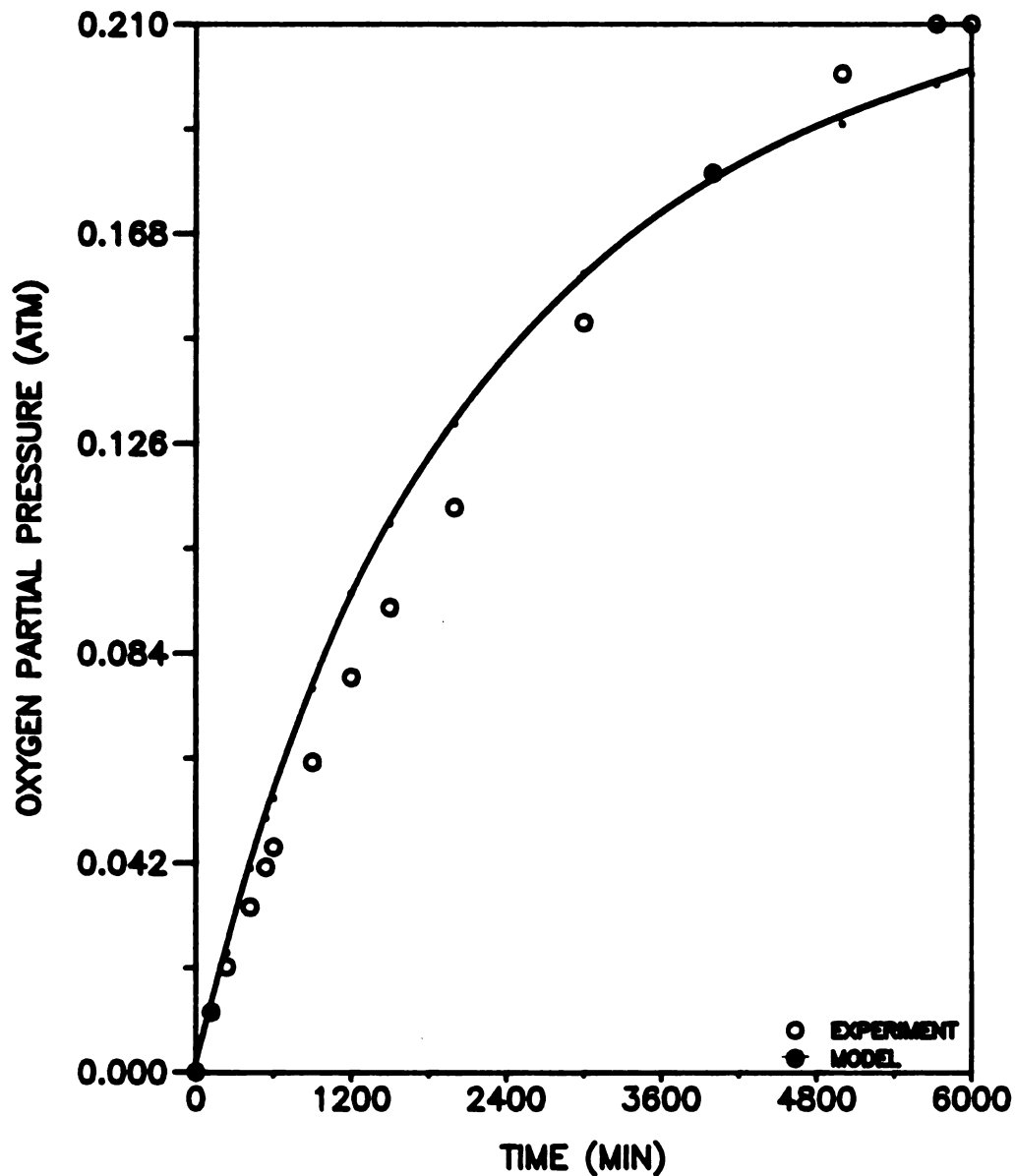


FIGURE 4.8 UNSTEADY STATE DIFFUSION FROM AIR INTO A CYLINDRICAL PERMEABLE (HDPE) CONTAINER. EXPERIMENTAL VALUES AND LUMPED MODEL PREDICTIONS.

The amount of oxygen which accumulates in the cell is determined by applying the diffusion Equation (4.5) at steady state in small time intervals:

$$F = \{2\pi L P_m / [\ln(r_2/r_1)]\} (p_a - p) \quad (4.5)$$

Where:

$F$  = Rate of oxygen passing through the film at small time intervals (cc/min)

$r_2$  = Outer radius of the cylindrical cell

$r_1$  = Outer radius minus the thickness of the film

$p_a$  = Oxygen partial pressure in the environment (0.21 atm)

$p$  = Oxygen partial pressure within cell at time  $t$  (sensor readings)

$L$  = Height of the cylindrical cell

Graphical integration of  $F$  (Figure 4.9) over a time of 5700 min, yields an oxygen accumulation of 46 cc while experimental measurements of partial pressure and cell volume gives 43 cc, representing about a 9% average absolute error. This greater value results from errors originated by cell length and radius measurements.

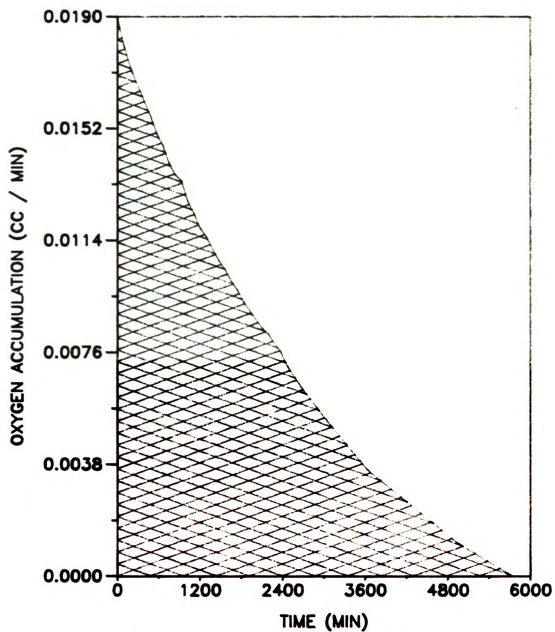


**FIGURE 4.9 LUMPED MODEL PREDICTIONS OF ACCUMULATING OXYGEN IN A CYLINDRICAL, PERMEABLE (HDPE) CONTAINER**



#### 4.5. Experimental determination of kinetic rate constants

##### 4.5.1. Optimum experimental conditions

The first step in the determination of kinetic rate constants in apple juice and water, was to test the performance of the oxygen sensors, with and without vitamin C reacting with dissolved oxygen in the liquid.

The sensor was capable of detecting differences in oxygen partial pressures (Figure 4.10) in water containing 0.31 mM vitamin C (open system).

The addition of vitamin C to water, containing zero oxygen, slowed the accumulation of dissolved oxygen due to consumption by oxidation (lower curve).

The upper curve is from the same system without chemical oxidation. The increasing oxygen partial pressure indicates greater accumulation of dissolved oxygen.

In the second step the addition of low (0.31 mM), and high (1.14 mM) amounts of vitamin C to water in an open system was done in order to select an optimum range of vitamin content and to obtain measurable changes of oxygen.

At low vitamin C contents (0.31 mM) a fairly fast oxygen consumption occurred (Figure 4.11). In about six hours oxy-

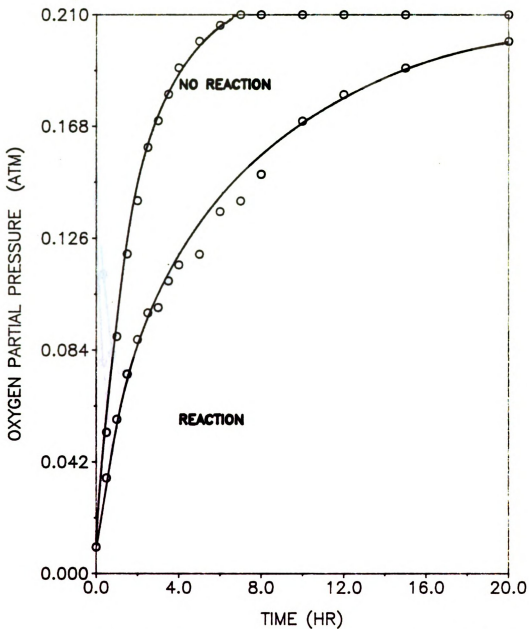


FIGURE 4.10 PRELIMINARY KINETIC EXPERIMENTS TO TEST OXYGEN SENSOR RESPONSE TO EFFECTS OF A CHEMICAL REACTION IN WATER.

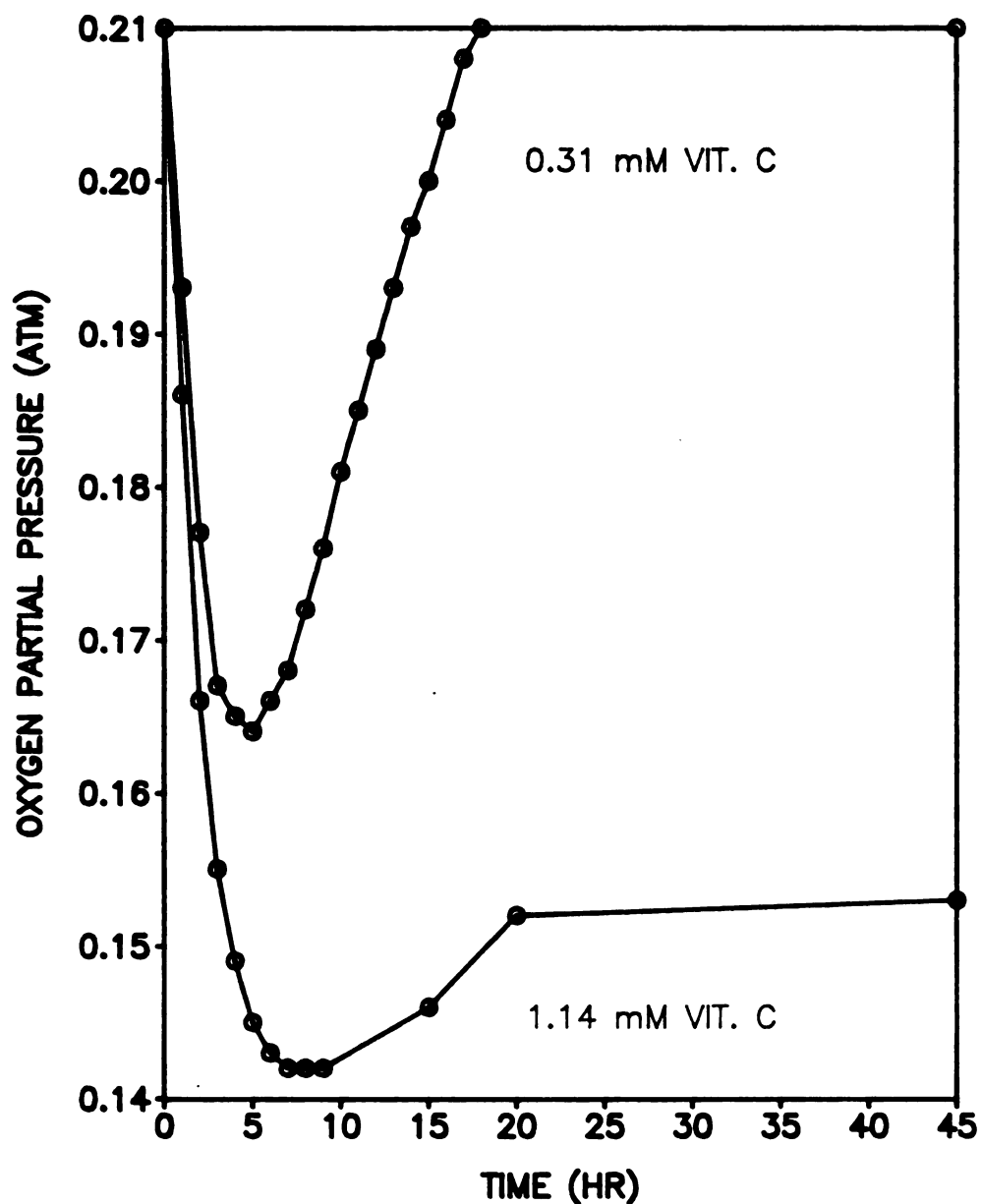


FIGURE 4.11 PRELIMINARY KINETIC EXPERIMENTS IN WATER TO VISUALIZE THE EFFECTS OF VITAMIN CONTENTS ON OXYGEN CHANGES (SEMI-INFINITE SYSTEM, NO HDPE).

gen starts to accumulate, and reaches steady state (0.21 atm) within 18 hours. This was a desirable response due to the short time calibration stability of the sensors ( about ten hours). The sensor response at high vitamin C contents (1.14 mM) was not desirable for modeling purposes due to longer times to reach steady state.

Three fruit juices were selected to provide a source of vitamin C; lemon (pH=2.85), grapefruit (pH=3.5) and apple juice (pH=3.6), with corresponding initial vitamin C contents of 6.81 mM, 5.56 mM and 0.19 mM.

Preliminary kinetics were performed on each juice at 25°C in a water bath as described in section Material and Methods (Section 3.6.1.) Vitamin C was added to apple juice to bring it up to 2.4 mM in order to obtain measurable changes in vitamin content.

In Figure 4.12 is shown the linear plot representing the zero order chemical reaction obtained for apple juice. The preliminary zero order kinetic rate constant value was  $1 \times 10^{-5}$  M/hr ( $r^2=0.97$ ).

This was termed a preliminary constant ( because of the assumed constant oxygen saturation levels in the liquid) to differentiate from the true rate constant that would be obtained if a constant supply of oxygen was provided to the juice.

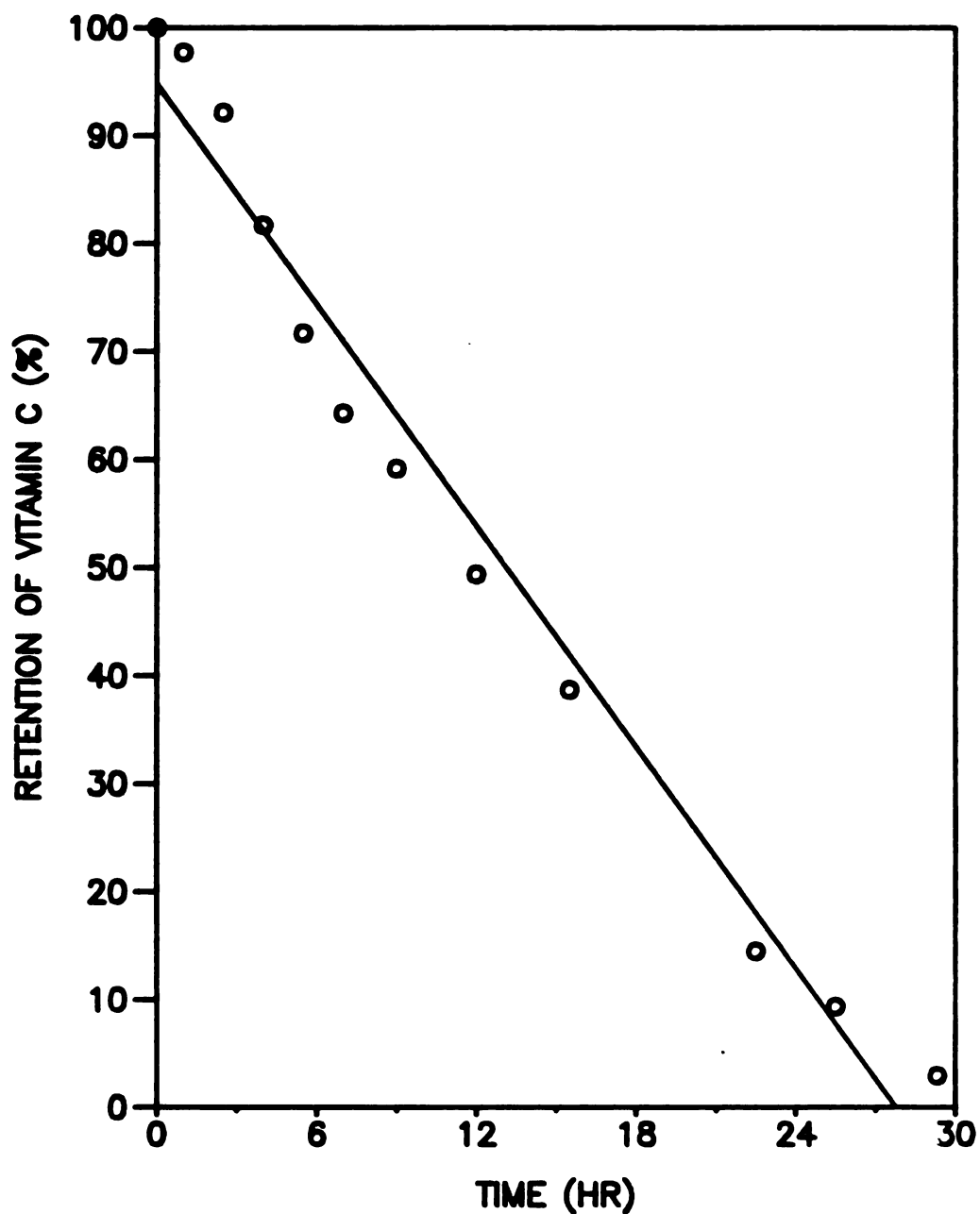


**FIGURE 4.12 PRELIMINARY ZERO ORDER CHEMICAL REACTION FOR DEGRADATION OF VITAMIN C IN APPLE JUICE. SHAKER WATER BATH SYSTEM AT 25°C**

Apple juice was selected over the other juices for further studies because no significant changes in vitamin C content occurred in three days in lemon and grape fruit juices.

#### 4.6. Experimental kinetic models

##### 4.6.1. Kinetic rate equations expressed in terms of oxygen partial pressure.

Kinetic rate equations were determined for water and apple juice with added vitamin C as follows.

##### 4.6.1.1. Water with added vitamin C (25°C)

In a closed system, water containing 0.341 mM vitamin C showed an average first order rate constant ( $k_{v,1}$ ) value of  $0.0049 \text{ min}^{-1}$  ( $r^2=0.95$ )(Table 4.1). All experiments were done in duplicate

The first order rate equation is expressed as follows:

$$-dp/dt = (k_{v,1})p \quad (4.6)$$

The rate constant was calculated using regression analysis (least square method) (Levenspiel , 1972).

**Table 4.1.- Kinetic data for water containing 0.341 mM vitamin C in a closed system (25<sup>0</sup>C). The first order rate constant was 0.0049 min<sup>-1</sup>**

<u>Oxygen partial pressure in water (atm)</u>					
<u>Time</u>	<u>Trial</u>		<u>Time</u>	<u>Trial</u>	
<u>(min)</u>	<u>1</u>	<u>2</u>	<u>(min)</u>	<u>1</u>	<u>2</u>
0	.21	.21	100	.100	.102
10	.195	.191	110	.093	.097
20	.175	.177	120	.089	.093
30	.161	.164	140	.081	.086
40	.151	.151	160	.073	.080
50	.142	.140	180	.067	.076
60	.135	.131	200	.062	.072
70	.127	.125	240	.055	.065
80	.118	.117	280	.050	.061
90	.109	.110			

**Table 4.2.- Kinetic data for water containing 11.35 mM vitamin C in a closed system (25<sup>0</sup>C). The zero order was 1.567x10<sup>-4</sup> atm/min**

<u>Oxygen Partial Pressure in water (atm)</u>				
<u>Time</u>	<u>Trials</u>			
<u>(min)</u>	<u>1</u>	<u>2</u>	<u>3</u>	<u>4</u>
0	.21	.086	.117	.100
10	.131	.084	.111	.095
30	.126	.080	.103	.089
60	.120	.076	.089	.081
90	.114	.070	.077	.076
120	.109	.065	.067	.071
150	.104	.061	.060	.064
180	.100	.057	.052	.060
210	.096	.054	.044	.056
270	.088	.045	.031	.048
300	.079	.041	.025	.044
360	.077	.036	.014	.037
390	.072	.033	.010	.035

In Figure 4.13 is shown the straight line derived from integrating the above equation. The slope represents  $k_{v,1}$ .

A zero order rate equation was found to best fit the kinetic data presented in Table 4.2 for water containing 11.4 mM vitamin C. A zero order rate constant ( $1.567 \times 10^{-4}$  atm/min,  $r^2=0.92$ ) was expected due to the excessive amount of vitamin in the water. The vitamin content was 47 times greater than the oxygen content.

The reaction rate equation for this zero order reaction is represented by Equation (4.7) which yields a straight line (Figure 4.14) by plotting  $p$  vs  $t$ . The slope represents  $k_{v,o}$ .

$$-dp/dt = k_{v,o} \quad (4.7)$$

Due to the saturation levels of vitamin C in the water the equation did not depend on oxygen partial pressure ( $p$ ) or vitamin C content. This is typical of zero order rate equations, whose rate is determined by some factor other than the concentration of the reacting materials (Levenspiel, 1972).



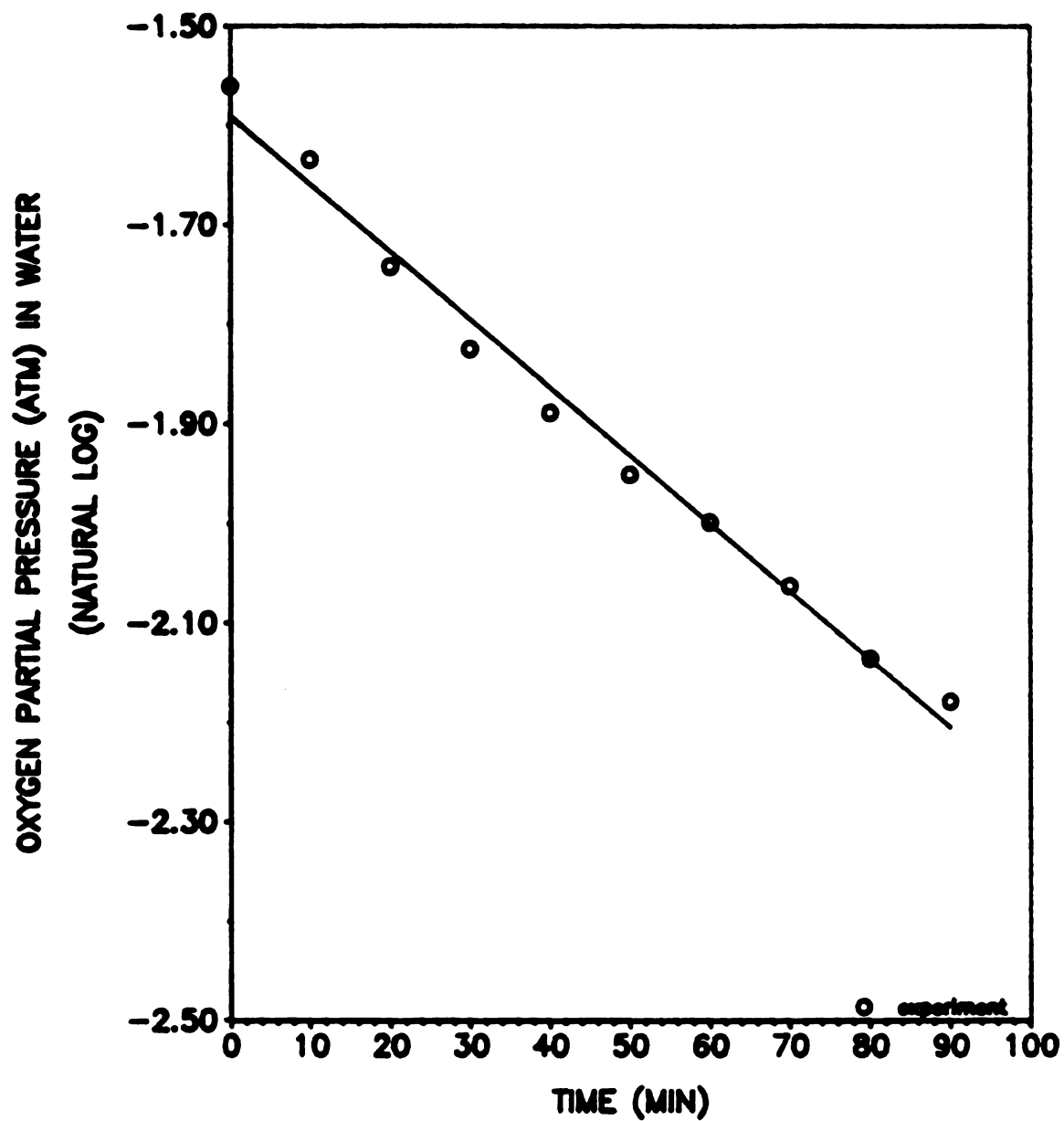
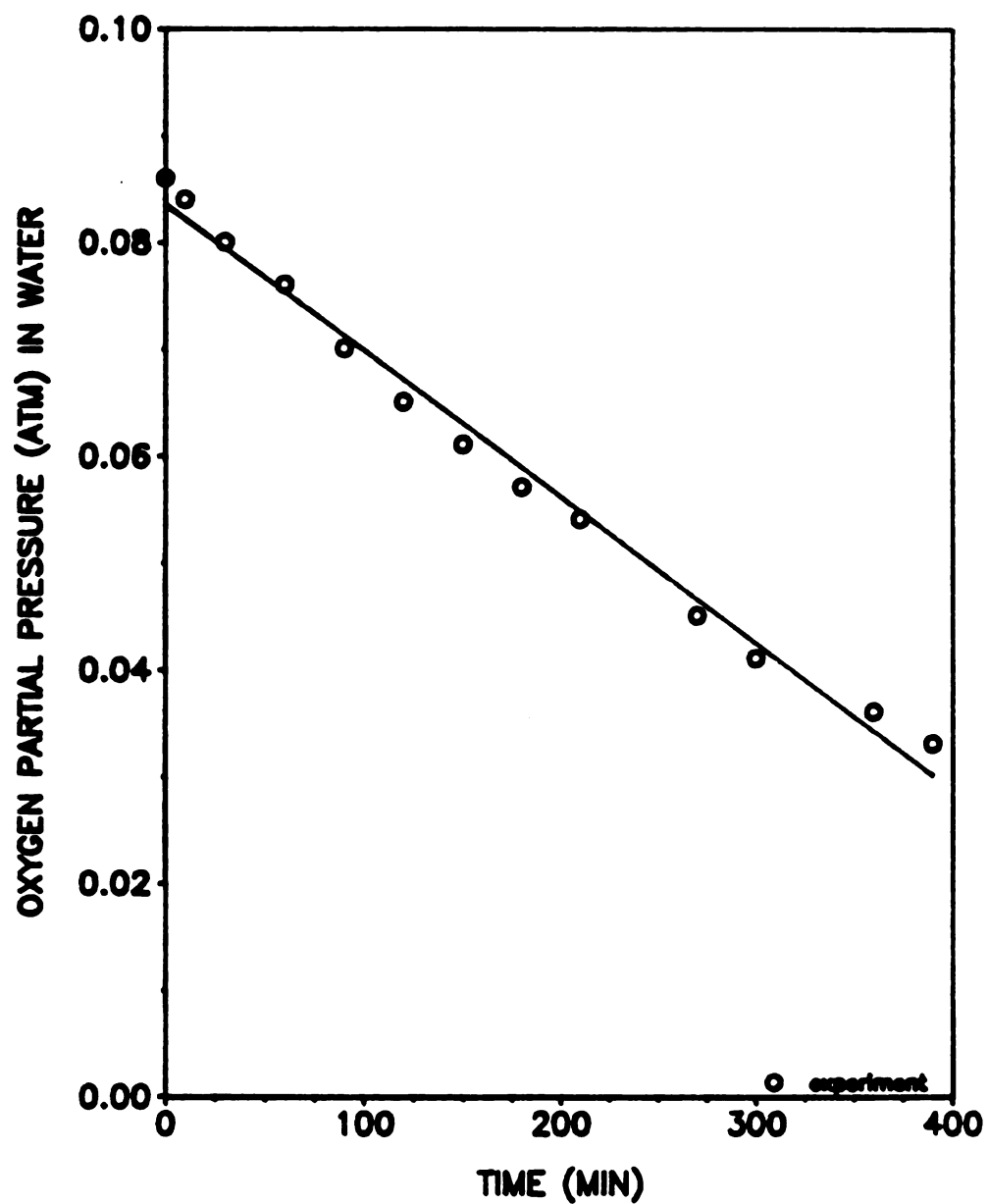


FIGURE 4.13 LINEAR PLOT REPRESENTING A FIRST ORDER RATE EQUATION FOR DEGRADATION OF VITAMIN C (0.341 mM) IN WATER



**FIGURE 4.14 LINEAR PLOT REPRESENTING A ZERO ORDER  
RATE EQUATION FOR DEGRADATION OF VITAMIN C  
(11.35 mM) IN WATER**

According to Levenspiel (1972), reactions are of zero order only at high concentrations of the reactants; and the reaction becomes concentration dependent if the concentration is lowered, causing the order to rise from zero order.

#### 4.6.1.2. Apple juice with added vitamin C (25°C)

Kinetic data (three trials, Table 4.3) for apple juice was developed which yielded a first order rate constant value of  $0.0073 \text{ min}^{-1}$  ( $r^2=0.909$ ).

#### 4.6.2. Kinetic rate equations expressed in terms of vitamin C

Kinetic rate constant values, based on vitamin C changes are not required to use the finite element model, since it simulates oxygen diffusion. However it was necessary to assess the extent of vitamin C degradation because of its dependence on the availability of oxygen during the reaction in water and apple juice.

Several empirical kinetic models were developed, including fractional order "n"; however, based on regression analysis other models resulted in the best fit.

All the kinetic models which describe vitamin C degradation

**Table 4.3.- Kinetic data for apple juice (0.272 mM vit. C) at 25°C in a closed system. The first order reaction rate constant was 0.0073 min<sup>-1</sup>**

<b><u>Oxygen Partial Pressure in the Juice (atm)</u></b>			
<b><u>Time *</u></b>	<b><u>Trials</u></b>		
<b><u>(min)</u></b>	<b><u>1</u></b>	<b><u>2</u></b>	<b><u>3</u></b>
0-0-0	.21	.21	.21
4-10-6	.202	.196	.205
10-20-10	.181	.177	.199
20-30-16	.158	.159	.188
30-40-20	.141	.145	.183
40-50-26	.130	.135	.176
50-60-30	.121	.127	.172
60-70-40	.115	.121	.166
70-80--	.112	.119	--
80 -- --	.109	---	--

**\* This time column contains the corresponding times for each trial separated by a dash.**

are based on total percentage (%), where the initial vitamin C content expressed in mM was used as a 100 %.

#### 4.6.2.1. Water with added vitamin C.

Experimental results showed no significant changes in the vitamin content in water containing 11.4 mM vit. C in a closed system (no oxygen diffusion into the water) at any of the following initial oxygen levels: 0.08, 0.12 and 0.21 atm. This was expected since dissolved oxygen was very limited and vitamin C was in excess.

Only 0.05 mM vitamin C was retained within the first two hours for water containing initially 0.284 mM vitamin C. It remained unchanged for the next 24 hours. No empirical model was developed for this case.

For water containing 0.34 mM vitamin C, with continuous supply of oxygen, an empirical model, represented by power Equation (4.8) was obtained:

$$C = (C_0)t^{-b} \quad (4.8)$$

where:

$C$  = Vitamin C content (mole/L)

$C_0 = 7.1 \times 10^{-4}$  mole/L (model constant)

$b = 0.249 \text{ min}^{-1}$  (model constant)

This power equation ( $r^2=0.927$ ) was also obtained by regression analysis of the experimental data shown in Table 4.4

#### 4.6.2.2. Apple juice added with vitamin C

Kinetic results for apple juice in a closed system indicate that no significant degradation of vitamin C occurred within 24 hours for juice containing 0.227 mM vitamin C, and within 50 hours for juice containing 2.23 mM vitamin C. The initial oxygen level was 0.21 atm.

No significant changes for the higher vitamin content were expected, since the vitamin C concentration was set to be about 9 times greater than oxygen.

**Table 4.4.- Kinetic data for vitamin C degradation in water at 25<sup>0</sup>C, with constant supply of oxygen and initial vitamin C content of 0.341 mM**

<u>Time</u> <u>(min)</u>	<u>Vit. C**</u> <u>(%) *</u>
0	100
15	98
45	93.5
225	47.67
765	41.17

**\* This percentage is calculated based on the initial vitamin C content of 0.341 mM taken as a 100%.**

**\*\* Average of two trials.**

**Table 4.5.- Kinetic data for vitamin C degradation in apple juice at 25<sup>0</sup>C with constant supply of oxygen and initial vitamin C content of 0.272 mM**

<u>Time</u> <u>(min)</u>	<u>Vit. C*</u> <u>(%)</u>
0	100
15	95.8
45	96.8
105	94.8
165	90.6

**\* Average of two trials**

The no significant vitamin content changes in the apple juice containing 0.227 mM might be due to some unidentified protective factors such as the high content of soluble solids (11.2 mg).

When oxygen was in constant supply to the reacting apple juice, then significant changes were noticed for juice samples containing 0.272 mM and 3.157 mM vitamin C.

In Table 4.5 are kinetic data for the apple juice containing 0.272 mM vitamin C. Regression analysis yielded an empirical linear model suggesting an "apparent" zero order chemical reaction. It is termed "apparent" as compared to the true value because the reaction was not carried out to at least its 75% completion (for a correct determination of kinetic constants).

However, in this study, the zero order constant value of  $2.7 \times 10^{-7} \text{ M/min}$  was useful to assess vitamin C degradation within the time frame covered by the finite element model.

Statistical analysis of the kinetic data for the 3.157 mM apple juice (Table 4.6) reveals an empirical power model (Equation 4.8) similar to that used for the 6mg water system. In this case, the constants were  $4.9 \times 10^{-3} \text{ mole/L}$  for  $C_0$  and  $0.196 \text{ min}^{-1}$  for b.



**Table 4.6.- Kinetic data for vitamin C degradation in apple juice at 25°C with constant supply of oxygen and initial vitamin content of 3.157 mM**

<u>Time</u> <u>(min)</u>	<u>Vit. C*</u> <u>(%)</u>
0	100
30	72.95
60	80.79
180	54.57
240	50.57
480	41.77
1170	41.27
1596	36.51

**\* Average of two trials**

**Table 4.7.- Experimental retention values of vitamin C in water and apple juice at 25°C. Semi-infinite and cylindrical cell systems.**

<u>Set No.</u>	<u>Elapsed time</u> <u>(min)</u>	<u>Init. Vit. C</u> <u>(mM)</u>	<u>Init. P</u> <u>(atm)</u>	<u>Vit. C Ret.</u> <u>(%)</u>	<u>System*</u>
1	2665	0.337	0.0	43.9	W., S.I., No barrier
2	4408	0.243	0.06	94.9	A.J., S.I., No barrier
3	2470	1.506	0.125	98.1	A.J., HDPE barrier
4	2490	1.303	0.21	94.5	A.J., HDPE barrier

**\* W = water; S.I. = semi-infinte system; A.J. = apple juice**

The nonconsistent kinetic models presented above suggest a complex reaction mechanism, and a simple rate equation would be only an approximation (Davidson and Grieger-Block, 1977). It was not the objective of this work to make an in depth study of the reaction mechanism for oxidation of vitamin C.

The kinetic models and the corresponding kinetic rate constants (atm) developed in this work, provided the necessary input parameters to the finite element computer programs in order to predict oxygen partial pressures in water and apple juice.

#### 4.7. Liquid resistance to oxygen absorption

The data in Figure 4.15 show that for about the first 200 minutes, the oxidation rate of vitamin C in the apple juice is much faster than oxygen diffusion to the center of the cylindrical cell. This is indicated by the rapid decrease in oxygen partial pressure, and it means that oxygen diffusion is the limiting factor during this initial period, regardless of vitamin C content (low or high)

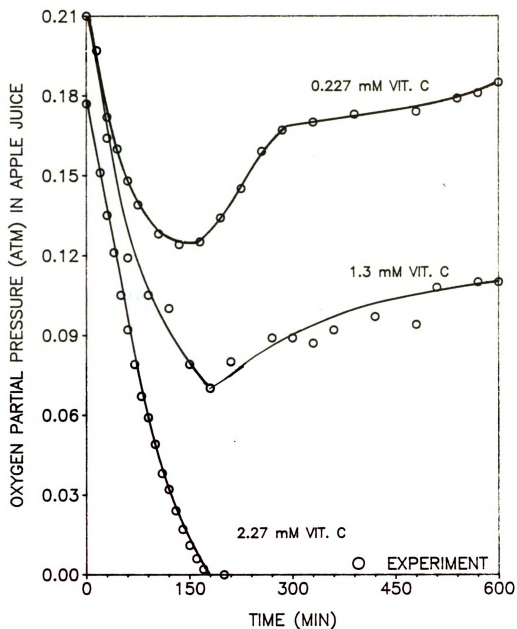


FIGURE 4.15 EFFECT OF VITAMIN C CONTENT ON THE RESISTANCE TO OXYGEN ABSORPTION IN APPLE JUICE (CYLINDRICAL PERMEABLE (HDPE) PACKAGE)

At a low initial vitamin content (0.227 mM), oxygen partial pressure begins to increase after about 200 min, indicating that the chemical reaction rate now becomes the limiting factor (Figure 4.15). A similar situation was observed in water (Figure 4.16) with low vitamin content (0.341 mM). Further discussion of this matter is presented in section 4.10.

#### 4.8. Experimental retention of vitamin C

Amount of vitamin C remaining after exposure to dissolved oxygen in apple juice is shown in Table 4.7 (page 108). For the two cases of apple juice in the HDPE barrier (sets 3 and 4), retention was about 95% (of the total) or better; indicating some barrier effect, which was similar to what happens in a closed system already described, where no absorption of oxygen from the outside air takes place, and negligible vitamin degradation is observed.

Even for the semi-infinite open system (set 2) with no permeable membrane, retention was still very high (94.9%) suggesting that combination of at least four factors: thickness of the juice layer (1.5 cm), pH, low oxygen levels, and soluble solids, exercise a protective effect against degradation of vitamin C.

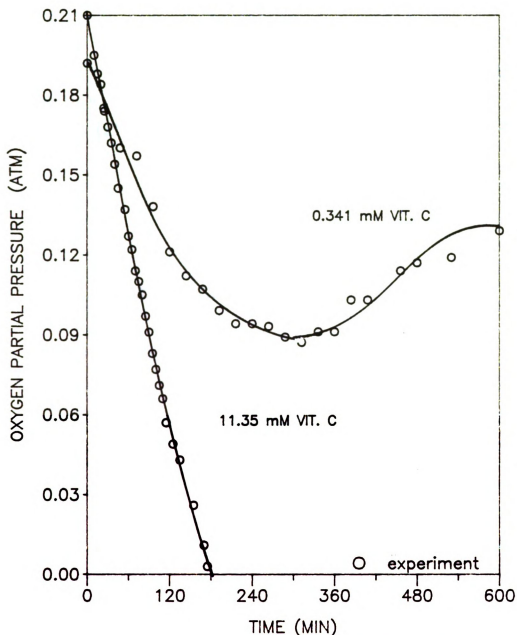


FIGURE 4.16 EFFECT OF VITAMIN C CONTENT ON THE RESISTANCE TO OXYGEN ABSORPTION IN WATER PACKAGED IN A CYLINDRICAL PERMEABLE (HDPE) CONTAINER

Lower retention (43.9%) was expected and observed for the semi infinite water open system, since the protective effect of soluble solids is not available in this case. Most of the retention power appears too be derived from the low oxygen levels (almost zero atm) and the 1.5 cm layer thickness.

#### 4.9. Finite Element Computer Models

##### 4.9.1. Rectangular coordinates ( one dimension)

##### 4.9.1.1. Oxygen diffusion

Uni-dimensional oxygen diffusion was modeled by two finite element computer models. One was developed by Segerlind (1984) and was described in the Materials and Methods chapter, and the second was adapted from ANSYS (1988) to represent a semi infinite liquid system (Figure 4.17) with no convective movements.

The finite element model for this system is identified as STIF 33 in the ANSYS computer programs, described in Materials and Methods. The input parameters and description for this model are presented in Table 4.8.

**Table 4.8 .- Description of input parameters to the ANSYS computer program. Oxygen diffusion in a semi-infinite liquid system.**

<b>/PREP7</b>	<b>Preparation routine command</b>
<b>/TTITLE</b>	<b>Title of this particular computer run</b>
<b>KAN,-1</b>	<b>Thermal analysis option</b>
<b>ET,1,33</b>	<b>Element type 1, STIF 33</b>
<b>R,1,4,374</b>	<b>Cross sectional area constant for element type 1</b>
<b>KXX,1,1</b>	<b>Oxygen diffusion</b>
<b>DENS,1,1</b>	<b>Model parameter not applicable in this situation, but necessary for computer compiling</b>
<b>C,1,1</b>	<b>Parameter not applicable but necessary for compiling</b>
<b>N,1</b>	<b>Node one at surface of liquid; zero distance</b>
<b>N,6,0.25</b>	<b>Node 6 at 0.25 cm from the surface</b>
<b>FILL</b>	<b>Command to generate more nodes between nodes 1 and 6</b>
<b>N,6,0.25</b>	
<b>N,11,0.75</b>	<b>Node 11 at 0.75 cm from the surface</b>
<b>N,16,1.5</b>	<b>Node 16 at 1.5 cm from the surface</b>
<b>FILL</b>	
<b>E,1,2</b>	<b>Nodes 1 and 2 to form element 1</b>
<b>EGEN,15,1,1</b>	<b>Command to generate 15 elements starting from element 1 and increasing the number by one</b>
<b>ITER 40,1,1</b>	<b>Number of iterations (time intervals) in increments of one</b>
<b>TIME,200</b>	<b>Total time (min)</b>
<b>TUNIF,0.21</b>	<b>Initial, uniform oxygen partial pressure</b>
<b>KBC,1</b>	<b>Step function at the boundary</b>
<b>NT,1,TEMP,0.21</b>	<b>Constant oxygen partial pressure of 0.21 atm at the surface boundary</b>
<b>AFWRIT</b>	<b>Compiling the program</b>
<b>FINISH</b>	<b>To terminate input</b>
<b>/EXE</b>	<b>To execute the program</b>
<b>/INPUT,27</b>	<b>To store results in file 27</b>
<b>/EOF</b>	<b>To terminate the session</b>

**The following parameters must be added to incorporate a zero order chemical reaction**

<b>KTEMP,-1</b>	<b>Command to indicate the presence of a chemical reaction</b>
<b>QE,1,-1.6E-4</b>	<b>Zero order kinetic rate constant in element 1</b>
<b>QEGEN,15,1,1</b>	<b>Generation of more kinetic constants in all 15 elements</b>





Equation (3.1) provides the basis to model a semi-infinite system or a symmetrical finite system, with  $k_{o,v} = 0$  and  $\lambda = 1$  for the no chemical reaction case.

#### 4.9.1.2. Oxygen diffusion and chemical reaction

In order to incorporate a chemical reaction factor into Equation (3.1), the  $k_{v,o}$  takes a definite value depending on the type of reaction. For zero order,  $k_{v,o}$  is equivalent to the constant generation rate  $q$  described in STIF 33.  $\lambda$  has a value of one. The ANSYS computer model requires three extra input parameters to simulate the simultaneous diffusion and chemical reaction: QE, QGEN and KTEMP, as shown in Table 4.8.

For a first order chemical reaction, the term  $q$  will depend on  $p$  becoming  $k_{v,1}(p)$ . This  $q$  term is obtained from the element type STIF 71, which is simultaneously implemented into the main computer program, as shown in Table 4.9.

For this first order case, the finite element model utilizes two types of elements: STIF 33 and STIF 71, in order to simulate the more complicated simultaneous oxygen diffusion and reaction.

**Table 4.9- Description of input parameters too the ANSYS computer program. Oxygen diffusion in a semi infinite liquid system with simultaneous chemical reaction. (\*)**

/PREP7	
/TITLE	
KAN,-1	
ET,1,71	Element type 1, STIF 71
ET,2,33	Element type 2, STIF,33
N,1	
N,5,0.25	
FILL	
N,5,0.25	
N,11,1.5	
FILL	
E,1	
RP11,1	Generation of eleven elements in increments of one
R,1,1,0,-0.0051	First order reaction rate constant
RP11,1	Generation of eleven rate constants (one for each element)
*CREATE,GPO	This is a subroutine to assign the rate constants to elements of the element type STIF71
TYPE,1	
REAL,ARG1	
*END	
*USE,GPO,1	
RP11,,1	Last command of subroutine
TYPE,2	To indicate that the following parameters will be assigned to element type 2: STIF 33
KXX,1,1.2E-3	
DENS,1,1	
C,1,1	
E,1,2	
EGEN,10,1,1	
R,12,4.374	
RP10,1	
*CREATE,GP2	
TYPE,2	
REAL,ARG1	
*END	
*USE,GP2,1	
RP10,1	
ITER,40,1,1	
TIME,200	
TUNIF,0.21	
KBC,1	

**(Table 4.9 continued)**

NT,1,TEMP,0.21

AFWRIT

FINISH

/EXE

/INPUT,27

/EOF

---

(\*) Model parameters not described here were already described in Table 4.8

#### 4.9.2. Cylindrical coordinates (two dimensions)

##### 4.9.2.1. Oxygen diffusion

Diffusion of oxygen in water or apple juice, packaged in a cylindrical permeable container, was modeled by element STIF 70 as described in Materials and Methods. A representative section (slice) of the cylindrical system is shown in Figure 4.18.

A description of the input parameters for this cylindrical model is shown in Table 4.10. Equations (3.21) through (3.30) represent the basis for the finite element model. Appropriate substitutions are made in order to suit the ANSYS nomenclature.

##### 4.9.2.2. Oxygen diffusion and chemical reaction

The use of appropriate reaction rate constants is necessary in order to include the effect of a chemical reaction in the oxygen diffusion process. The rate constant is represented by  $q$  (Equation 3.9).

For a zero order, the rate constant  $k_{v,0}$  is represented by Equation (3.45) in oxygen partial pressures.

For a first order, the rate constant  $k_{v,1}$ , dependent upon oxygen partial pressure and is represented by Equation 3.46 in

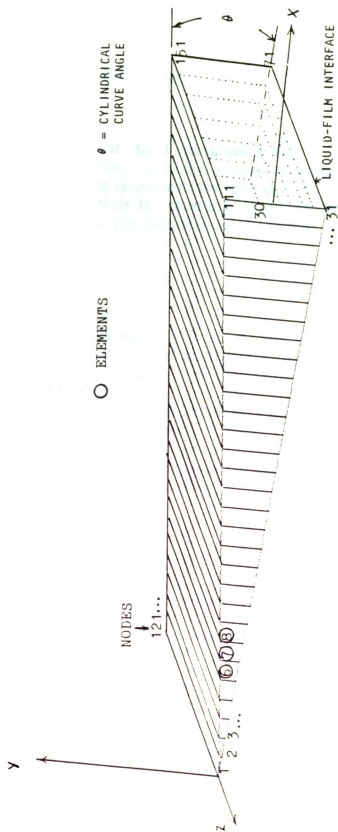


FIGURE 4.18 FINITE ELEMENT MODEL FOR A CYLINDRICAL PERMEABLE CELL.  
REPRESENTATION OF A CYLINDRICAL (SLICE) SECTION.

**Table 4.10 - Description of input parameters to the ANSYS computer program. Oxygen diffusion in a cylindrical permeable cell.**

```

/REP7
/TITLE
KAN,-1
ET,1,70          Element type 1, STIF 70
KXX,1,8.5E-4
DENS,1,1
C,1,1
CSYS,1          Cylindrical coordinates option
N,1,0,-5        Node one located at center of cylinder (0 cm) with a 5 angle
                  to approximate the curve surface
N,31,3.512,-5   Node 31 located at 3.512 cm from the center with a 5 angle
                  to approximate the curved surface

FILL
N,41,0,5
N,71,3.512,5
FILL
NGEN,2,80,1,71,1,,,7.62
                  Generation of 2 sets of nodes, increments of 80, starting from
                  node 71, and proceeding one by one. 7.62 is the height of the
                  cylindrical
E,1,2,42,42,81,82,122,122
                  First element formed by 8 nodes with the corresponding
                  node numbers
E,2,3,43,42,82,83,123,122
EGEN,29,1,2      Generate 29 elements in increments of one starting with
                  the second element

KBC,1
ITER,40,1,1
TIME,200
TUNIF,0.21
CV,31,71,8.7E-4,0.21,,,151,111
                  Permeability properties at the surface, identified with node
                  31,71,151,and 111. 0.21 atm is oxygen partial pressure in air
                  9.44E-4 is the converted value of permeability constant.

AFWRIT
FINISH
/EXE
/INPUT,27
/EOF
Add the following parameters to incorporate a zero order reaction
KTEMP,-1
QE,1,1.567E-4
QGEN,30,1,1

```

oxygen partial pressures.

In Tables 4.10 and 4.11 are shown the respective descriptions of input parameters for the zero and first order models.

The ANSYS computer programs are very flexible and useful to cover a variety of modeling situations. The most difficult task is to identify the physical problem and to adapt it to the appropriate element or elements available in ANSYS.

#### 4.10. Validation of the Finite Element Computer Models

Exhaustive verification of the FE computer models has been carried out by their developers (ANSYS,1982) as demonstrated on a verification manual with more than a 100 solved problems taken from the literature.

In this study, additional verification was generated using the analytical method to solve a comparative heat transfer problem (Geankoplis,1984).

The same analytical method was used to predict dissolved oxygen in water packaged in an Alethan cylindrical cell to compare with predictions using the FE model as shown in Figure 4.19. The average absolute error was 9%. The oxygen coefficient in water (Section 3.2.3) was used to convert oxygen partial pressures.

**Table 4.11 - Description of input parameters to the ANSYS computer program. Simultaneous oxygen diffusion and chemical reaction in food liquids packaged in a permeable cylindrical cell.**

```
/PREP7
/TITLE
KAN,-1
ET,1,70

ET,2,71
KXX,1,8.5E-4
DENS,1,1
C,1,1
CSYS,1
N,1,0,-5
N,31,3.512,-5
FILL
N,41,0,5
N,71,3.512,5
FILL
NGEN,2,80,1,71,1,,,-7.62
E,1,2,42,42,81,82,122,122
E,2,3,43,42,82,83,123,122
EGEN,29,1,2
TYPE,2
E,1
RP31,1
TYPE,2
E,41
RP31,1
TYPE,2
E,81
RP31,1
TYPE,2
E,121
RP31,1
R,1,1,0,-0.0073
RP124,1
*CREATE,GRP
TYPE,2
REAL,ARG1
*END
*USE,GRP,1
RP124,,1
ITER,20,1,1
TIME,200
```



**(Table 4.11 continued)**

TUNIF,0.21  
CV,31,71,8.7E-4,0.21,,,151,111  
AFWRIT  
FINISH  
/EXE  
/INPUT,27  
/EOF

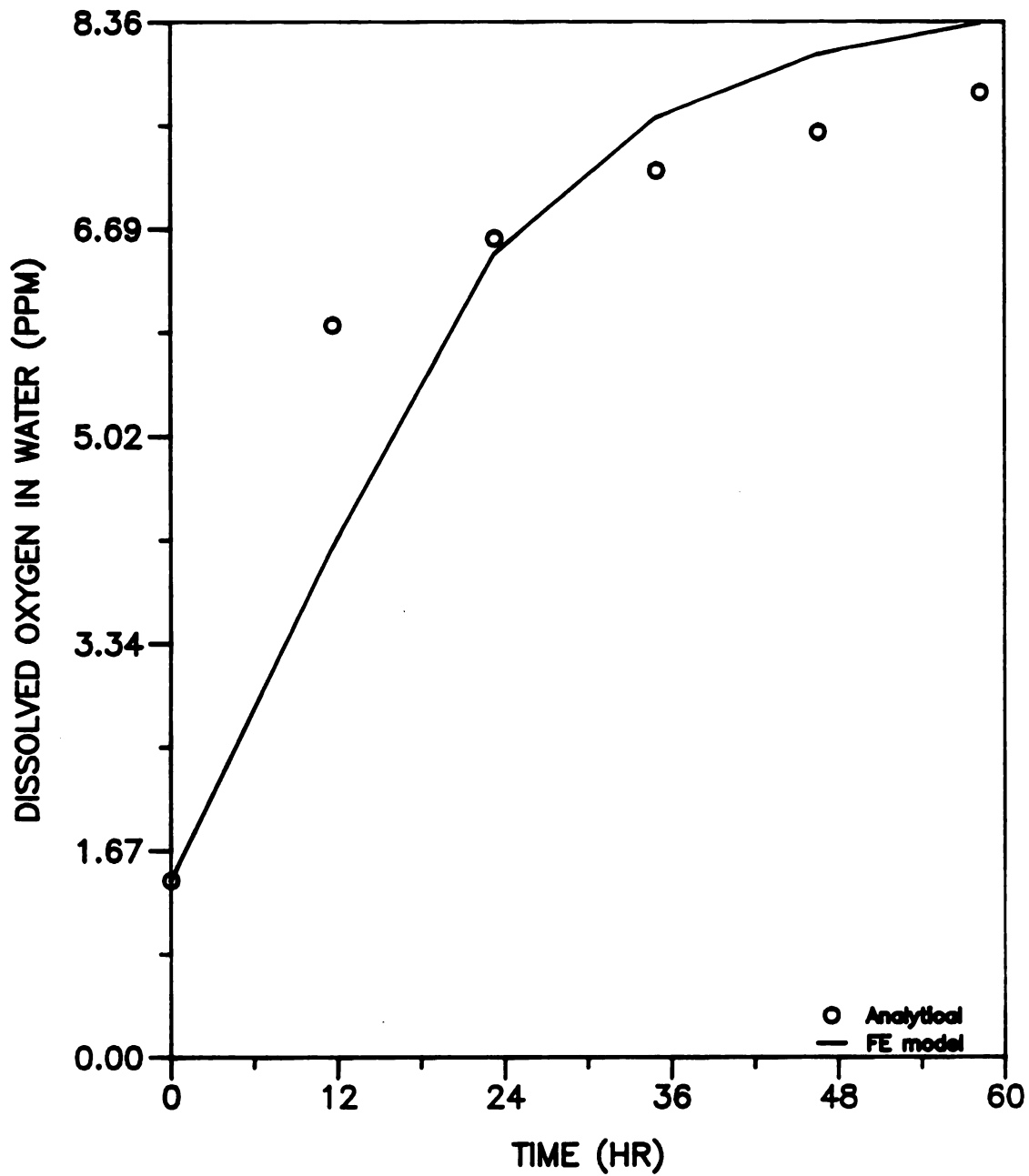


FIGURE 4.19 PREDICTED DISSOLVED OXYGEN IN WATER PACKAGED IN A CYLINDRICAL PERMEABLE (ALETHAN) CONTAINER. ANALYTICAL AND FINITE ELEMENT ESTIMATES

#### 4.10.1. Model verification for oxygen diffusion

Three basic FE computer models were developed and are verified as described below for representative cases.

Case 1. Water system (semi-infinite), with no permeable membrane (Figure 4.20).

Case 2. For this particular case, the FE model developed by Segerlind (1984) was also validated (Figure 4.21) for the one dimension diffusion in a 0.5 cm water layer (Figure 3.4). No chemical reaction and permeable membrane were used.

Case 3. Apple juice (semi-infinite system) contained in a long glass graduated cylinder (Figure 4.22).

Case 4. Water contained in a cylindrical permeable membrane (Alethan) (Figure 4.23).

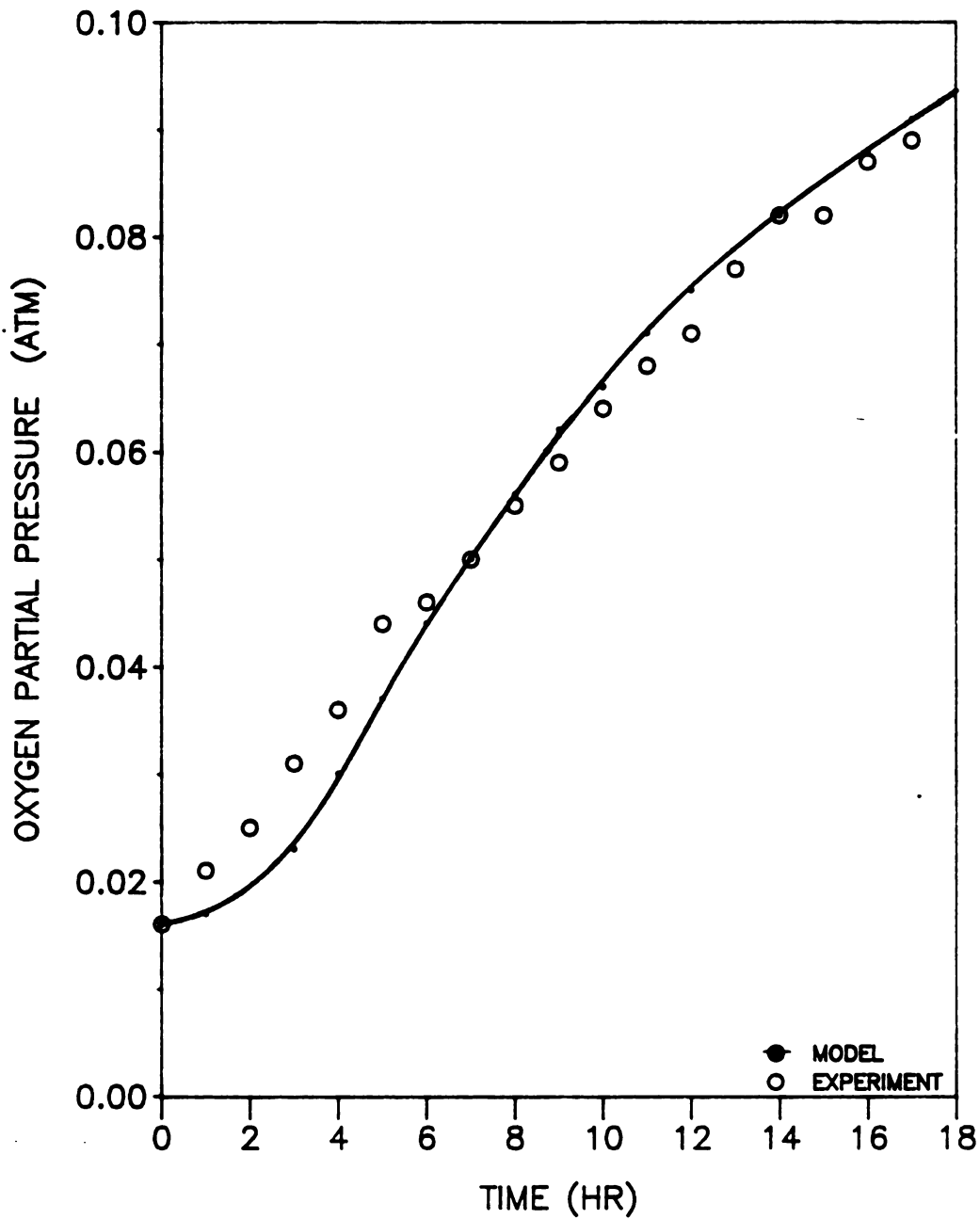


FIGURE 4.20 PREDICTED (FE) AND EXPERIMENTAL OXYGEN LEVELS IN A SEMI-INFINITE WATER SYSTEM. ONE DIMENSIONAL DIFFUSION

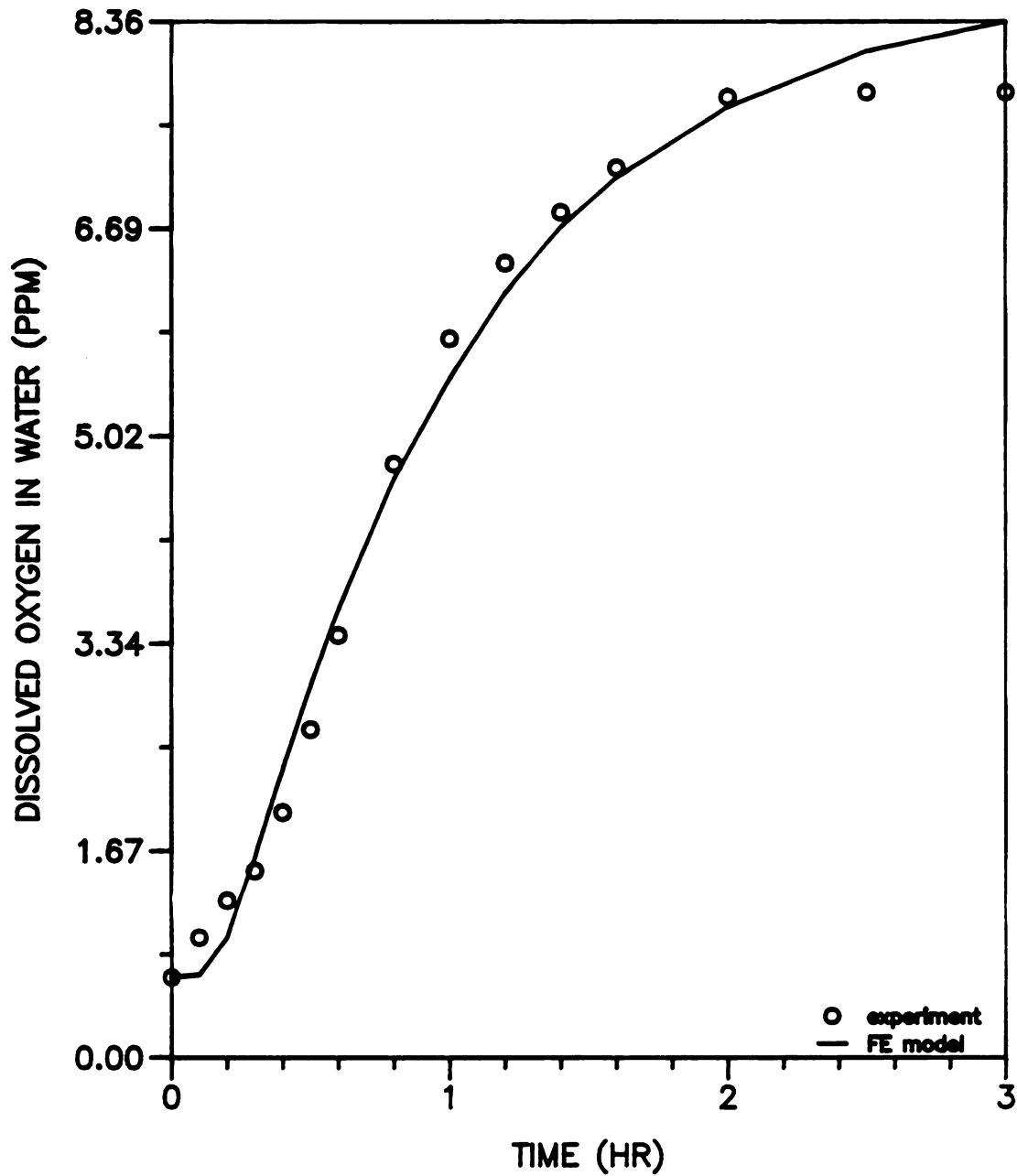


FIGURE 4.21 PREDICTED (FE, SEGERLIND,1984) AND EXPERIMENTAL DISSOLVED OXYGEN IN A 0.5 CM LAYER OF WATER AT 25°C. ONE DIMENSIONAL DIFFUSION

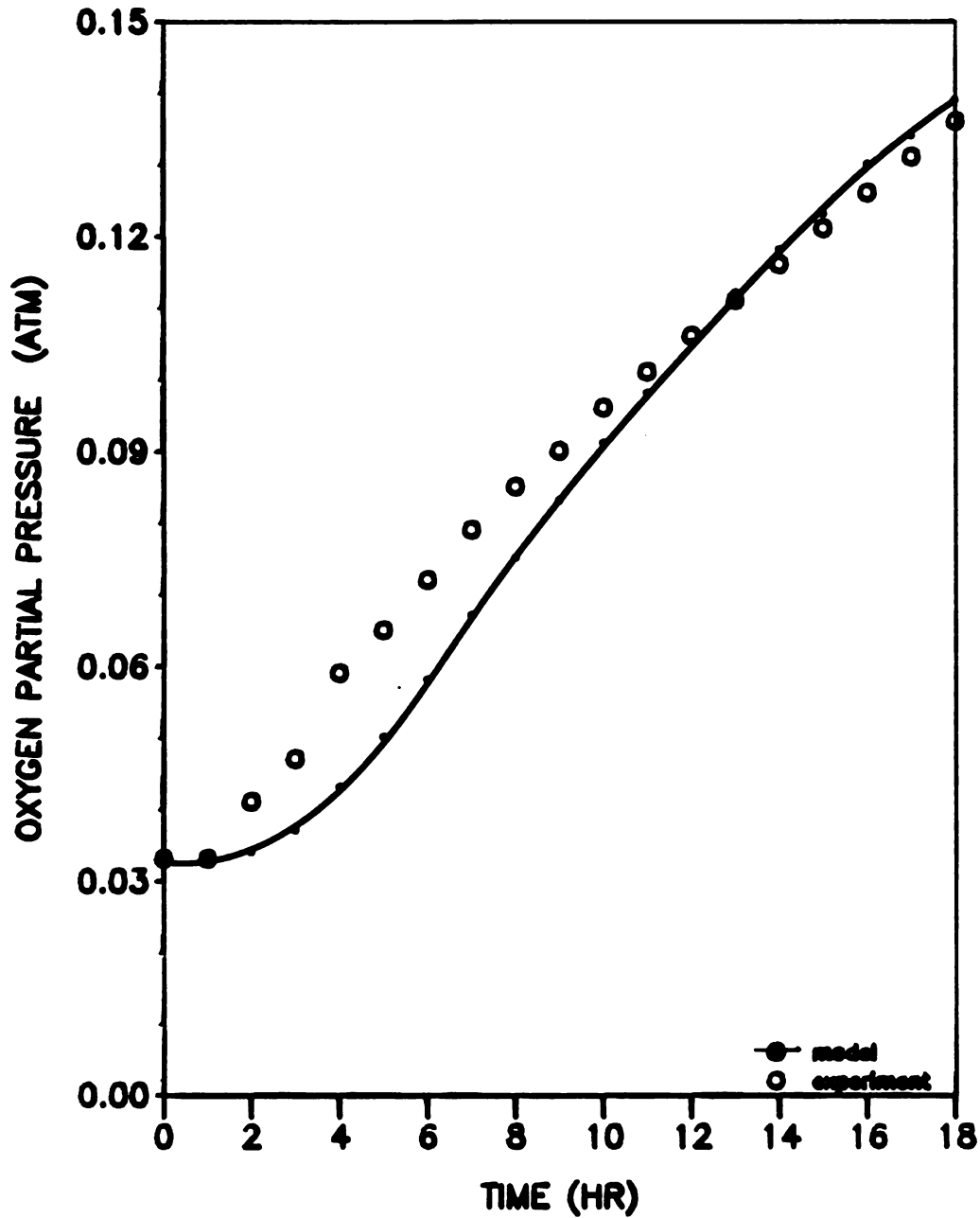


FIGURE 4.22 PREDICTED (FE) AND EXPERIMENTAL OXYGEN LEVELS IN A SEMI INFINITE APPLE JUICE SYSTEM. ONE DIMENSIONAL DIFFUSION

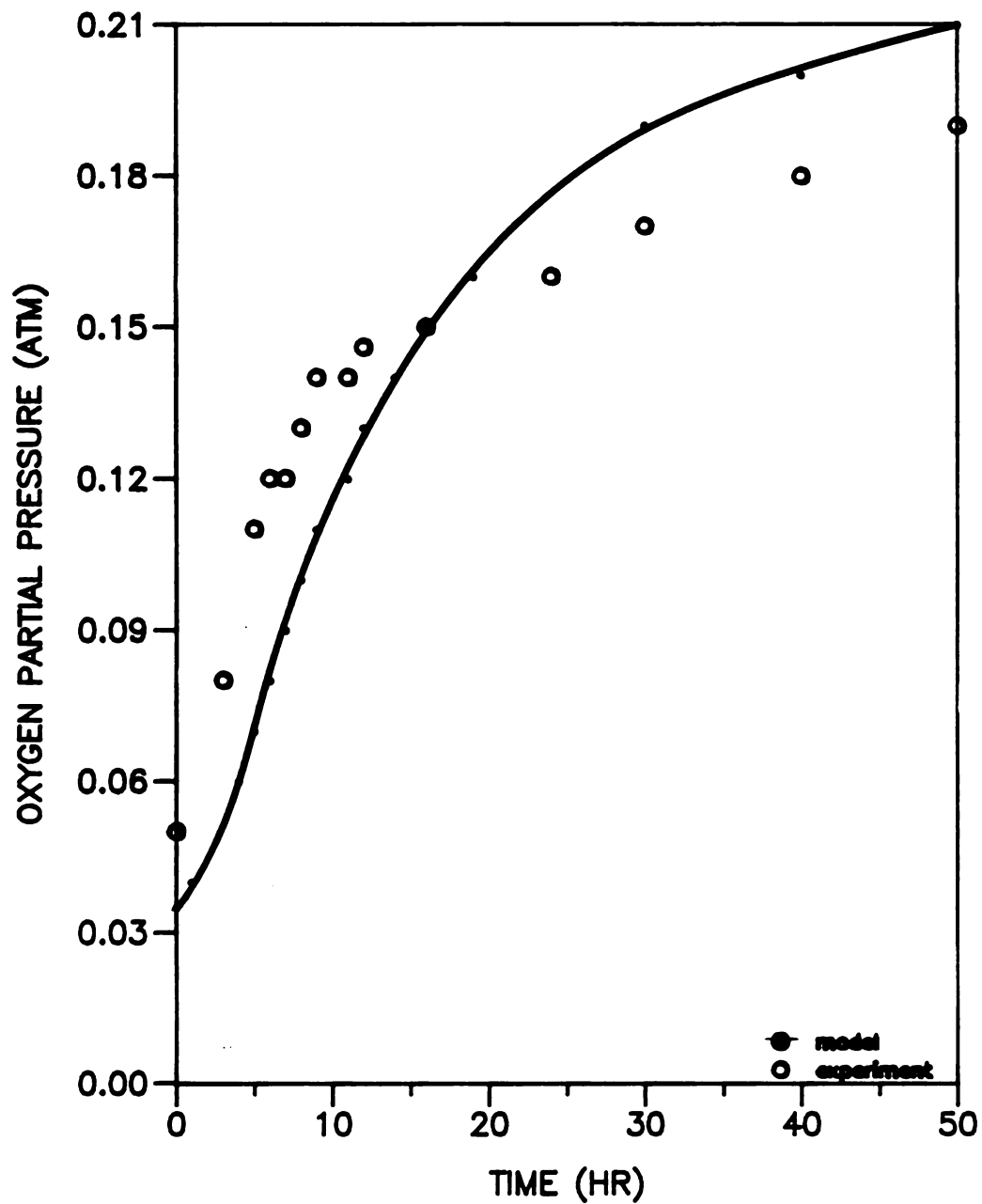


FIGURE 4.23 PREDICTED (FE) AND EXPERIMENTAL OXYGEN LEVELS IN WATER PACKAGED IN A CYLINDRICAL PERMEABLE (ALETHAN) CONTAINER

#### 4.10.2. Model verification for simultaneous oxygen diffusion and chemical reaction with vitamin C.

The simultaneous diffusion and first order reactions modeled in this study typically present a "U" oxygen profile, which can be divided into three parts: The first part of the "U" correspond to the oxygen decrease, following a minimum plateau as the second part. Finally, increase oxygen levels begin to show in the third part of the process.

As the amount of oxygen increases, it will eventually reach steady state values (0.21 atm)

Excess vitamin content in liquids requires large amounts of dissolved oxygen for total destruction of vitamin C. If diffusion of oxygen to the reaction site is limited, it will take a long time for total vitamin degradation and accumulation of oxygen.

This is the reason for having only the decreasing part of the oxygen "U" profile in the diffusion and a zero order reaction. The increasing part of the "U" profile begins as soon as accumulation of oxygen occurs.

Verification of the FE models for the simultaneous oxygen diffusion and chemical reaction is demonstrated in the following representatives cases:



Case 5. Water containing 0.341 mM vitamin C (semi infinite) with no permeable membrane (Figure 4.24).

Case 6. Water with 0.341 mM vitamin C contained in a cylindrical permeable cell (HDPE) (Figure 4.25).

Case 7. Apple juice with 1.303 mM vitamin C contained in a cylindrical permeable cell (HDPE) (Figure 4.26).

In general, acceptable predictions were obtained for all representative cases. The average absolute error ranged from 2.3% (Figure 4.21) to 12.5% (Figure 4.23).

This indicates that the FE models are capable of simulating the oxygen diffusion alone or simultaneous with a chemical reaction where oxygen is consumed.

Apparently, the major source of the above stated errors is caused by the variable sensor response, which is more critical at the beginning of the diffusion process, especially when a reaction is taking place. The variable response appears to be related to the teflon membrane at the tip of the sensor.

This membrane is responsible for allowing oxygen from the liquid into the electrode housing where it is then detected and subsequent voltage readings result.

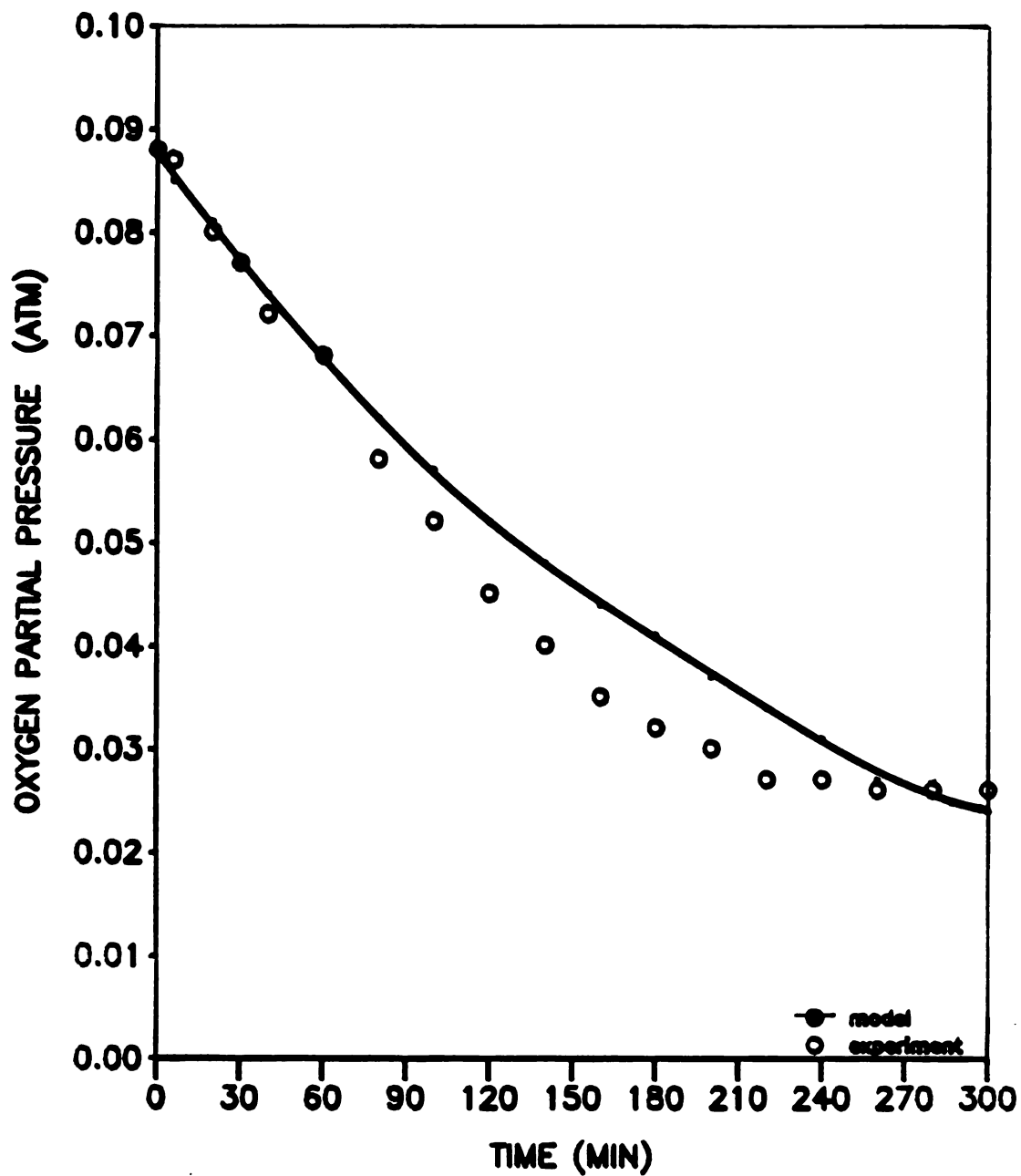


FIGURE 4.24 PREDICTED (FE) AND EXPERIMENTAL OXYGEN LEVELS IN A SEMI-INFINITE WATER SYSTEM REACTING WITH VITAMIN C (0.341 mM)

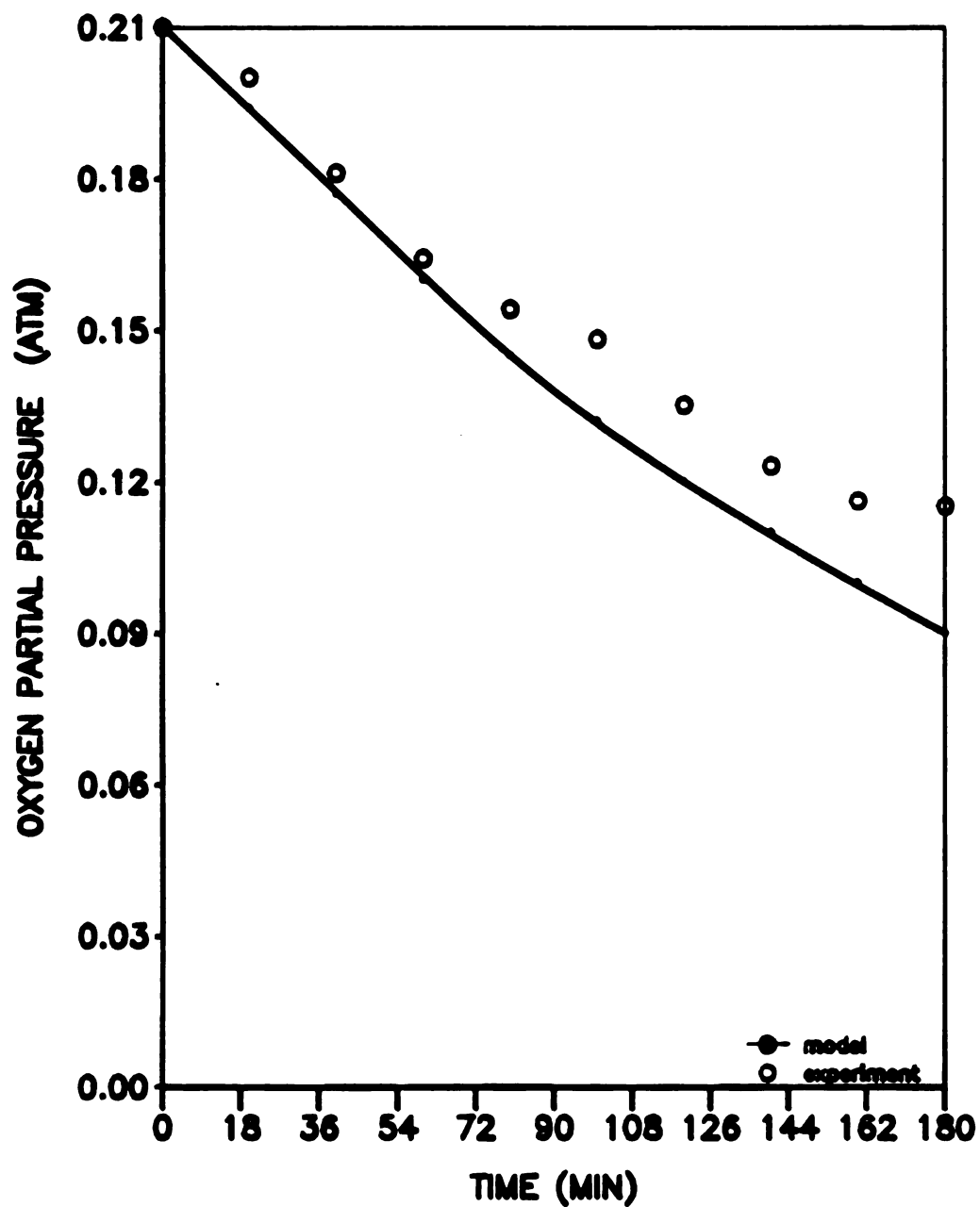


FIGURE 4.25 PREDICTED (FE) AND EXPERIMENTAL OXYGEN LEVELS IN WATER (HDPE) WITH SIMULTANEOUS DIFFUSION AND REACTION (0.341 mM VITAMIN C)

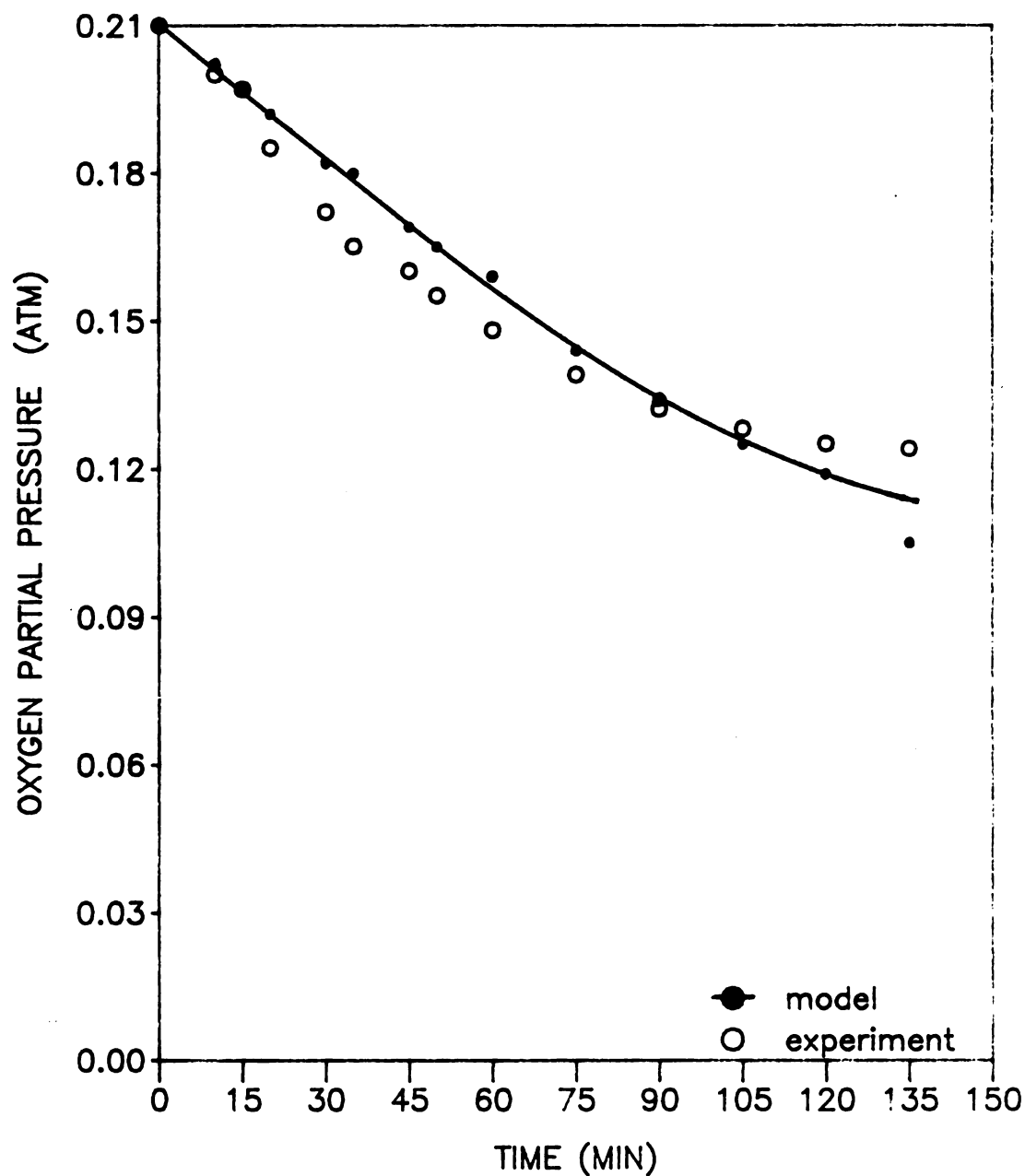


FIGURE 4.26 PREDICTED (FE) AND EXPERIMENTAL OXYGEN LEVELS IN APPLE JUICE (HDPE) WITH SIMULTANEOUS DIFFUSION AND REACTION (1.303 mM VIT. C)

According to manufacturers (Microelectrodes, Inc.), the teflon may allow water to pass into the electrode housing which can affect the reacting properties of the electrolyte solution. During the course of this study, improvements in this membrane were suggested and achieved, but the sensors still need to be perfected by the manufacturing company.

Saturation around the sensor tip area is another source of potential error. This originates due to the still conditions of the liquids. Other errors with apparent less effect are a result of the nonhomogeneous film thickness, location of the sensor in the cell, and measurements of cell dimensions. These errors were already discussed in appropriate sections.

#### 4.11. Effects of packaging variables on oxygen diffusion

A description of the effect of an oxygen saturated water surface on vitamin oxidation is shown in Figures 4.27 and 4.28. In Figure 4.27 it is shown that the lowest oxygen partial pressure levels exist below the water surface, in a thin layer of about 0.125 cm, which indicates that the reaction rate is faster than the oxygen diffusion rate during the first 100 min of the reaction process.

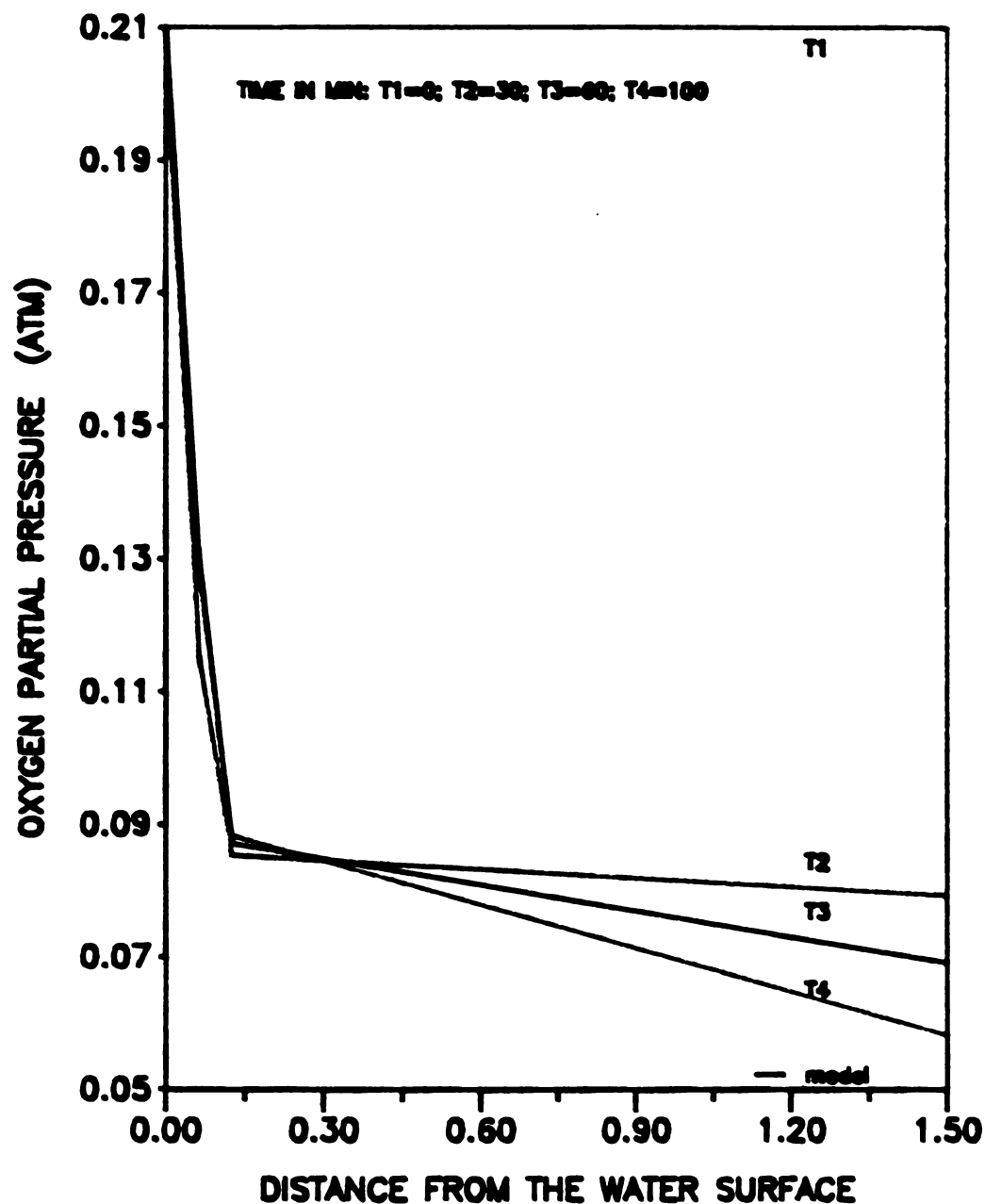


FIGURE 4.27 OXYGEN PROFILE IN A SEMI-INFINITE WATER SYSTEM WITH SIMULTANEOUS DIFFUSION AND REACTION WITH VITAMIN C (0.341 mM)

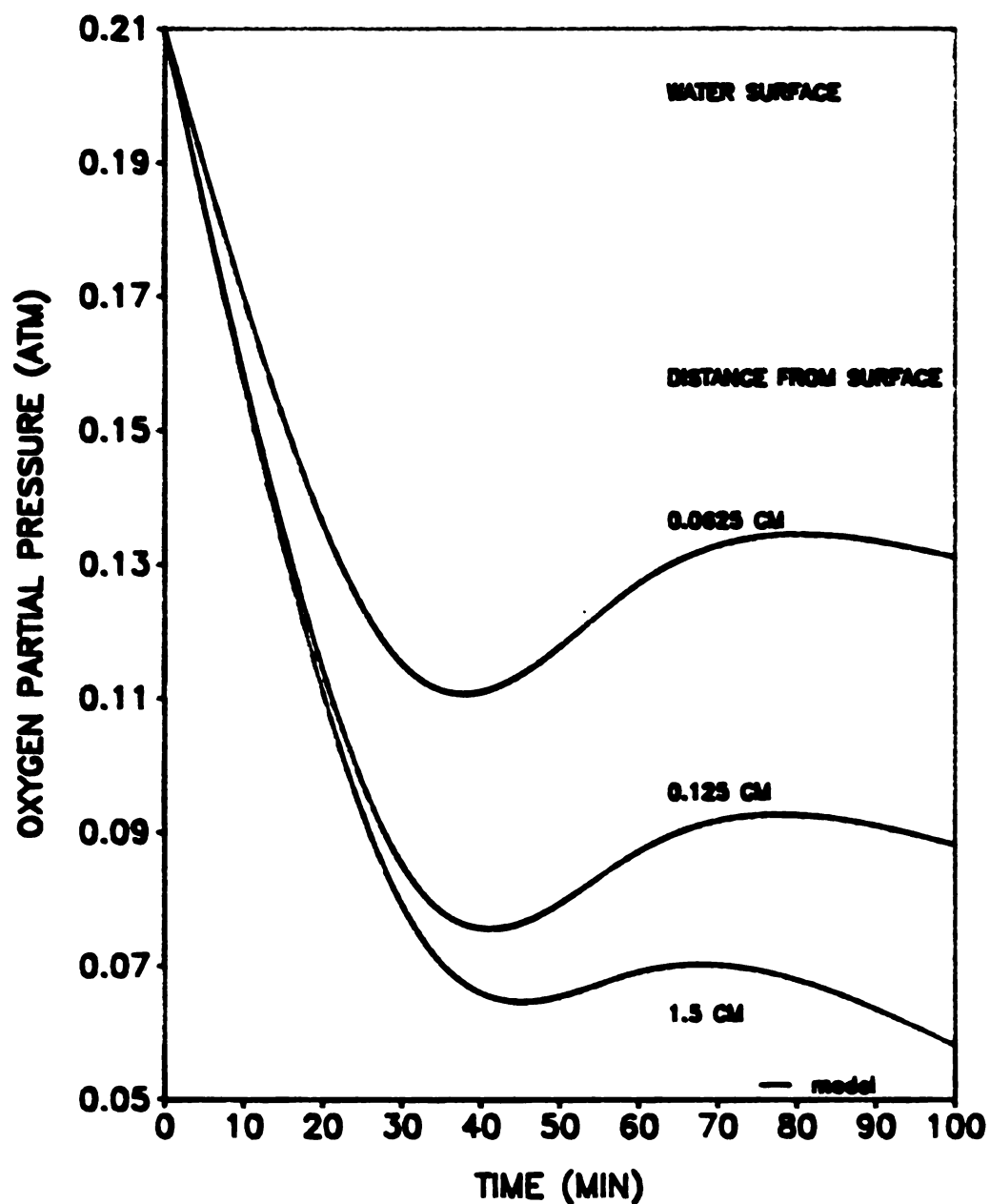


FIGURE 4.28 UNSTEADY STATE OXYGEN DIFFUSION AND REACTION IN A SEMI-INFINITE WATER SYSTEM (0.341 mM VIT. C)

At 1.5 cm from the surface, oxygen is still being consumed; at a distance closer to the surface, oxygen starts to accumulate during the first 100 min of the reaction (Figure 4.28). This indicates that the degradation of vitamin C is higher closer to the water surface than away from it.

Increasing levels of oxygen at the surface are indicative of vitamin degradation or that oxygen diffusion was faster than degradation of vitamin C. These observations agree with the fact that vitamin C retention drops to about 16% (total) within 120 min in the closed water system (Section 4.5.2.1).

The effect of the HDPE membrane on oxygen diffusion and reaction of vitamin C (0.341 mM) is shown in Figure 4.29. Uniform oxygen levels were predicted throughout the cylindrical container, at every time step.

As time increases, the oxygen levels decrease. These oxygen levels are slightly higher close to the surface membrane. This is due to the oxygen permeating in from the environment through the HDPE film.

The protective effect of the HDPE film is demonstrated by the oxygen gradients close to the membrane. These levels are not as steep as those observed in the open system, where the surface was not protected with HDPE.



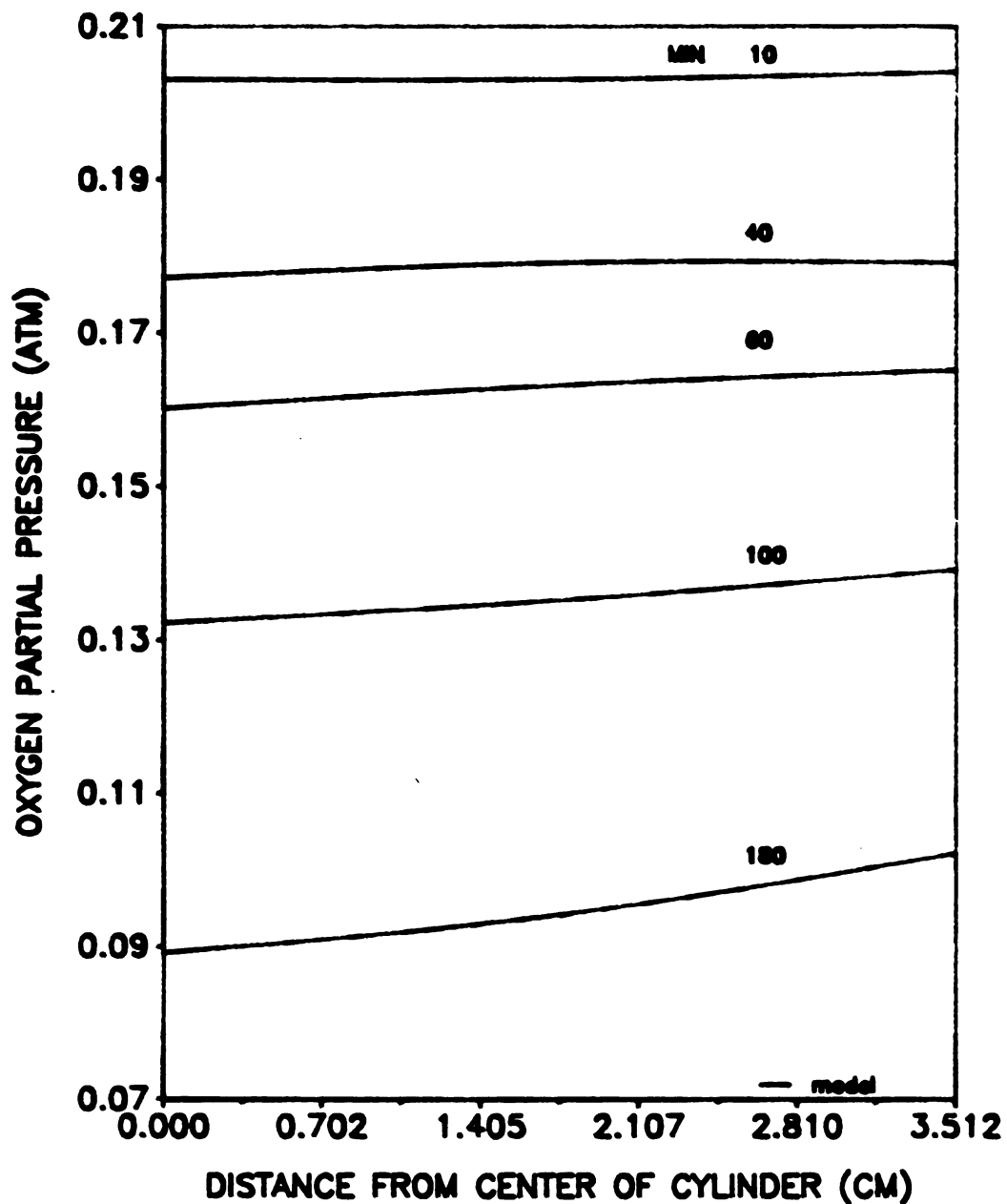


FIGURE 4.29 OXYGEN LEVELS AS A FUNCTION OF TIME AND LOCATION IN A CYLINDRICAL HDPE WATER SYSTEM REACTING WITH VITAMIN C (0.341 mM)

Within 180 minutes, the degradation of vitamin C is faster than oxygen diffusion at any location within the container (Figure 4.30). This means that oxygen molecules do not arrive the center of the container as fast as they are consumed by the reaction.

Similar results were obtained for apple juice (Figure 4.31 and 4.32) packaged in the HDPE cylindrical cell.

The FE model could be used to visualize the effect of other variables on oxygen diffusion, including the kinetic order of a degradative reaction, package permeability to oxygen, package shape and dimensions, physical properties of liquids (Diffusion coefficients), deaeration effects (initial oxygen levels) etc. The model could be applied to situations with specific purposes such as selecting packaging materials based on known permeability constants, or estimating oxygen distribution in a packaged liquid with known oxygen diffusivity.

As a sample application, assume that a liquid food, with similar characteristics as for water ( $D = 1.2 \times 10^{-3} \text{ cm}^2/\text{min}$ ), has a zero order rate constant of  $6.073 \times 10^{-4} \text{ atm/min}$  for a quality degradation reaction. The food is packaged in a cylindrical container of 7.024 cm diameter and has a permeability constant of  $10593.1 \text{ cc.mil/m}^2.\text{atm.day}$ .

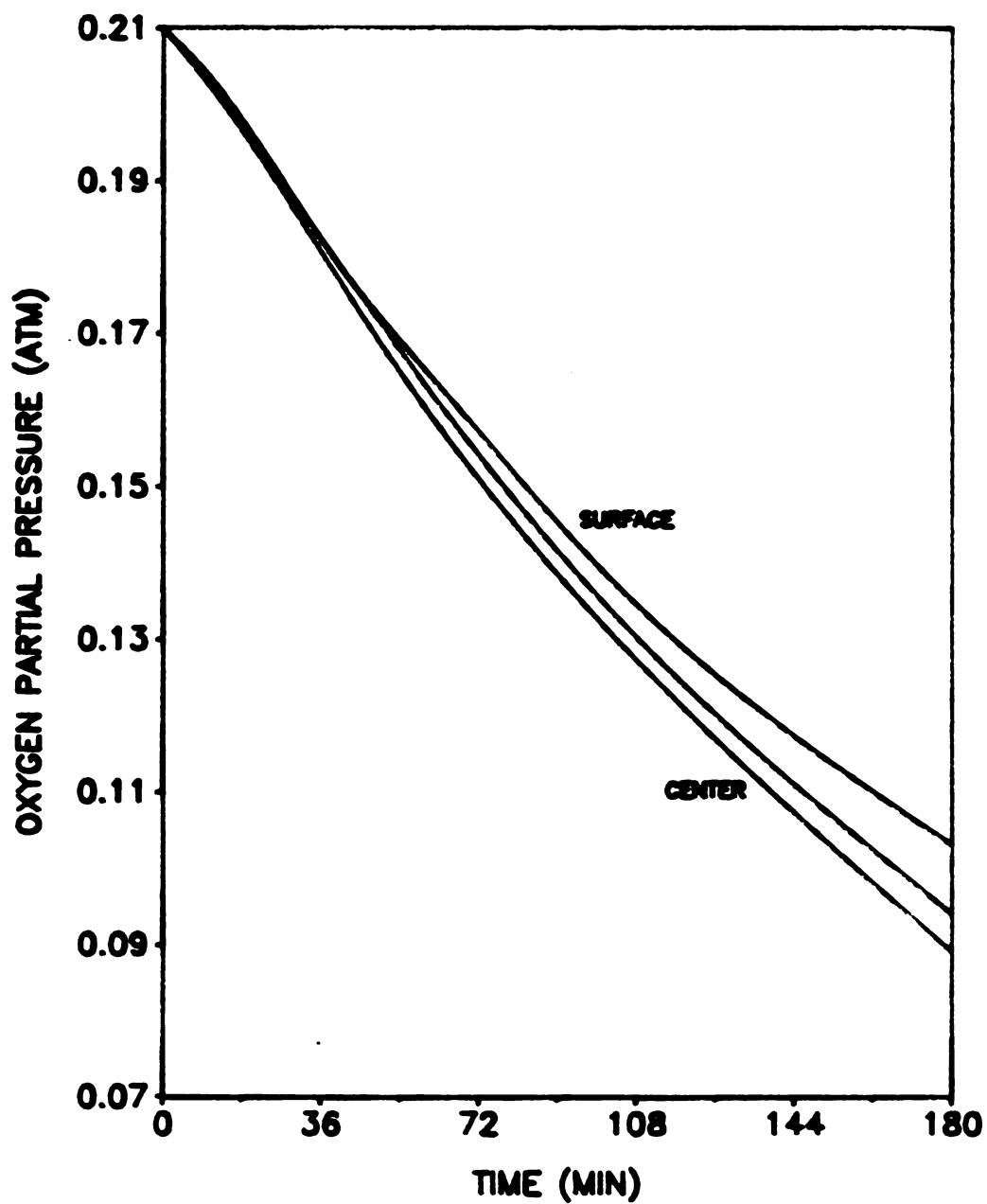


FIGURE 4.30 UNSTEADY STATE OXYGEN DIFFUSION AND REACTION IN A CYLINDRICAL HDPE WATER SYSTEM (0.341 mM VIT. C)

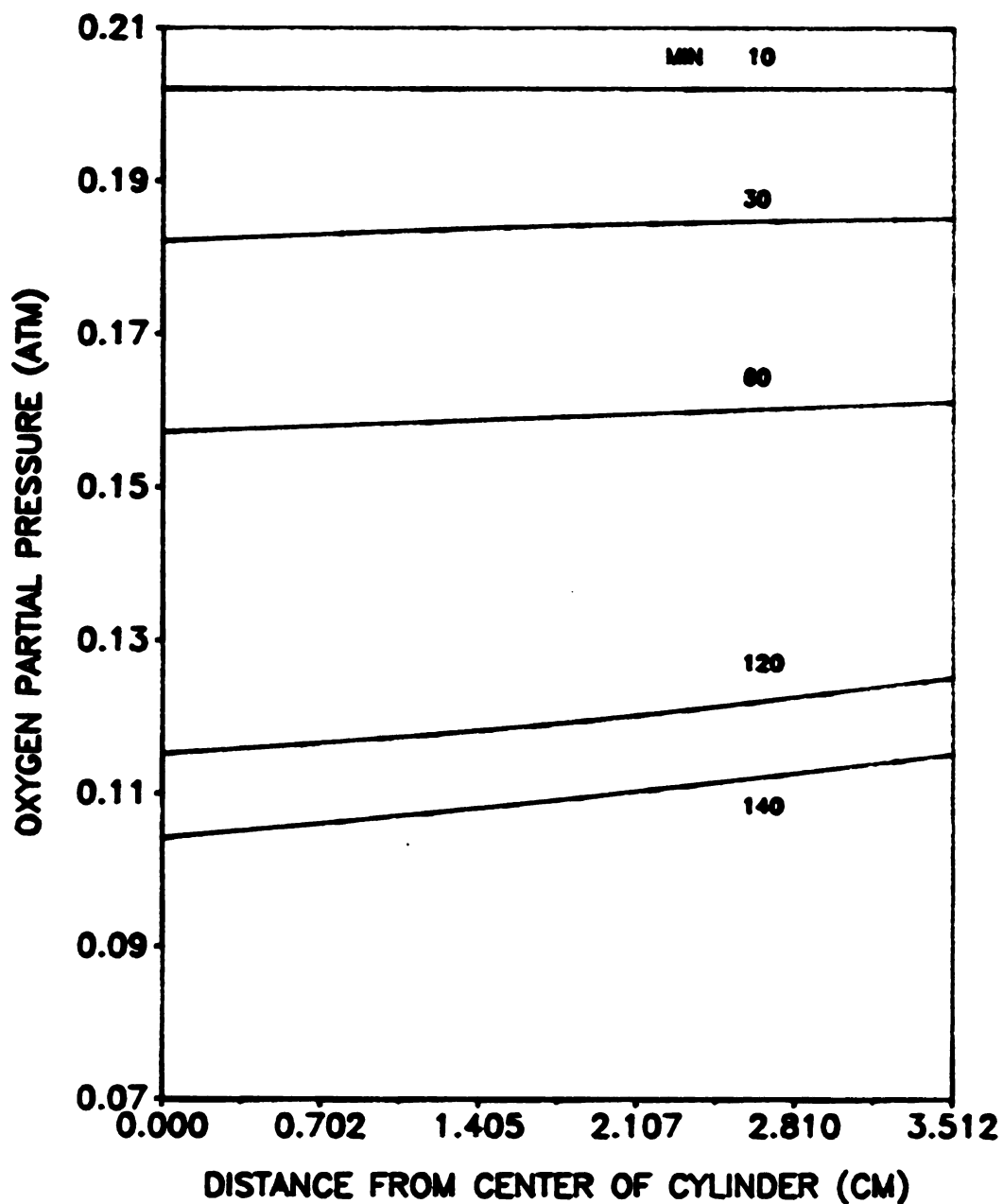


FIGURE 4.31 OXYGEN AS A FUNCTION OF TIME AND LOCATION IN A CYLINDRICAL HDPE APPLE JUICE SYSTEM REACTING WITH VITAMIN C (1.303 mM)

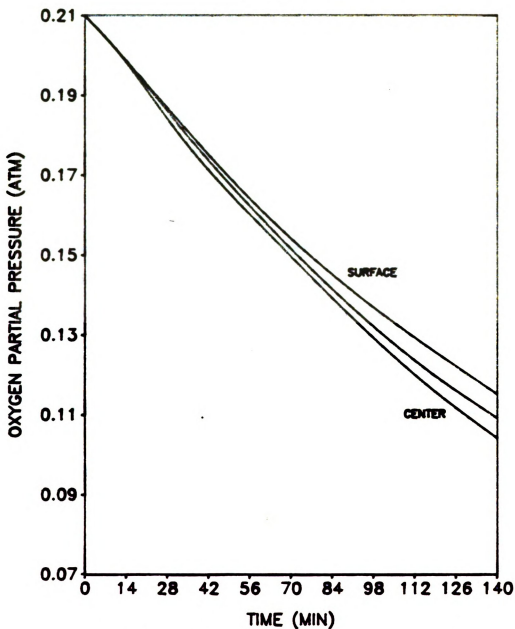


FIGURE 4.32 UNSTEADY STATE OXYGEN DIFFUSION AND REACTION IN A CYLINDRICAL HDPE APPLE JUICE SYSTEM (1.303 mM VIT. C)

deaeration was not performed, thus the product has an initial dissolved oxygen level of 0.10 atm. It is desirable to predict the diffusion of oxygen with and without the reacting quality factor, and what would be the effect of the diameter of the package on oxygen predictions. The simulation of the diffusion process is shown in Figure 4.33.

Steep oxygen gradients are observed in a layer of about 0.6 cm close to the surface, therefore quality degradation is expected to be high in this critical region, which is about the same thickness regardless of the presence of the quality factor (dotted vertical line). The distance (package diameter) is not important since the critical region is very thin, about 16% of the radius.

Oxygen absorption rates (lines above the 0.10 atm level) are smaller than the oxygen consumption rates (below 0.10 atm) (Figure 4.34). This limitation presented by the diffusion rate is in agreement with the results from the similar situation described for the first order case in water and apple juice (Section 4.6)

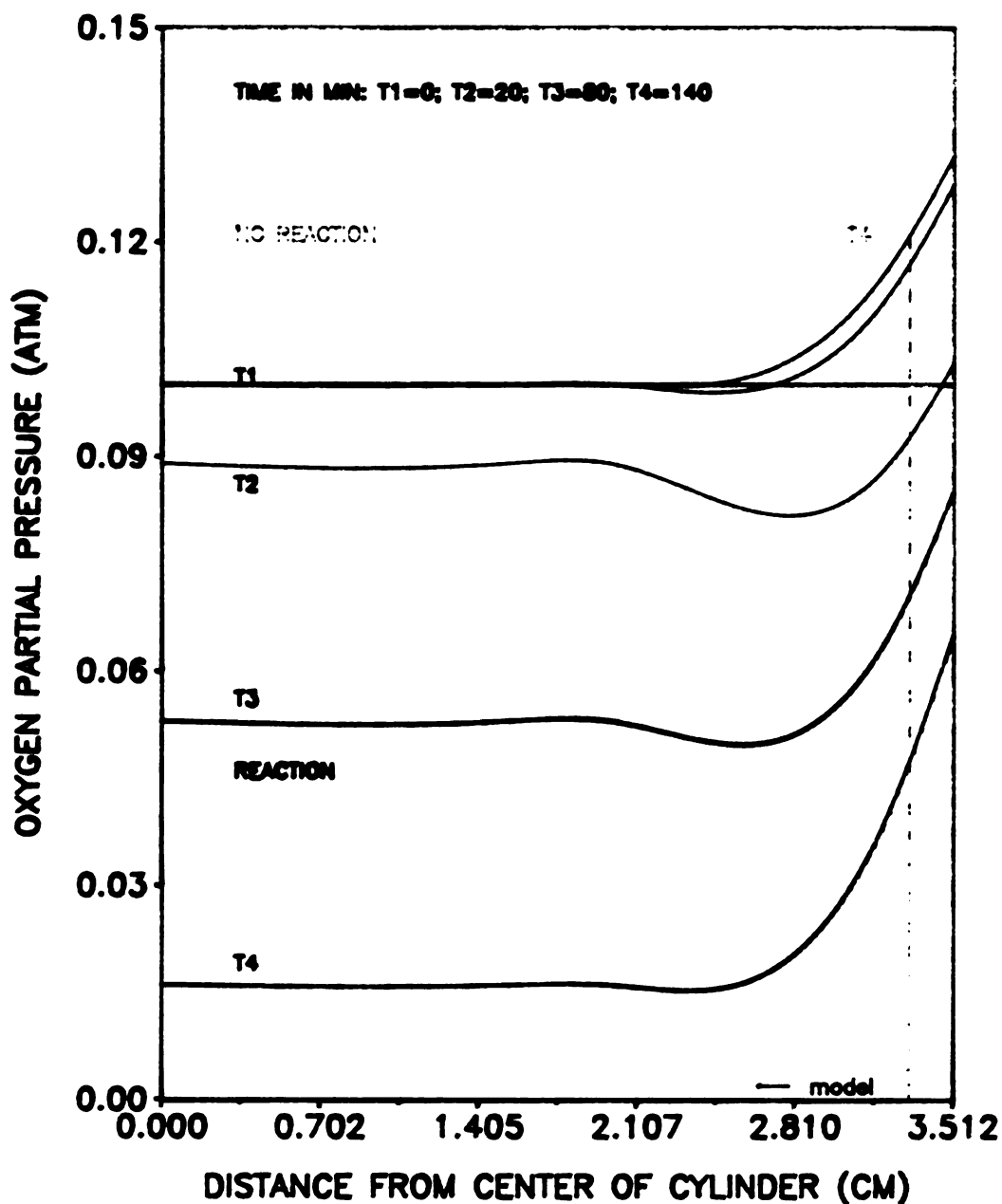
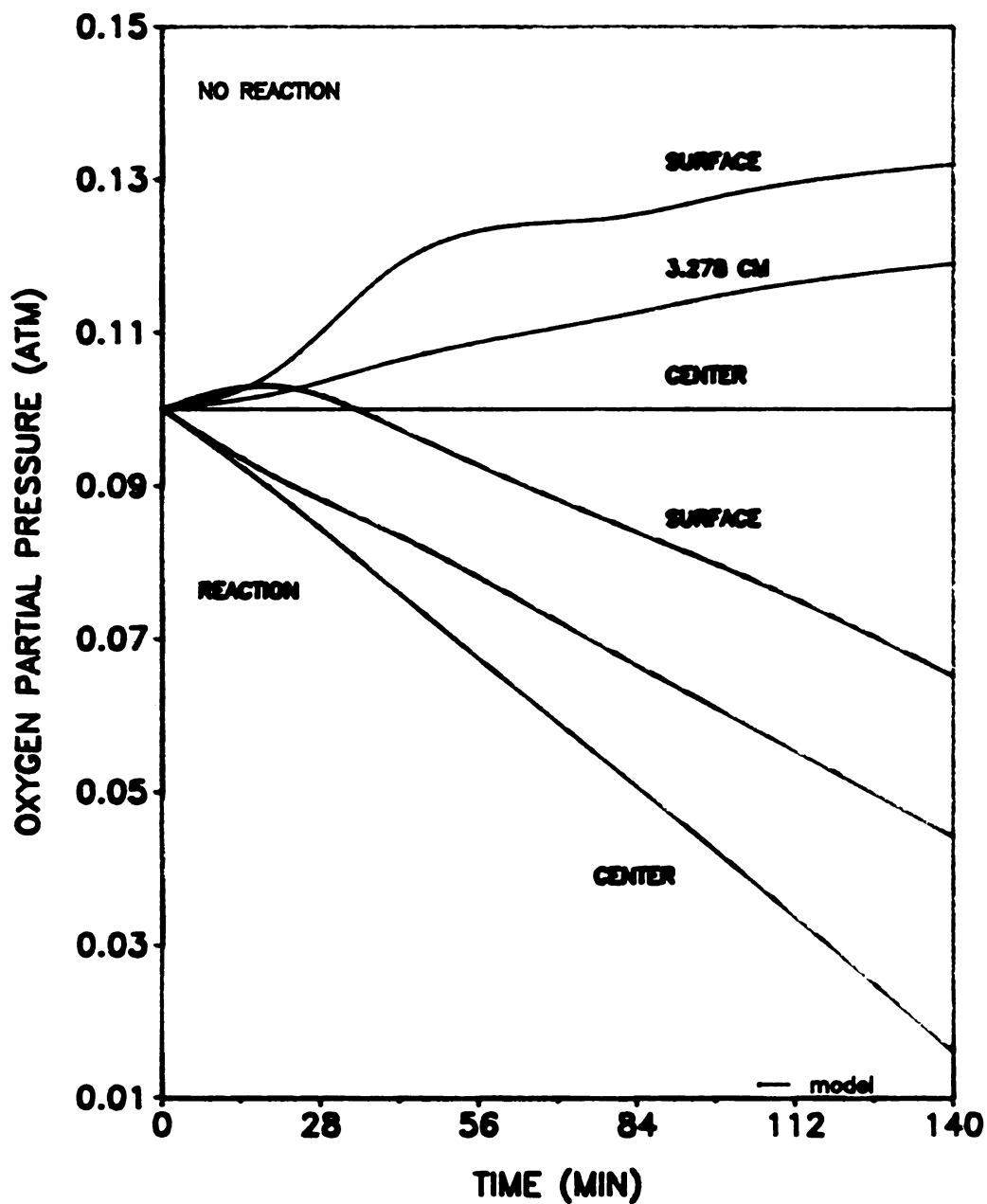


FIGURE 4.33 PREDICTED (FE) OXYGEN LEVELS IN A LIQUID FOOD, WITH AND WITHOUT A ZERO ORDER REACTION (HDPE CYLINDRICAL CONTAINER)



**FIGURE 4.34 UNSTEADY STATE OXYGEN DIFFUSION WITH AND WITHOUT REACTION IN A LIQUID FOOD SYSTEM (HDPE CYLINDRICAL CONTAINER)**



## V CONCLUSIONS

Three finite element computer models were used to simulate the oxygen diffusion in water and apple juice. Each computer model simulated a particular diffusion situation: A one dimensional, symmetrical (finite) diffusion system, and a semi infinite system, both in absence of a permeable membrane.

In the third model the liquids were packaged in a cylindrical permeable container (two dimensions, cylindrical coordinates).

Simultaneous oxygen diffusion and oxidation of vitamin C were also simulated in the semi infinite and cylindrical systems. The permeable packages were made with HDPE and Alethan.

Three model input parameters were determined: Oxygen diffusion coefficients ( $D$ ) in water and apple juice; Oxygen permeability constant ( $P_m$ ) of the packaging material, and kinetic rate constants related to degradation of vitamin C.

Results show that the method used in this study for determination of  $D$  in the food liquids provided reasonable data. The  $D$  value ( $8.5 \times 10^{-4}$  cm<sup>2</sup>/min) in apple juice was smaller than that found in water ( $1.2 \times 10^{-3}$  cm<sup>2</sup>/min),

The method could be applied to other liquids such as fruit juices and drinks.

Suspended particles which could affect sensor response must be avoided. Integral seal and water impermeable teflon membrane in the sensor are necessary to avoid electrode contamination by food which would result in corresponding inaccurate response.

A lumped air system method was developed to verify permeability constants and to estimate magnitude of error due to package design. Results show that the lumped method accurately predicted oxygen levels in a cylindrical permeable cell, and it may be applied to other situations such as head space determinations and oxygen consumption rates.

Two kinetic rate constants related to degradation of vitamin C were determined: one was obtained by measuring the percent retention of vitamin C in the liquid food.

The second kinetic rate constant was expressed in terms of oxygen (atm) since it was obtained by monitoring oxygen changes in the liquid. This constant was a necessary input parameter for the FE computer model to simulate oxygen diffusion.

Zero and first order rate equations expressed in atm of oxygen were obtained for high and low vitamin contents in the liquids. Vitamin C rate equations did not fit simple zero or first orders, but an empirical power law equation, suggesting a complex rate mechanism of destruction of vitamin C. Selected kinetic rate equations were used in the finite element modeling in this study. Attempts were not made to determine the rate mechanism for the oxidation of vitamin C.

Regardless of the presence of a protective package (oxygen permeable), the liquid systems show decrease in oxygen levels within the first two hours of each experimental run; levels then increased towards saturation (0.21 atm) steady state values. The decrease was related to a limiting diffusion rate, and the increase to a limiting reaction rate in water and apple juice with low vitamin content (0.341 mM and 0.227 mM vit. C respectively).

A protective effect which reduced destruction of vitamin C in apple juice was apparently related to the following factors: Thickness of the liquid, packaging membrane, pH and soluble solids in the apple juice. This protective effect was less evident in water probably due to a more alkaline pH and very low soluble solids content.

In any event, most of the vitamin C in apple juice was destroyed after the liquid reaches saturation oxygen levels. This condition may not occur in a real situation where more

This condition may not occur in a real situation where more impermeable packages are used and the product is consumed in a reasonable short period of time (six months),

The initial oxygen levels in the apple juice did not have a significant impact (within time frame in this study) on destruction of vitamin.

Computer modeling using the three FE models provided accurate predictions of oxygen levels in combination with degradation of vitamin C. Further experimentation with the models is necessary in order to simulate increasing oxygen levels in the diffusion-reaction process.

The models can be adapted to various food liquid packaging situations to include the effects of the following parameters:

- Permeability properties of packages
- Reaction kinetics of a quality factor
- Shape and dimensions of a package
- And Oxygen diffusion coefficients.

The following studies are suggested:

1. Oxygen diffusion studies to improve oxygen sensor design with emphasis on the thickness and water permeability of the teflon (tip) membrane.
2. Determination of oxygen diffusion coefficients in a wide variety of liquid foods: fruit juices, enriched drinks, wine, beer etc.
3. Development of charts using dimensionless parameters in order to visualize effects of packaging permeability, liquid diffusivity, package dimensions etc. in a wide range of oxygen diffusion situations.
4. Development of a FE model capable of simulating the diffusion of oxygen and other reacting components resulting from a second order kinetic rate equation.
5. Modification of the FE model to include the effects of convective movements in a liquid food.

## **APPENDIX A**

### Oxygen diffusion in a symmetrical system

The unsteady state diffusion of oxygen in stationary water can be represented by the following diffusion equation (Geankoplis, 1971):

For one dimensional flow

$$\partial p / \partial t = D \partial^2 p / \partial x^2 \quad (\text{AA.1})$$

Defining

$$Y = (p - p_b) / (p_o - p_b) \quad (\text{AA.2})$$

Where  $Y$  is dimensionless pressure variable

$$\text{I.C.} \quad Y = (p_o - p_b) / (p_o - p_b) = 1, \text{ all } x, t = 0 \quad (\text{AA.3})$$

$$\text{B.C.1} \quad Y = (p_b - p_b) / (p_o - p_b) = 0, x = 0, t = t \quad (\text{AA.4})$$

Boundary Condition 2 is similar to B.C.1, since both surfaces:  $x = 0$  and  $x = 2H$ , originally at  $p_o$ , are suddenly changed to  $p$ . ( $2H=L$ )

Solution:

$$Y(x,t) = (4\pi) \exp\{-\pi^2 D t / 4H^2\} \text{SIN}(\pi x / 2H) \quad (\text{AA.5})$$

Rearranging, and expressing in log terms:

$$2.303 \log [Y(x,t)] = 2.303 \log\{4/\pi + \text{SIN}(\pi x / 2H)\} - D\pi t / 4H^2 \quad (\text{AA.6})$$

$$\text{If } A = \log\{4/\pi + \text{SIN}(\pi x / 2H)\} \quad (\text{AA.7})$$

and

$$B = D\pi^2 / [2.303(4H^2)] \quad (\text{AA.8})$$

Then

$$\log [Y(x,t)] = A - Bt \quad (\text{AA.9})$$

and

$$D = 2.303[4BH^2 / \pi^2] \quad (\text{AA.10})$$

## **APPENDIX B**



**Development of equations for the oxygen diffusion in a semi infinite stagnant liquid system (Danckwerts, 1951a).**

The variation in time and space of the concentration  $C$  of dissolved oxygen in the liquid is governed by the diffusion equation (AB.1).

$$D \frac{\partial^2 C}{\partial x^2} = \frac{\partial C}{\partial t} \quad (\text{AB.1})$$

The rate of transfer of  $C$  across unit area of any plane parallel to the surface is:

$$R = -D \frac{\partial C}{\partial x} \quad (\text{AB.2})$$

Where  $x$  is the distance measured from the surface, where  $x=0$ .

$$\text{I.C. } C = C_0; \quad x \geq 0, \quad t = 0 \quad (\text{AB.3})$$

$$\text{B.C.1. } C = C^*; \quad x = 0, \quad t > 0 \quad (\text{AB.4})$$

$$\text{B.C.2. } C = C_0; \quad x = \infty, \quad t > 0 \quad (\text{AB.5})$$

The solutions is:

$$C - C_0 = (C^* - C_0) \text{erfc} \left\{ \frac{x}{2 \sqrt{Dt}} \right\} \quad (\text{AB.6})$$

It follows from (AB.3) and (AB.6) that

$$R = (C^* - C_0) \sqrt{D/\pi t} \quad (\text{AB.7})$$

and the amount of oxygen absorbed per unit surface area in time  $t$  is:

$$Q = RDt = 2(C^* - C_0) \sqrt{Dt/\pi} \quad (\text{AB.8})$$

plotting  $Q$  vs  $\sqrt{t}$  a straight line is obtained with a slope equal to  $2(C^* - C_0) \sqrt{D/\pi}$ , from which  $D$  can be calculated.

## **APPENDIX C**

## ISOSTATIC METHOD

### MEASUREMENT OF OXYGEN PERMEABILITY CONSTANT

(MOCON,1981)

The OX-TRAN 100 is an instrument for measuring the transmission rate of oxygen through synthetic films, coated papers, and other flexible or semirigid packaging materials.

The basic instrument consists of a  $100\text{ cm}^2$  diffusion cell in which the test specimen is clamped; an oxygen-specific coulometric detector, bubblers for humidifying gases, and associate controls.

Data is recorded by a strip chart millivolt potentiometer. The output of the coulometric detector is consistent with the fundamental electro chemical relationship described by Faraday's law.

Test specimens are clamped in the  $100\text{ cm}^2$  diffusion cell. Both sides of the cell are initially purged with an oxygen free carrier gas to remove residual oxygen from the system and desorb oxygen from the sample.

When a stable zero reading has been established, oxygen is introduced in the upper half of the diffusion chamber. The carrier gas continues to flow through the lower half and into the coulometric oxygen detector.

After a short period of time, the diffusion of oxygen through the film begins to be detected by the sensor, and the recordings of the millivolts continues to rise until leveling off, indicating the steady state has been reached. This voltage represents the equilibrium transmission rate of the oxygen through the film. From here, data conversion will yield the oxygen permeability constant  $P_m$ .

## **APPENDIX D**

## DETERMINATION OF ASCORBIC ACID (VITAMIN C) (Morell,1941)

### SOLUTIONS

1. Metaphosphoric acid (3%) (MPA) or Oxalic acid (1%)(OA).
2. 2,6- Dichlorophenol indophenol dye: 17.2 mg/500 ml water. Boil distilled water and pour dye in a filter paper. Cool and bring to 500 ml in a volumetric flask.

### SAMPLE DETERMINATION AND PREPARATION

1. If sample is juice, shake a volume of juice with 100 ml of 3% MPA or 1% OA for one min.  
If sample is solid, blend 25 gm of sample as above.
2. Filter through Whatman #1 filter paper. pour first filtrate back through paper to obtain a clear sample.
3. If dilutions are necessary, use sample and one of the acid solutions.
4. For color determination place 2 ml of dye in spectrophotometer tube and add 2 ml of sample, always adding the dye first.
5. Shake sample and read at 520 nm in the spectrophotometer within 15 -20 seconds.
6. Use the Optical Density (O.D.) readings to determine the mg AA/100 ml sample, by using a standard curve.

## **REFERENCES**

## REFERENCES

- Aiba, S., and Huang, S.Y. 1969. Oxygen permeability and diffusivity in polymer membranes immersed in liquids. Chem. Eng. Sc. 24:1449.
- ANSYS, 1988. "Engineering Analysis Systems Heat Transfer Seminar". Swanson Analysis Systems, Inc. Houston, PA.
- ANSYS, 1987. "Engineering Analysis Systems User's Manual." Swanson Analysis Systems, Inc. Houston, PA.
- ANSYS, 1983. "Engineering Analysis Systems Theoretical Manual." Swanson Analysis Systems, Inc. Houston, PA.
- ANSYS, 1982. "Engineering Analysis Systems Verification Manual." Swanson Analysis Systems, Inc. Houston, PA.
- Barron, F. 1981. Texture of Cooked Potatoes. M. S. Thesis, Washington State University. Pullman, WA.
- Battino, R., and Clever, H. L. 1966. The solubility of gases in liquids. Chem. Reviews, 66:395.
- Branner, S., V.O. Wodicka, and Dunlop, S.G. 1948. Effect of high temperature storage on retention of nutrients in canned foods. Food Technology 2:207
- Brian, P.L.T. 1964. Gas absorption accompanied by an irreversible reaction of general order. A.I.Ch.E. J. 10:5
- Brown, R. B. 1981. "Handbook of Plastic Test Methods." George Godwin Ltd.
- Comini, G., Del Giudice, S., Lewis, R.W., and Zienkiewicz, O.C. .1974. Finite Element solution of nonlinear heat conduction problems with special reference to phase change. Int. J. Num. Methods Eng. 8,613-624.
- Crank, 1975. "The Mathematics of Diffusion." Clarendon Press, Oxford.
- Chapra, S., and Canale, R. P. 1988. Numerical Methods for Engineers." Second Ed. McGraw-Hill, New York, N. Y.

Danckwerts, P.V. 1951a. "Gas-Liquids Reactions." McGraw-Hill Book Co. New York.

Danckwerts, P.V. 1951b. Absorption by simultaneous diffusion and chemical reaction into particles of various shapes and into falling drops. Trans. Faraday Soc. 47:1014.

Davidson, R. S., and Grieger-Block, R. A. 1977. The effect of mass transfer on apparent Ascorbic Acid autoxidation kinetics. A.I.Ch.E. J. 23, No, 4, 529

De Baerdemaeker, J., Singh, R. P., and Segerlind, L.J. 1977. Modeling heat transfer in foods using the finite element method. J. Food Processing Eng. 1,37-50.

Eison-Perchonok, M.H., and Downes, T.W. 1982. Kinetics of Ascorbic acid autoxidation as a function of dissolved oxygen concentration and temperature. J. Food Sc. 47:766.

Fatt, I. 1976. "The Polarographic Oxygen Sensor." CRC Press, Cleveland.

Fennema, O.R. 1996. "Principles of Food Science, Part I, Food Chemistry." Mercel Dekker, Inc. New York, N.Y.

Geankoplis, Ch.J. 1984. "Transport Processes and Unit Operations." Allyn and Bacon, Inc. Boston.

Geankoplis, Ch.J. 1971. "Mass Transport Phenomena." Holt, Rinehart and Winston, Inc. New York

Gilliland, E.R., Baddour, R.F., and Brian, P.L.T. 1958. Gas absorption accompanied by a liquid-phase chemical reaction. A.I.Ch.E. J. 4,223.

Goldstick, T. K., and Fatt, I. 1970. Diffusion of oxygen in solutions of blood proteins. Chem. Eng. Prog. Symp. Series 66:101.

Hay, G.W., B.A. Lewis and F. Smith. 1967. Chemistry of ascorbic acid, in "The Vitamins", Vol. 1, pp. 307. Academic Press, New York.



Hayakawa, K.I., Nonino, C., Succar, J., Comini, G., and Del Giudice, S. 1983. Two dimensional heat conduction in food undergoing freezing: development of computerized model. J. Food Sc. 48:1849. ✓

Hayduk, W., and Laudie, H. 1974. Prediction of diffusion coefficients for nonelectrolytes in dilute aqueous solutions. A.I.Ch.E. J. 20, 611-615.

Heldman, D.R., and Singh, R. P. 1981. "Food Process Engineering." Second Ed. The AVI Publishing Co., Inc. Westport, Conn.

Hernandez, R.J. 1984. Permeation of toluene vapor through glossy polyethylene terephthalate film. M.S. Thesis, Michigan State University, E. Lansing, MI.

Hikita, H., and Asai, S. 1964. Gas absorption with (m,n)-th order irreversible chemical reaction. Intl. Chem. Eng. 4:232

Hong, Y.C., Bakshi, A.S., and Labuza, T.P. 1986. Finite element modeling of moisture transfer during storage of mixed multicomponent dried foods. J. Food Sc. 51:554 ✓

Huelin, F.E. 1953. Studies on the anaerobic decomposition of Ascorbic acid. Food Res. 18:633.

Jameson, R.F., and Blackburn, N.J. 1976. Role of copper dimers and the participation of copper III in the copper catalyzed autoxidation of Ascorbic acid. Part II. J. C.S., Dalton, 534.

Lee, Y.C., Kirk, J.R., Bredford, L.L., and Heldman, D.R. 1977. Kinetics and computer simulation of Ascorbic acid stability in tomato juice as a function of temperature, pH, and metal catalyst. J. Food Sc. 42:640. ✓

Levenspiel, O. 1972. "Chemical Reaction Engineering." John Wiley and Sons. New York.

Lomauro, C.J., and Bakshi, A.S. 1985. Finite element analysis of moisture diffusion in stored foods. J Food Sc. 50:392. ✓

Luh, B.S., and Sharpe, R. 1982. Stability of tomato pastes packaged in plastic laminated pouches. A.I.Ch.E. Symp. Ser., V.78, No. 218.

Meyers, G.E. 1974. "Analytical Methods in Conduction Heat Transfer." McGraw-Hill Book Co. New York.

Mocon, 1981. "Operating Manual for the OX-TRAN 100 Oxygen Permeability Tester." Modern Controls, Inc. Elk River, Minn.

Morell, S.A. 1941. Rapid photometric determination of ascorbic acid in plant materials. Ind. Eng. Chem. Anal. ed. 13:793.

Pitts, R., and Sisson, E.L. 1977. "Theory and Problems of Heat Transfer." McGraw-Hill Book Co. New York.

Purwadaria, H.K. 1980. A Numerical Prediction Model for Food Freezing Using Finite Element Methods. Ph.D. dissertation, Agricultural Eng. Dept. Michigan State University.

Quast, D., and Karel, M. 1971. Effects of oxygen diffusion on oxidation of some dry foods. J. Food Tech. 6: 95.

Robertson, G.L., and Samaniego, C.M.L. 1986. Effect of initial dissolved oxygen levels on the degradation of Ascorbic acid and the browning of lemon juice during storage. J. Food Sc. 51: 184.

Russel, W.P., and Walton, J.H. 1943. The autoxidation of Ascorbic acid. J. Am. Chem. Soc. 65:1212.

Sadler, G.D. 1984. A Mathematical Prediction and Experimental Confirmation of Food Quality Loss for Products Stored in Oxygen Permeable Polymers. Ph.D. thesis, Purdue University.

Segerlind, L.A. 1984. "Applied Finite Element Analysis." John Wiley and Sons, New York.

Singh, R.P. 1974. Computer Simulation of Liquid Food During Storage. Ph.D. thesis, Michigan State University.

Van de Vusse, J.G. 1961. Mass transfer and chemical reaction. Chem. Eng. Sc. 16:21

Zhang, T.Y., Bakshi, A.S., Gustafson, R.J., and Lund, D.B. 1984. Finite element analysis of nonlinear water diffusion during rice soaking. J. Food Sc. 49:246.

Zienckiewicz, O.C., and Cheung, Y.K. 1965. Finite elements in the solution of field problems. *The Engineer*, pp. 507-510.